Frontispiece; Coring lake sediments on Trough Lake, Pyramid Trough 1987.

SEDIMENTATION IN ANTARCTIC PROGLACIAL LAKES.

University of Waikato
1989

A thesis
submitted in partial fulfilment
of the requirements for the degree of
Master of Science in Earth Sciences
at the
University of Waikato
by

ANTHONY JOHN SADLER

ABSTRACT

A variety of Antarctic lakes occur either as proglacial lakes to glaciers, or as detached lakes within an enclosed drainage system in the Dry Valleys of McMurdo Sound, Antarctica. Some of these are the evaporated remnants of much larger proglacial lakes that formed during the last glacial, when the Ross Ice Shelf thickened, grounding on the continental shelf, and advanced landward entering many of the Dry Valleys. These former proglacial lakes have been the source of datable material using U/Th methods on the products of evaporation ($CaCO_3$), and ^{14}C on algal deposits associated with many lacustrine sediments. These methods provide dates for glacial advances and hence allow correlation with similar northern hemisphere events.

Interpretation of both the data generated, and morphologic evidence for paleo-lacustrine environments, requires a knowledge of how these former lakes developed and the processes occurring within them. To this end a modern proglacial lake, Trough Lake in Pyramid Trough, was selected to study and provide a model for sedimentation in the former lakes as well as a guide for interpretation of former proglacial environments.

Although Trough Lake is proglacial to an alpine glacier, not a large ice sheet, and it is much smaller than the former lakes, it makes a satisfactory surrogatte. The principle aim was to examine the sedimentary processes occurring within the lake and to use this information to construct a facies model for the interpretation of former proglacial lacustrine environments.

The transport of ice-rafted, formerly glacial material, across the lake ice and the changes that occur to it have been examined. The results indicate that aeolian processes, as well as extraction of the fine fraction through the lake ice, occur concentrating the coarse fraction in ice-cored domes at the distal end of the lake. The fine fraction if it migrates through the lake ice becomes part of the normal, predominantly silt, lacustrine sediments. However, the distance a sand particle can move through the ice is size dependent, the coarser the material the smaller the distance it can migrate downward. This sand/ice interaction manifests itself in bimodal lacustrine sediments becoming progressively coarser away from the glacier until a point is reached where all the sand fraction that can migrate through the ice, has done so, and beyond this, lacustrine sediments will be unimodal. Thus it is apparent, that grain size distribution analysis of proglacial lacustrine sediments, and their associated drift, can be very useful in determining the size and structure of former Antarctic proglacial lakes.

The calving of icebergs from the glacier snout and their eventual replacement by lake ice provides a mechanism by which lake ice can move at a rate of about 18 m per year (at Trough Lake) away from the glacier.

The formation of the characteristic ice-cored domes found on many proglacial or former proglacial lakes in the McMurdo Sound area was demonstrated in a laboratory experiment designed to model the Antarctic environment. These domes are important as they often cover and preserve underlying lacustrine silts and algae when left behind by falling lake levels through retreat of the associated glacier. In addition these deposits can be used to gauge the extent of former lakes as well as providing samples for ^{14}C dating.

Evidence of seasonal cracks within the lake was observed and a core of sediment deposited through such a crack was extracted. This suggests another method by which lacustrine silts may be preserved in a very dry and windy Antarctic environment.

The physics of sand/ice interactions was examined in some detail, and it was demonstrated that the feasibility of sand moving through ice was not size related as had been suggested by some workers, however the rate at which sand moves through ice is inversely proportional to grain size. This provides a non-structural mechanism by which sand can move through lake ice and accumulate within the normal lacustrine sediments.

By measuring temperature and chemical variation through the water column and the light penetrating the lake ice a model for a reverse convection cell operating within the lake was devised, and this explains how such a deep lake can maintain a very homogeneous water temperature and chemistry.

Finally with the accumulated information a model for present and past proglacial lacustrine sedimentation was developed and this was used as the basis for a proposed facies model for paleo-proglacial lacustrine environments.

ACKNOWLEDGEMENTS

I would like to gratefully acknowledge the contribution of the many people who have helped in the coarse of this thesis. Principally I would like to thank Dr. Chris Hendy of the Chemistry Department who suggested the topic and arranged for the field work necessary. In addition he supplied valued information and advice from his extensive Antarctic background, helping to interpret results, and apply them to the Antarctic situation.

I would also like to thank my other supervisor, Willem deLange of the Earth Sciences Department for his help with the sedimentary side of this thesis and his time and patience demonstrated in reading and helping structure this thesis, especially while Chris was overseas. I would also like to acknowledge Associate Professor Evan Byder of the Physics Department for his aid in the interpretation of the physics of sand/ice interactions.

I wish to acknowledge the valued contribution of the Ross Dependency Research Commitee without who's sponsorship this project would not have gone aheadas well as the D.S.I.R. for logistics support. Thanks also to the staff and personal of Scott Base as well as the other member of Event K021 Fiona Judd now residing in England.

A special thanks to the technicians and staff of both the Chemistry and Earth Science Departments for their assistance during the coarse of this thesis. To the many students I have known especially my fellow inmates in F 2.04 Allen, Tony , Shane, Fiona and Heather, thanks for the friendship and the best of luck for the future.

Finally I would like to thank the staff and fellow patrons of H Block for their ample supply of good humour and liquid refreshment.

TABLE OF CONTENTS

LIST OF FIGURES

LIST OF TABLES

LIST OF PLATES

CHAPTER ONE

INTRODUCTION

1.1 ANTARCTIC DRY AREAS

The Antarctic continent is occupied by two very large ice sheets, the East Antarctic Ice Sheet and the West Antarctic Ice Sheet which together cover 96% of the land area and are separated by the Transantarctic Mountains. Along the western shores of the Ross Sea embayment, the Transantarctic Mountains form an impediment to the flow of ice from the East Antarctic Ice Sheet to the sea. Throughout the mountain range large valleys have been calved by outlet glaciers from the ice sheet, most of which are still occupied by ice. However in a few locations, insufficient ice enters the western ends of the valleys to sustain a through glacier. Dry air, heated by adiabatic compression flows through the valleys from the 4000 m high ice sheet to the sea, and results in the most extreme aridity found anywhere on earth. The degree of aridity is evidenced by the presence of very deliquescent salts, such as $CaCl_2.6H_2O$ which may crystalize from ice-free saline ponds (eg. Don Juan Pond [House *et al*, 1966]). The McMurdo Sound area of Antarctica contains a number of "Dry Valleys", so called because they are predominantly devoid of ice and snow, with the exception of some enclosed drainage basins which contain ice-covered lakes (Wilson, 1967/a).

Precipitation is restricted to snowfall due to the extreme cold, and very little of the snow which falls in the dry valleys melts, most being lost by sublimation. The precipitation/evaporation balance (Wilson, 1967/a) defines whether or not ice and snow may accumulate. The relationship of precipitation to evaporation (or more correctly sublimation) can be considered as the net precipitation, which is equal to the total precipitation minus the total evaporation. Hence a dry area can be considered a place where the net precipitation is negative since evaporation exceeds precipitation. Ice and snow covered areas are places where the precipitation exceeds evaporation, and hence the net precipitation is positive. The snow line represents the point where net precipitation becomes positive (Charlesworth, 1957).

Ice and snow may move below the snow line from an area of high positive net budget to an area of low net budget as a glacier. Such a glacier will flow into a valley until an equilibrium between the positive region, above the snow line, and the negative budget

below is achieved. In summer, during the hottest days, glaciers may melt, forming streams and lakes in enclosed drainage basins. The amount of water in such a lake, and hence lake level, is controlled by (fig. 1.1):

-the surface area of the lake;
-the sublimation rate; and
-the fluvial inflow

The volume of water in the lake, and its dimensions, determine the lake's surface area, and hence sublimation rate. For a lake to remain at a static level, the inflow during summer must equal the losses through sublimation over the total lake surface during the year, assuming, as is the case for most lakes in the area, there is no outflow controlling lake level. Although Cartwright and Harris (1981) claim a ground water flow into some lakes, there is no geochemical or isotopic evidence to show that this phenomena has a measurable effect on the water balance (Hendy, *in press*).

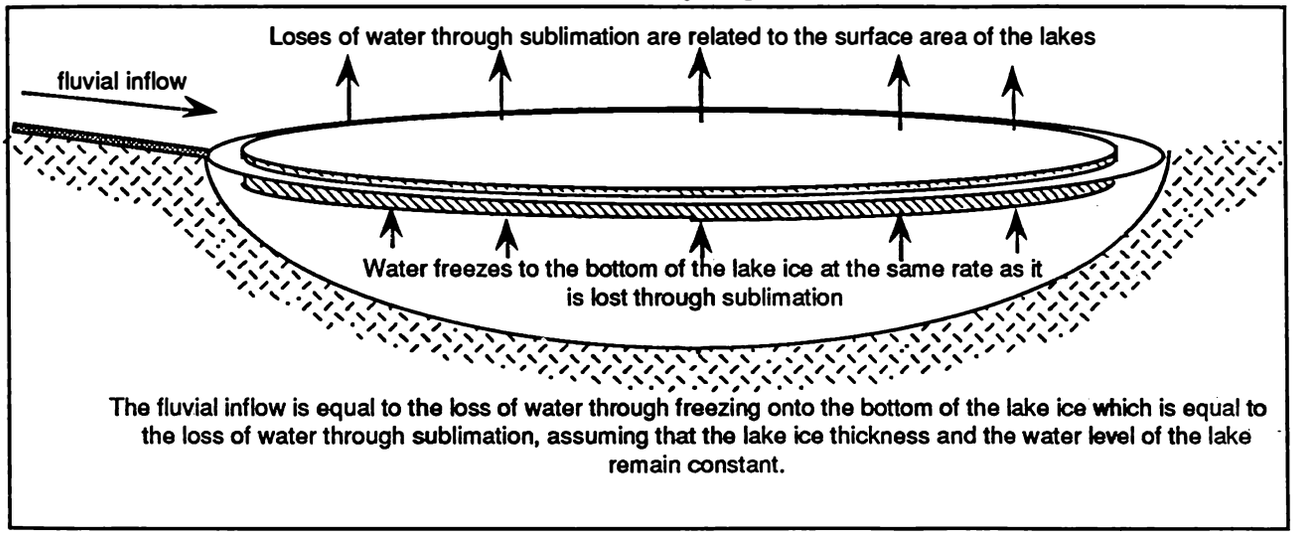

Figure 1.1 An idealized water budget for an enclosed drainage system lake in a McMurdo dry valley.

1.1.2 Dry Valley Climate

The mean annual temperature in the McMurdo area is about -20°C, with a range of -55°C in winter to +10°C for a few hours on some days in the late summer (Bull, 1966; Thompson *et al*, 1971), although higher temperatures have since been recorded (deLange, *pers. comm.*). At higher elevations the air temperature decreases rapidly, so that above about 1000 m it is unlikely to exceed 0°C. Mean annual precipitation is about 50-100 kg/m^2 (Thompson *et al.*, 1971), while the potential sublimation figure for low elevations is about 500 kg/m^2 (Ragotzkie and Likens, 1964; Anderton and Fenwick, 1976; Chinn,1983). This ensures a substantial over-potential for sublimation, by about one order of magnitude, for the valleys.

1.1.3 Dry Valley Hydrology

Water in the dry valleys moves as glaciers, in rivers that flow infrequently during summer, or as ground water above a frozen water table. In the Antarctic dry valleys, the water table consists of a pan of hard ice-cemented debris, often found beneath the ground surface, and is locally, but incorrectly, referred to as "perma-frost". The depth at which the ice cement occurs, appears to be controlled by position relative to the snow line, and hence is controlled by the net precipitation in a similar manner to the snow line (Wilson, 1981). Work conducted during the Dry Valley Drilling Project (DVDP) has shown that this "perma-frost" zone is between 240 and 970 m thick (Decker and Bucher, 1982).

On the basis of their ice cover two types of lake are recognized in the dry valleys (Wilson, 1981):

(1) Perennially ice-covered lakes, which have a permanent cover of ice that does not melt out during summer. This ice cover is generally between 3.5 and 6.5 m thick, the thickness being determined by the relative losses through ablation and the gains through freezing of ice on to the bottom of the ice raft; and

(2) "Ice-block" lakes, which are permanently frozen to their base. Losses through ablation are replaced by seasonal inflow of water over the surface of the lake, where it freezes.

The factor which controls the type of lake present, is the relative proximity to the snow line. Lakes in low areas, such as the Taylor Valley (eg. Lake Fryxell), are perennially ice-covered while those closer to the snow line such as those in the Victoria Valley (eg. Lake Vida), are ice-block lakes. The thickness of the floating ice cover is therefore related to the relative position of the lake with respect to the snow line, as well as the relative ablation and freezing rates.

In addition to the distinctions recognized by Wilson (1981), we can further sub-divide the Antarctic lakes according to their containment into:

(1) Topographic depression lakes, which may be enclosed drainage (eg. Lakes Vanda, Vida, Don Juan and Fryxell) or may overflow (eg. Lakes Miers and Canapus) and;

(2) Ice dammed lakes, in which a glacier occupies the lowest point of a drainage system physically damming melt waters in a proglacial lake (eg. Lakes Trough, Wilson, Joyce, Hoare and Brownworth).

1.1.3 Dry Valley Hydrology

Water in the dry valleys moves as glaciers, in rivers that flow infrequently during summer, or as ground water above a frozen water table. In the Antarctic dry valleys, the water table consists of a pan of hard ice-cemented debris, often found beneath the ground surface, and is locally, but incorrectly, referred to as "perma-frost". The depth at which the ice cement occurs, appears to be controlled by position relative to the snow line, and hence is controlled by the net precipitation in a similar manner to the snow line (Wilson, 1981). Work conducted during the Dry Valley Drilling Project (DVDP) has shown that this "perma-frost" zone is between 240 and 970 m thick (Decker and Bucher, 1982).

On the basis of their ice cover two types of lake are recognized in the dry valleys (Wilson, 1981):

(1) Perennially ice-covered lakes, which have a permanent cover of ice that does not melt out during summer. This ice cover is generally between 3.5 and 6.5 m thick, the thickness being determined by the relative losses through ablation and the gains through freezing of ice on to the bottom of the ice raft; and

(2) "Ice-block" lakes, which are permanently frozen to their base. Losses through ablation are replaced by seasonal inflow of water over the surface of the lake, where it freezes.

The factor which controls the type of lake present, is the relative proximity to the snow line. Lakes in low areas, such as the Taylor Valley (eg. Lake Fryxell), are perennially ice-covered while those closer to the snow line such as those in the Victoria Valley (eg. Lake Vida), are ice-block lakes. The thickness of the floating ice cover is therefore related to the relative position of the lake with respect to the snow line, as well as the relative ablation and freezing rates.

In addition to the distinctions recognized by Wilson (1981), we can further sub-divide the Antarctic lakes according to their containment into:

(1) Topographic depression lakes, which may be enclosed drainage (eg. Lakes Vanda, Vida, Don Juan and Fryxell) or may overflow (eg. Lakes Miers and Canapus) and;

(2) Ice dammed lakes, in which a glacier occupies the lowest point of a drainage system physically damming melt waters in a proglacial lake (eg. Lakes Trough, Wilson, Joyce, Hoare and Brownworth).

Plate 1.1 Aerial photograph looking south-west toward Mt Dromedary and Mt Kempe of the Royal Society Range from over the Koettlitz Glacier, showing Trough Lake and the surrounding area (Trough Lake's dimensions are 3 km by 2 km at their greatest).

In addition some topographic depression lakes, may also be proglacial, in that a glacier advances into the lake, but not necessarily damming it (eg. Lake Bonney).

The unexpected occurrence of these lakes, and their ability to remain liquid in an area where the mean temperature is only -20°C, has been the subject of some research. The temperatures of bottom waters of these lakes have been measured, and they range from -5°C to 26°C. Numerous mechanisms have been proposed for this, but the two major ones are:

-solar heating (Wellman and Wilson, 1962); and
-a high geothermal gradient below the lake (Nichols, 1962; Armitage and House, 1962; Angino and Armitage,1963).

It has been demonstrated that the primary mechanism for heating in most lakes is solar heating, as in Lake Fryxell and Lake Bonney (Hoare *et al*, 1964: 1965), and, in an extreme case, Lake Vanda where the dense $CaCl_2$ saturated bottom waters reach temperatures of 26°C.

The solar mechanism was proven during the Dry Valley Drilling Project, when temperature logs of the holes drilled below the deepest part of the lake showed heat decreased downward, eliminating a high thermal gradient below the lake as a possible source of heat (Wilson *et al*, 1974). Solar heating is made possible by the lack of snow covering the lake ice during summer, as this would seriously restrict penetration of light. The very clear lake ice therefore ensures high transmission rates through the ice into the water below (6% solar energy transmission was recorded through 4 m of ice on Lake Vanda [Wilson, 1981]). This high level is achieved as a result of the manner in which the ice forms. Water freezes onto the bottom of the ice raft, resulting in large ice crystals several square centimetres in cross-section, and in excess of 4 m long. These crystals have their c-axis aligned vertically, and thus the ice crystals act as light pipes through which the solar energy can be transmitted into the underlying water.

1.2 OBJECTIVES

The University of Waikato Antarctic Research Unit has previously conducted work on Antarctic lacustrine sediments (Gumbley, 1975; Laurence, 1982; Judd, 1986; Clayton-Greene, 1986), in lakes of the McMurdo dry valleys. The bulk of this work was conducted on detached, or former proglacial lakes, all of which generally imply some degree of evaporation and therefore concentration of salts within the water column and lacustrine sediments. To gain an insight into the sedimentary processes active in the former large lakes proglacial to the Ross Sea Ice (Clayton-Greene *et al.*, 1987) a survey

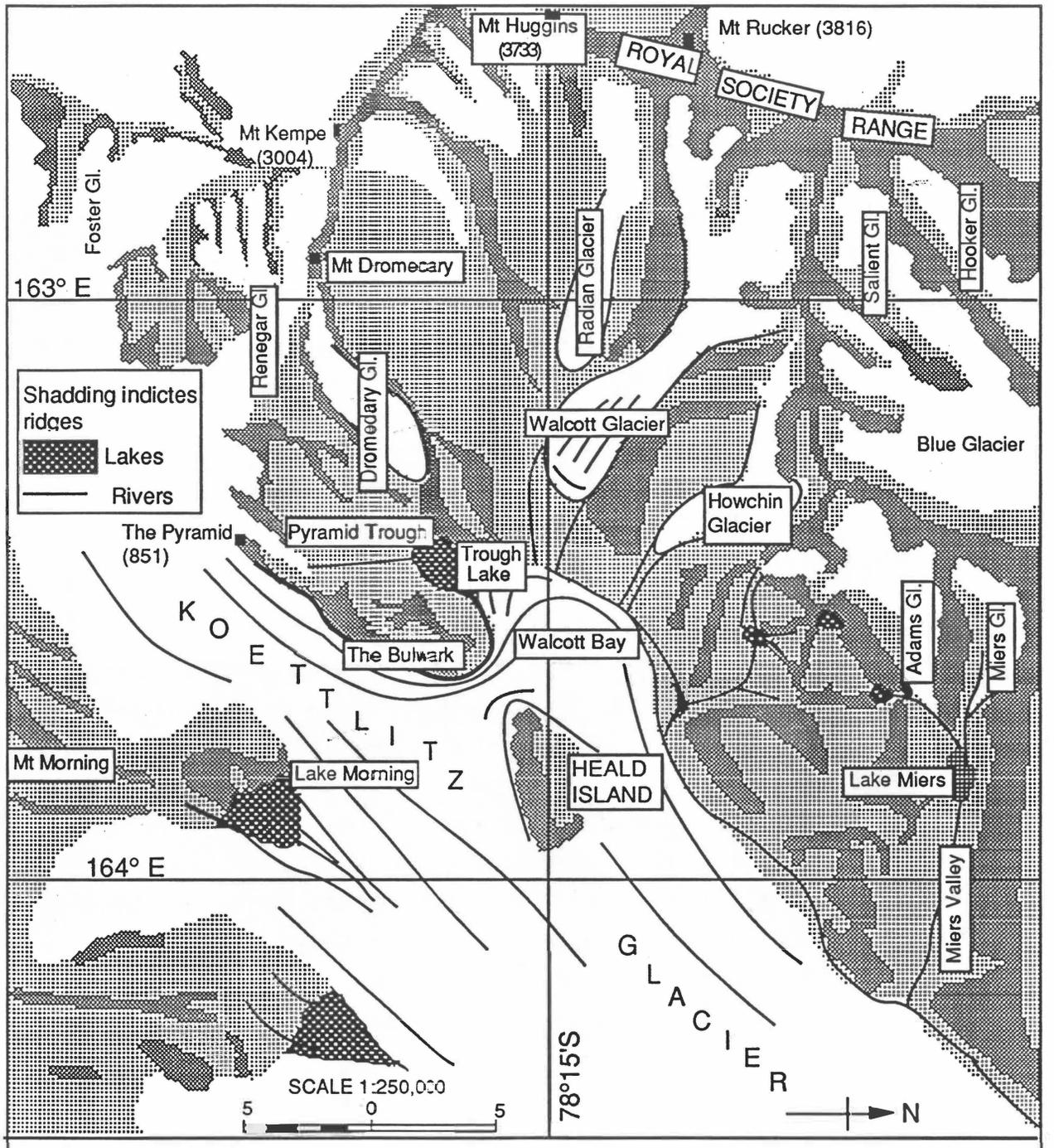

Figure 1.2 **Physiography of the Koettlitz Glacier area of the Royal Society Range, Antarctica.**

of modern proglacial lakes was under-taken to find a suitable lake to study. After an initial survey, Trough Lake in Pyramid Trough was selected as a suitable model for the much larger former proglacial lakes.

1.3 PYRAMID TROUGH

1.3.1 Location

Trough Lake is situated in Pyramid Trough (fig. 1.2) one of the McMurdo dry valleys, and trends north to south, between The Bulwark and Mount Dromedary, at 78° 16' 53" S and 163° 26' 01" E respectively. The Koettlitz Glacier occupies both the northern and southern extremes of the valley. This glacier has its source in a névé formed between Mt Kempe and Mt Morning, and thus the Koettlitz Glacier is an alpine glacier, albeit a very large one, and not an outlet of the East Antarctic Ice Sheet.

1.3.2 Topography

Pyramid Trough is a glacial valley that parallels the Royal Society Range of southern Victoria Land (Plate 1.1). The Royal Society Range is the section of the Transantarctic Mountains bordering McMurdo Sound between the Ferrar Glacier in the north and the Koettlitz Glacier in the south. The Royal Society Range is dominated by Mt Morning, Mt Kempe, Mt Dromedary, Mt Huggins, Mt Rucker, Mt Hooker and Mt Lister, all of which are about 3000 m in height.

Pyramid Trough was formed by a branch of the Koettlitz Glacier which flowed down the valley, forming the steep sides characteristic of the valley today (Lyon, 1979). The Koettlitz Glacier flows past the southern extreme of the valley and down the eastern side of The Bulwark, although a branch of it does impinge into Pyramid Trough to the south (fig. 1.3). This branch is separated from the glacier by a ridge of resilient granite, on the extremity of which is a pyramid shaped hill (The Pyramid [851 m]), from which the valley gains its name. Northeast of Pyramid Trough, the Koettlitz Glacier is divided in two by Heald Island. The eastern branch flows into McMurdo Sound and the Ross Ice Shelf while the western branch flows into Walcott Bay where it enters the northern extreme of Pyramid Trough. A proglacial lake to the Koettlitz Glacier (Trough Lake) has formed extending up Pyramid Trough some 2.5 km.

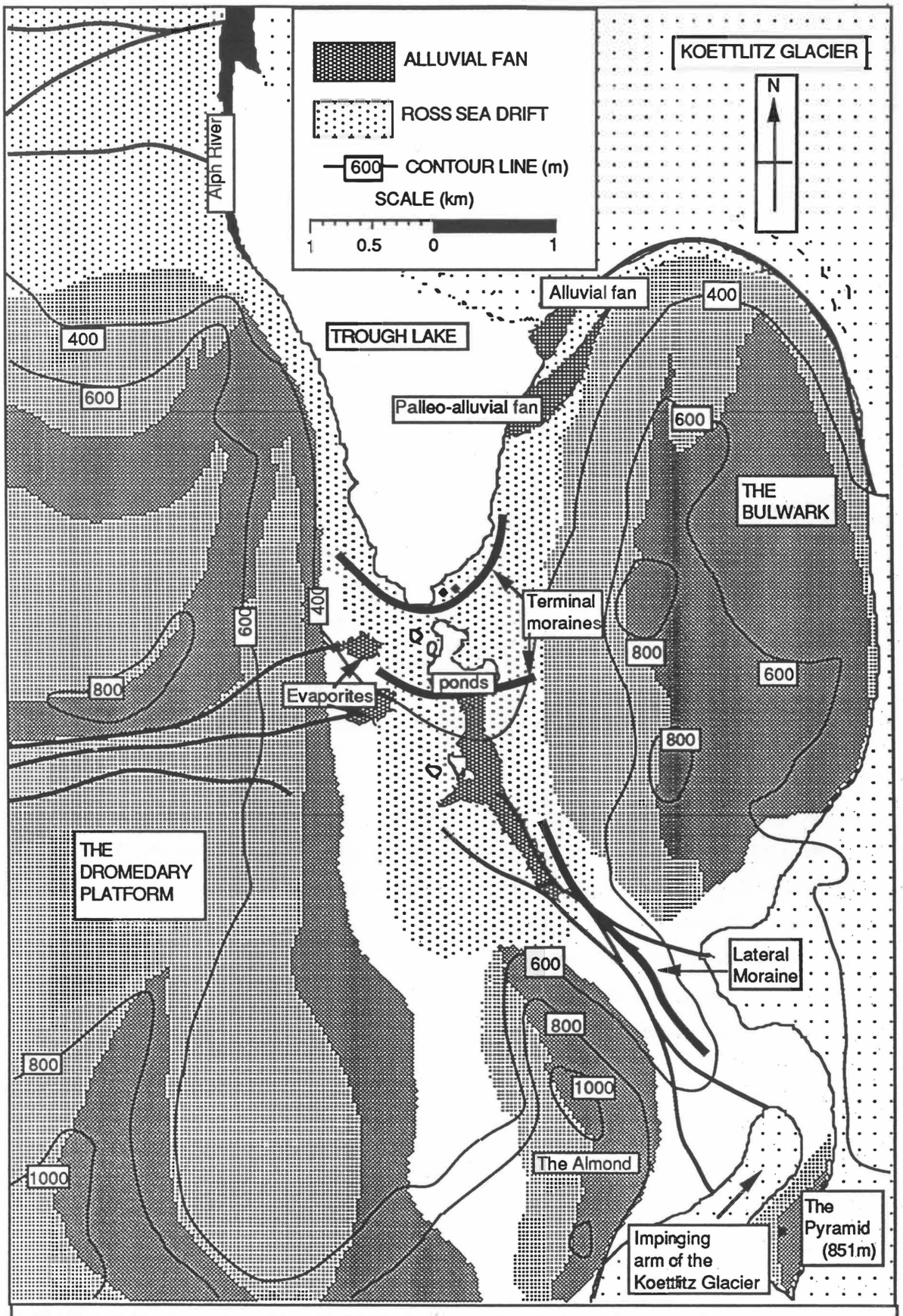

Figure1.3 Topography of Pyramid Trough, McMurdo Sound, Antarctica.

The eastern margin of the valley is formed by The Bulwark, a hill of some 900 m in height. The western margin of the valley is bordered by the Dromedary Platform (altitude approx. 600 m) onto which the Dromedary Glacier flows from neighbouring Mt Dromedary (2760 m). The southern end of the valley is dominated by The Almond (Blank *et al*, 1963), a triangular shaped outcrop of granite in excess of 1000 m in height. The valley is divided in two by The Almond, forming a southwestern and northeastern branch.

Trough Lake's water level, about 200 m, above sea level is controlled by the height of the Koettlitz Glacier which blocks the northern extremity of Pyramid Trough. Some ponds occur just south of the lake and are separated from the lake by a ridge of drift. The remainder of the valley floor consists of predominantly hummocky drift with some lateral moraines. The southeastern side of the valley is bordered by a large lateral moraine presumably left during the last withdrawal of the Koettlitz Glacier, in a southerly direction up the valley.

1.3.3 Hydrology

The Alph River drains Trough Lake at the northwestern extreme and flows north along the Koettlitz Glacier margin. This river is also fed by streams from numerous valley glaciers, such as the Radian, Walcott and Howchin Glaciers as it flows north.

The major inflow to Trough Lake occurs at the northeastern corner of the lake, where a river marginal to the Koettlitz Glacier flows around The Bulwark and into Trough Lake forming an alluvial fan at the northeastern extremity of the lake. Inflow also occurs at the southern end of the lake, where streams draining the impinging arm of the Koettlitz Glacier enter the lake. Seasonal streams occur on the western side of the lake, which have their source at the Dromedary Glacier, 600 m above Trough Lake on the Dromedary Platform. These streams flow down the western side of the valley over alluvial fans at the base of the slope, where evaporatic salts have precipitated. Blank *et al*, (1963) mapped these two alluvial fans as volcanic features pertaining to the McMurdo Volcanics. In addition, water is probably added to the lake by the Koettlitz Glacier melting directly into the lake.

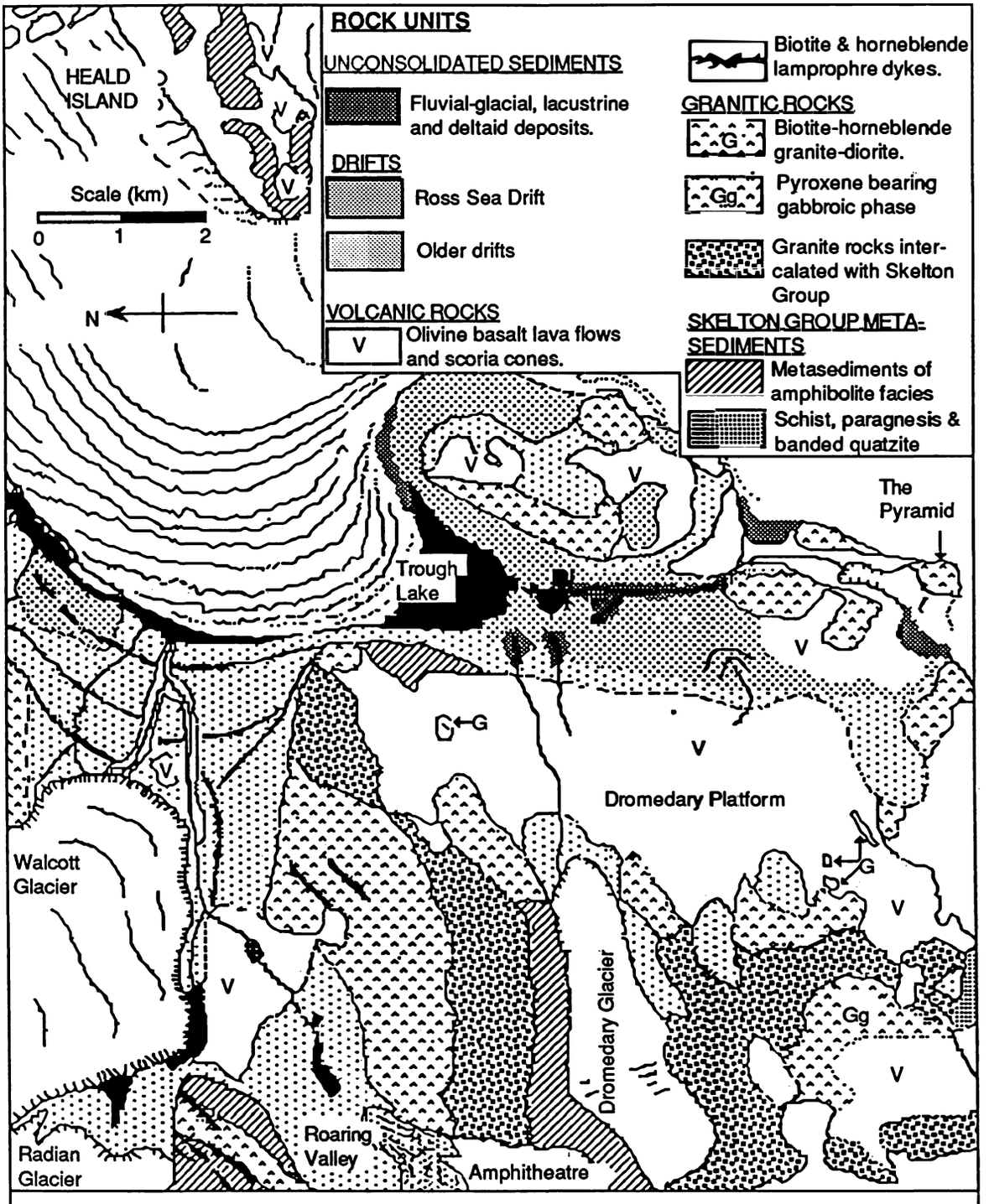

Figure 1.4 Geology of the Koettlitz Glacier area of McMurdo Sound, (Blank *et al*, 1963).

1.4 GEOLOGY OF THE KOETTLITZ GLACIER AREA

1.4.1 Basement Geology

The basement geology of the Koettlitz Glacier area (fig. 1.4) is predominantly Precambrian to Cambrian in age. The basement consists of metasediments belonging to the Skelton Group which have been folded and metamorphosed during an Ordovician orogeny. Associated with this orogenic event, was the intrusion of a syn-tectonic granodiorite batholith, and subsequently, the post-tectonic deposition of a sheet-like granite batholith with lamprophyre and porphyry dyke swarms of at least two generations (fig. 1.5), that strike generally northeast (Blank *et al,* 1963; Neall and Smith, 1967). The basement geology of the eastern margin of Pyramid Trough, namely The Bulwark and The Almond, is dominated by the granite of the post-tectonic batholith. However, the western margin of Pyramid Trough becomes progressively dominated by the Skelton Group metasediments, with less influence of granitic rocks.

In general, a westward increase in metamorphic grade and a decrease in the influence of orogenic granites can be recognized. This is reflected by the change in geology toward the west, ranging from the granite of the batholith, to the Skelton Group metasediments comprising firstly an amphibolite facies, then schists and banded quartzites.

Following the Ordovician Orogeny, an extensive period of erosion led to the development of the Kuriki Peneplain Surface (Neall and Smith, 1967), which was followed by a long period of continental marine sedimentation from Devonian times. The sediments were subsequently intruded by dolerite sills and dykes, during the Jurassic, to form the characteristic Beacon Sandstone and Ferrar Dolerites of the Royal Society Range. The McMurdo Sound area was subsequently uplifted, and sub-aerially exposed.

1.4.2 Cenozoic Geology

Due to uplift and erosion , no Cenozoic sediments have survived, with the exception of fluvial-glacial deposits. The McMurdo Volcanics in the Koettlitz area are centred on the Dromedary Platform which forms the western margin of Pyramid Trough. The volcanics consist of cinder cone remnants, scoria mounds, lava flows and spatter cones (Blank *et al,* 1963), and show no evidence of alignment (Wright, 1978). The volcanics have been described as basanitoid by McIver and Gevers (1970) and Goldich *et al,* (1975) using the chemical definition of MacDonald and Katsura (1964). They are typically glassy or fine-grained lavas with phenocrysts of olivine, or xenocrysts of kaersutite.

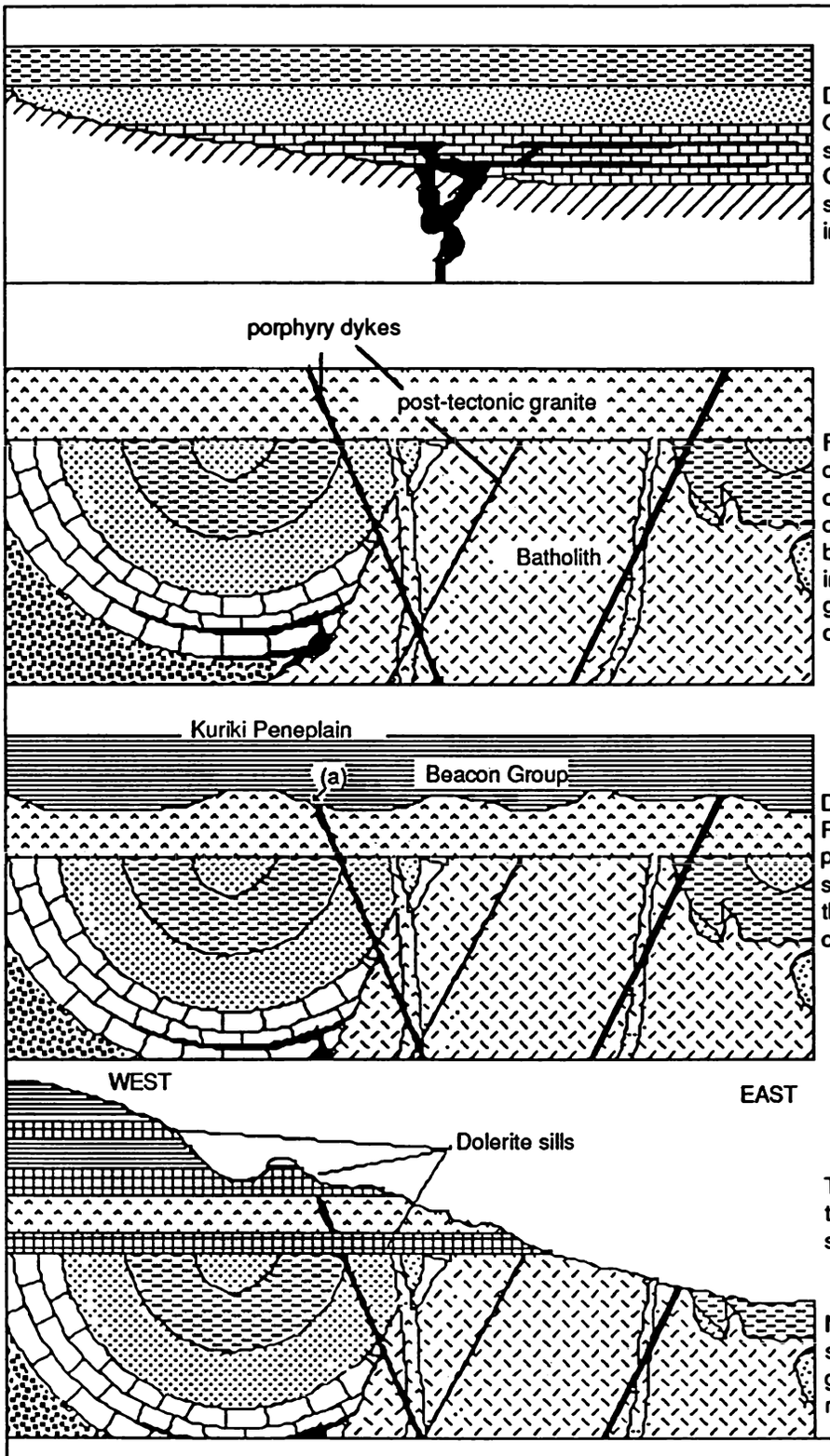

Deposition of the Skelton Group sediments in a geo-syncline of Pre-cambrian to Cambrian age, with subsequent igneous intrusion.

Ordovian Orogeny

Folding and metamorphism of the sediments with contemporaneous intrusion of syn-tectonic granodiorite batholith. Post-tectonic intrusion of a sheet-like granite with porphyry dykes of two generations.

Development of the Kuriki Peneplain surface (a) on the post-tectonic granite with subsequent deposition of the Beacon Group un-conformably on the granite.

The basement geology of the dry valleys today in a section from east to west.

N.B. the intrusion of dolerite sills within the post-tectonic granite and at the base and middle of the Beacon Group.

Figure 1.5 Diagrammatic representation of the development of the basement geology of the McMurdo Sound dry valleys, Antarctica (Neall and Smith, 1967).

The volcanics are generally truncated by the last glacial advance up the valley and therefore are believed to be older than this event (Blank *et al*, 1963). Some evidence of post-glacial volcanism is apparent on the eastern side of the valley where a lateral drift is draped with basalt associated with the McMurdo Volcanics.

The McMurdo Volcanics constitute the bulk of the western margin to the Pyramid Trough forming the Dromedary Platform as well as a large area of the western branch of the valley between The Almond and the Dromedary Platform. Outcrops also occur on The Bulwark and on the ridge leading up to The Pyramid.

Large areas of undifferentiated drift, mapped by Blank *et al,* (1963), cover the floor of the valley and areas of The Bulwark, as well as the area surrounding the Walcott Glacier, and into Roaring Valley. The McMurdo Volcanics appear to post-date this drift generally, as they overlie the drift surrounding The Bulwark and that present in the Roaring Valley-Walcott Glacier region. An additional drift (Blank *et al*, 1963) consisting of predominantly black basaltic material, as well as kenyite, in the Miers Valley area has been subsequently identified as the Ross Sea Drift by Denton and Hughes (1981). This relationship was not established by Blank *et al*, (1963), who recognized it as a Koettlitz Glaciation, as mapped by Péwé (1960). The drift differs from the established description of Ross Sea Drift "...cored with glacial ice that exhibits debris bands. Ross Sea drift is little weathered, and the drift surface is kettled and marked by bands of erratics." (Denton and Hughes, 1981). The drift in the Pyramid Trough area is characterized by a lack of basalt and consists primarily of large dolerite and granite blocks and is not ice-cored (Blank *et al*, 1963). Denton and Hughes, (1981) has dated some lava flows underlying the Ross Sea Drift using the K/Ar method and obtained dates of 226,000 +/-1100 and 236,000 +/-4,000 yr BP. This places some time constraints on the last glacial advance, although these dates are much older than dates obtained in other areas for the Ross 1 Glaciation (24,000 - 10,000 yrs BP.[Stuvier *et al*, 1981]).

Plate 2.1 View of the northeast corner of Trough Lake showing the glacial ice ridges decreasing in size with distance from the glacier. The sediment trapped behind the ridges and the broad glacial out-wash zone are visible in the foreground. The englacial material of the glacier and the glacial icebergs are evident. The outer margin of the Ross Sea Drift is also clearly visible on The Bulwark where it is marked by ice marginal fluvial sediments (photo C. Hendy).

CHAPTER TWO

FIELD OBSERVATIONS AND DESCRIPTION OF TROUGH LAKE AND PYRAMID TROUGH

2.1 THE KOETTLITZ GLACIER

The Koettlitz Glacier, where it contacts Trough Lake, is about 50 m higher than the lake surface, and consequentially forms the northern margin of the lake and controls the lake level. In the northeast corner of the lake, debris bands of englacial material occur where the glacier flows around The Bulwark. These bands occur as discrete layers within the glacier of basaltic gravels and sands (Plate 2.1). In addition, similar material occurs trapped between ridges on the surface of the glacier itself. The ridges characteristically have a vertical face exposed to the north, with a gentle slope to the south, allowing aeolian and fluvially transported basalt sands to be trapped in the lee of these ridges (Plate 2.2).

These features have been attributed to the combined effects of the sun's position relative to the glacier and the strong southerly katabatic winds in the area (Lyon, 1979). Lyon speculated that the sun produced the steep northern face through its position due north of the lake and the shade provided by the valley walls. The strong southerly winds and their associated high ablation rates were assumed to produce the gentle sloping southern side. Evidence that this is not the case can be found further to the west and east where the coast is orientated north to south and these glacial features parallel the coast (eg. The Bulwark in Plate 1.1). Lake Brownworth in the Wright Valley is also a proglacial lake and the same features appear in the glacier adjacent to the lake (Hendy *pers. comm.*). However in this case the lake is orientated east to west and therefore so are the glacial features. This eliminates solar factors as the cause and attention must be turned to structural mechanisms.

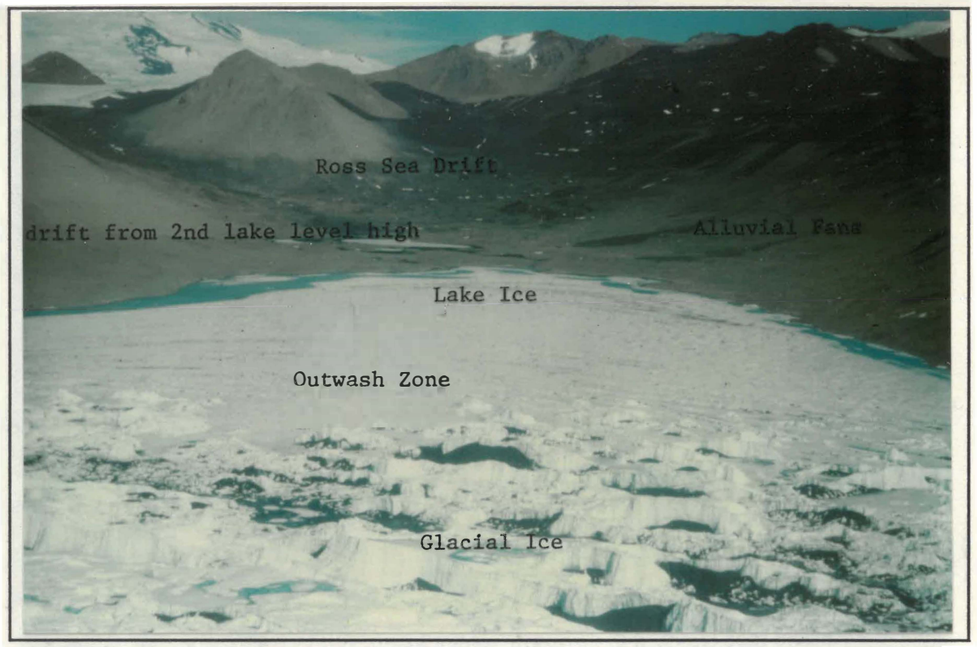

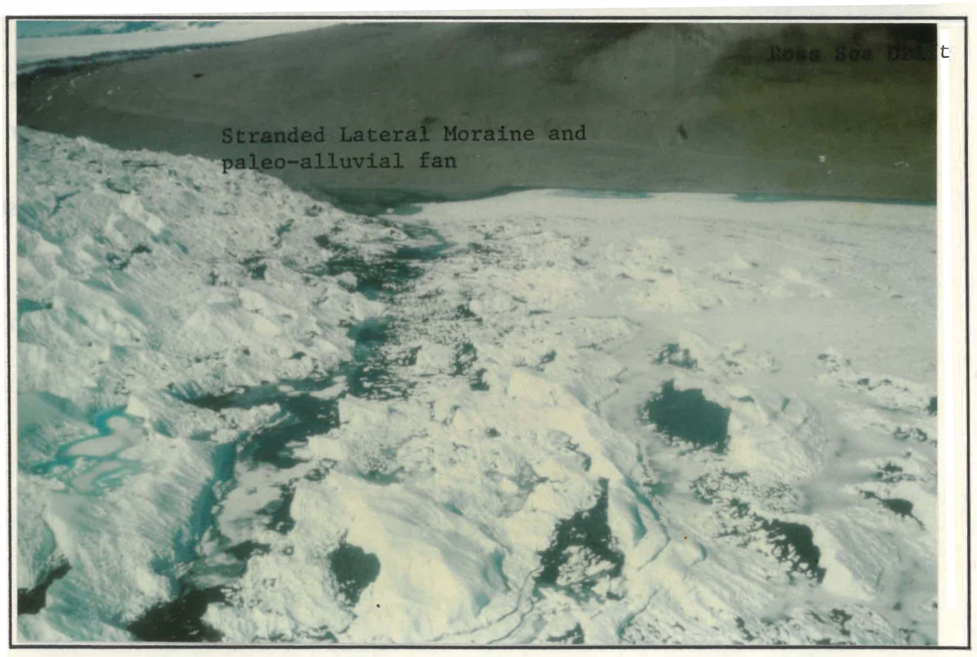

Plate 2.2 View south from the Koettlitz Glacier up Pyramid Trough showing the steep north facing ridges of glacial ice in the foreground with basaltic sands trapped at their base. The blue ice surrounding the lake is the result of compressional forces producing swales into which melt water has flowed and refrozen. The alluvial fans of basaltic sands on the western side of the valley clearly show three previous higher lake levels. The lower fan of the nearest pair corresponds with the paleo-alluvial fan and stranded lateral moraine on the eastern valley wall which rings The Bulwark (Plate 2.3). The higher fan of the nearest pair corresponds with the lower fan of the more distant pair of fans as well as the debris line on the eastern side of the valley indicating a second lake level. The highest fan appears to truncate the black basaltic drift around The Almond indicating a third previous lake level high. Finally the basaltic drift (Ross Sea Drift) suggests a fourth lake level high on The Almond.The ice covered ponds can be seen beyond Trough Lake from which they are separated by a terminal moraine. Beyond these are the alluvial fans of the stream draining the eastern arm of the valley which are separated from the ponds by another terminal moraine. The glacial ice ridges on the lake surface are in the centre foreground with the glacial outwash zone separating them into two groups to the left and right. At the other end of the lake the ice-cored domes of silicic material can be seen. The radiating nature of these surface features indicates movement of the lake ice and entrained sediment away from the glacier (Photo. C. Hendy).

Plate 2.3 View west from the Dromedary Platform of the lake ice/glacier ice contact showing melt water flowing from the glacier face and the associated basaltic sands deposited. The characteristic vertical northern face and sloping southern face of the icebergs is apparent to the south. The outer margin of the Ross Sea Drift can be seen rounding The Bulwark and merging into a terrace and paleo-alluvial fan which can be seen in the background attesting to the first of the previous high lake levels (Plate 2.2). The modern counterpart of this paleo-alluvial fan can be seen immediately below at the lake glacier contact..

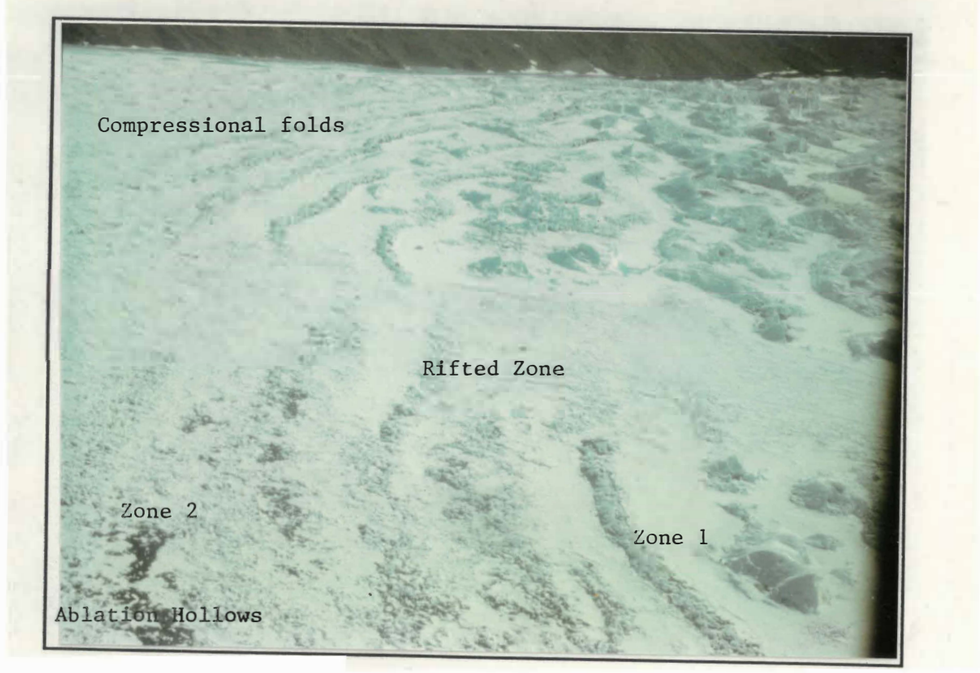

Plate 2.4 View north from the surface of Trough Lake toward the Koettlitz Glacier showing the lake/glacier contact zone and the basaltic sands deposited. The englacial material is also clearly visible as bands of basaltic sand in the glacier itself. A ridge formed by an iceberg can be seen in the foreground.

Plate 2.5 View west across Trough Lake, showing the transition from lake surface zone 1 (glacial ice ridges) to zone 2 (surficial sediments). These surficial sediments trapped in ablation hollows are visible in the bottom left hand corner. To the upper right can be seen a zone of iceberg ridges parallel to the glacier front. To the upper left are the somewhat more subdued compressional folds of the lake ice. Across the centre of the photograph is a zone of rifting of the lake ice dividing the fast moving thick ice to the west, from the slower thinner ice to the east. Glacial melt water appears to flow along this rift zone and can be seen ponded in the centre of the photo (photo C. Hendy).

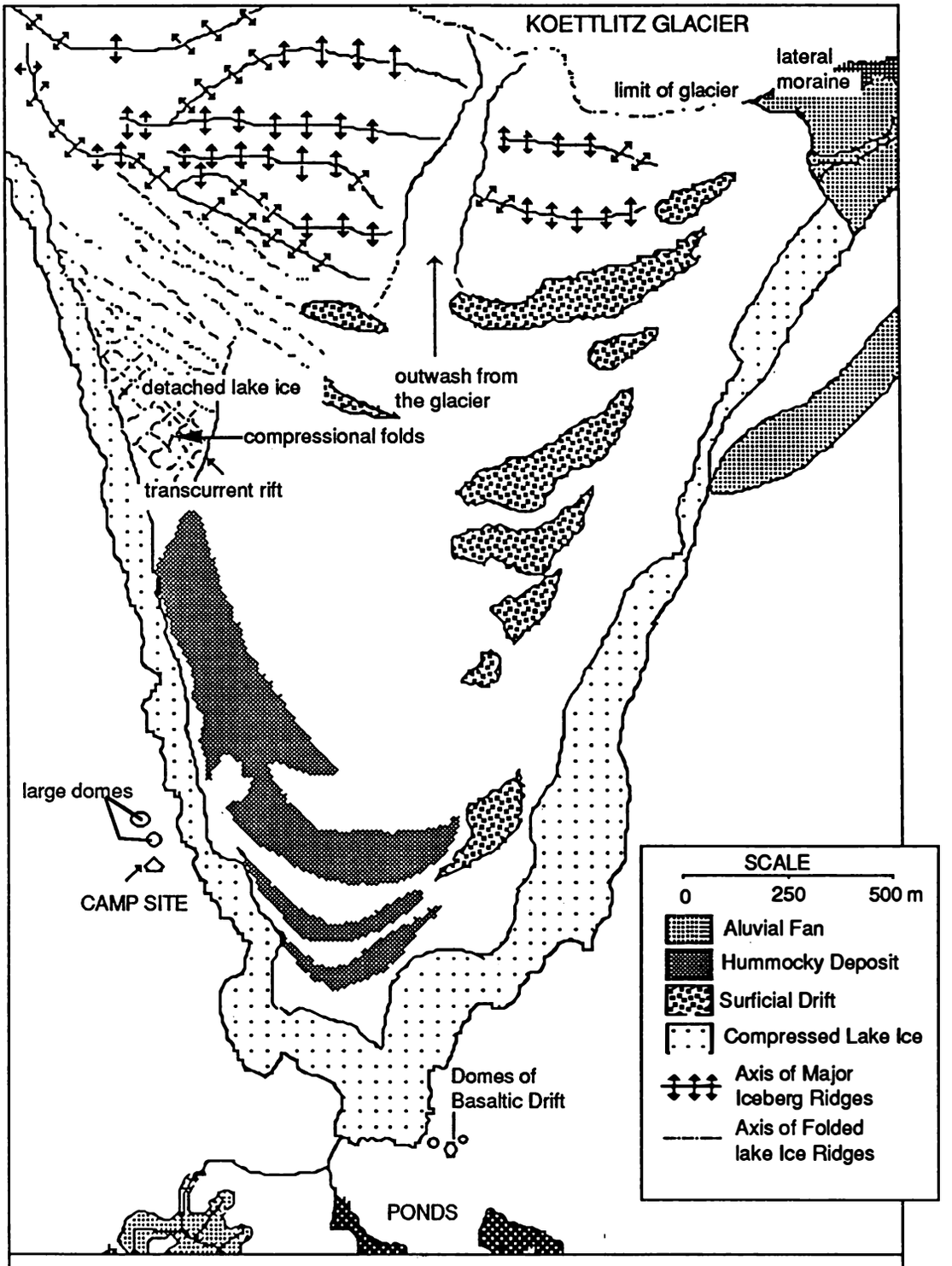

Figure 2.1 Surface features of the lake ice on Trough Lake, Antarctica.

As most Antarctic glaciers are frozen to their base and do not scour the basement there is a flow rate differential between the stationary base of the glacier and the relatively fast moving centre of the glacier. This is achieved by plastic flow within the glacier. Closer to the surface the pressure of the overlying ice is insufficient to produce plastic flow and the top 20 m of ice flows non-plastically. This implies that over a smooth surface the glacier flows plastically with a crust of non-ductile ice on the surface.

The situation changes when the glacier flows into a basin, such as Walcott Bay, and the surface cannot take up the resulting increase in flow rates by plastic deformation. This results in large cracks in the surface crust at 90° to the flow direction to accommodate the flow differential.These cracks allow the extension of the non-ductile zone deeper into the glacier extending the cracks until an iceberg is eventually calved from the snout of the glacier.

At the contact between glacial and lake ice there is a zone of debris consisting of both en-glacial and supraglacial sediments that are being actively deposited on to the lake ice surface (Plate 2.3). This glacial lake ice interface is characterized by large volumes of basaltic sands and surface melt waters flowing to both the east and west (Plate 2.3 and 2.4). Channels across the surface of Trough Lake indicate that these melt waters also occasionally flow southwards across the lake ice.

2.2 TROUGH LAKE

The surface of Trough Lake is ice-covered, however this ice cover is not smooth and uniform. A series of curved lineaments on the lake ice surface radiating from the glacier face were observed from the air (Plate 2.6).The lineaments are similar in appearance to ripples on a pond, and suggest some sort of progressive movement, away from the glacier, the rate of which is greatest in the middle of the lake. The lineaments can be divided into three zones based on their morphology and the sediments associated with them (fig. 2.1 and 2.2).

(1) Ice Ridges

The first zone, closest to the glacier, consisted of "icebergs" of glacial ice calved from the Koettlitz Glacier, forming curved ridges (Plate 2.5). These ridges are considered to be glacial ice, as opposed to lake ice, since they have a milky appearance and contained englacial sediment. These glacial icebergs are rafted onto the lake between sheets of lake ice which separate successive ridges. In the lee of these ridges basaltic sands are trapped and form aprons that drape the north and south flanks of the ridges (Plate 2.7). The height of these ridges decreases with distance from the glacier

Plate 2.6 View northeast from the Dromedary Platform of Trough Lake and the Koettlitz Glacier showing the radiating nature of the surface features. The outer ring of sediments, in the left hand foreground, is zone 3 (hummocky deposits). The blue depressed ice is visible surrounding the lake while the white thin ice shoreward is moat ice. The hummocky nature of the valley floor is also visible in the foreground.

Plate 2.7 View east down a valley between successive glacial ice ridges at the northern end of the lake (zone 1), showing basaltic sands trapped behind the ridge protecting underlying ice from sublimation (photo C. Hendy).

Plate 2.8 Ice-cored debris domes composed of predominantly silicic material, at the southern end of Trough Lake. Note the hummocky till on land in the background suggesting much wider activity of this type in the past (Photo. C. Hendy).

suggesting that melting and/or sublimation is reducing them, until the ridges disappear altogether, leaving predominantly basaltic sands behind (Plate 2.1). The progressive reduction in size of the ridges indicates that transport of glacial ice occurs across the lake surface, with the glacial icebergs transported within a block of lake ice. The progressive rotation of entrained gas bubbles and sediments in these icebergs with distance from the glacier suggests that a systematic rotation of the icebergs is occurring toward the south. This is interpreted as the result of ablation above the lake ice occurring at a rate greater than melting below. The result is that the ridges are rising up out of the water due to their buoyancy and rotating as a result.

(2) Surficial Sediments

The next zone starts where the ridges fade out and consist of concentric lines of surface basaltic sediment within ablation hollows, with the lake surface dominated by large silicic blocks. The ablation hollows are characteristically about 40 cm in depth and are believed to represent the annual ablation from the surface of the lake (Henderson, *et al*, 1966). Henderson noted in 1963 that wind blown dust tended to accumulate on the lake surface during the year, and during the summer, by absorbing solar energy, pass downwards to form pits in the lake ice. The same process appears to be operating on Trough Lake with the glacial derived basaltic sands.

The downward movement of sediment in this manner is in direct contradiction to work conducted by Rhodes *et al*, (1987) who, when working on the formation of ablation hollows in snow in Washington State noted that "dirty" snow tended to be less susceptible to ablation and thus be preserved as ridges. This was backed up by experiments carried out involving the sprinkling of volcanic ash on snow. The relationship between ice and snow in this mechanism has not been established and therefore parallels may not necessarily be drawn. Aside from the obvious crystallographic differences between ice and snow the differences in transparency will also affect the ability of sediment to melt underlying ice and snow.

(3) Hummocky Deposits

At the extreme southern end of the lake the debris ridges form ice-cored domes characteristic of this hummocky zone (Plates 2.8 and 2.9). These ice-cored mounds have been examined previously in other areas such as Lake Miers (Bell, 1962; Bradely and Palmer,1967) and Deep Lake at Cape Barne (Hendy, *et al*, 1972). These mounds, however, are not covered by the basaltic sands characteristic of the other two zones, but the sediments tend to be coarser and more siliceous, being generally meta-sediments, similar to those surrounding the lake.

Plate 2.9 The exposed ice core of a debris dome on Trough Lake. Note that the sediments overlying the ice core are not cemented by ice and relatively easily removed.

The entire lake, with the exception of the glacier lake contact, is surrounded by moat ice. This ice is thinner (about 10 cm thick in January) than the permanent lake ice and may melt out seasonally. The distribution of this moat ice is related to bathymetry and represents the point where the water becomes shallower than the permanent lake ice. Shoreward of this only seasonal moat ice can exist as solar heat is absorbed by the underlying sediments and is transferred to the overlying ice and water.

Substantial quantities of green algae were present within the moat ice. These algae float upward on gases produced by photosynthesis and move through the ice by maintaining a bubble of liquid water around them, derived by heating from intercepted sunlight (Plate 2.10).

Compression features occur around the edge of the lake, especially at the extreme southern end, attesting to the pressure being exerted on the lake ice by the Koettlitz Glacier. These features manifest themselves as a system of non-fractured ridges and swales surrounding the lake. Melt water has flowed into the swales, filling the trough, and freezing, producing "blue" ice (Plate 2.6), which is smooth and easily identified on aerial photographs. This ice is only a surface crust of about 20 cm in thickness, underlain by water about 1 m in depth (fig. 2.2).

Compressional features also appear between the glacial ice ridges.These appear as zones of blue ice between successive ice ridges, although they are not as extensive as the lake edge features.

A triangular area of the lake ice on the western side of the lake appears to differ in morphology to the rest of the lake ice. This section exhibits a different topography to the bulk of the lake ice. Although the same east-west orientated ridges, characteristic of the ridge zone, are apparent, there is also a system of ridges running north-south. These ridges are composed of lake ice, devoid of the bubbles and englacial sediment characteristic of the icebergs, and generally are broader, exhibiting gentler slopes and often fractured longitudinally. They also appear to be compressional features.This section of ridges is bounded by a large crack in the lake ice which exhibits transcurrent motion along it. This crack and the ridges that parallel it are at an angle of about 60° to the shore. Other cracks also occur in the lake ice and these may or may not extend completely through the ice.

Plate 2.10 Algae moving up through the moat ice by floating on gas bubbles and surrounded by liquid water produced by absorbed solar heat (Photo. F. Judd.).

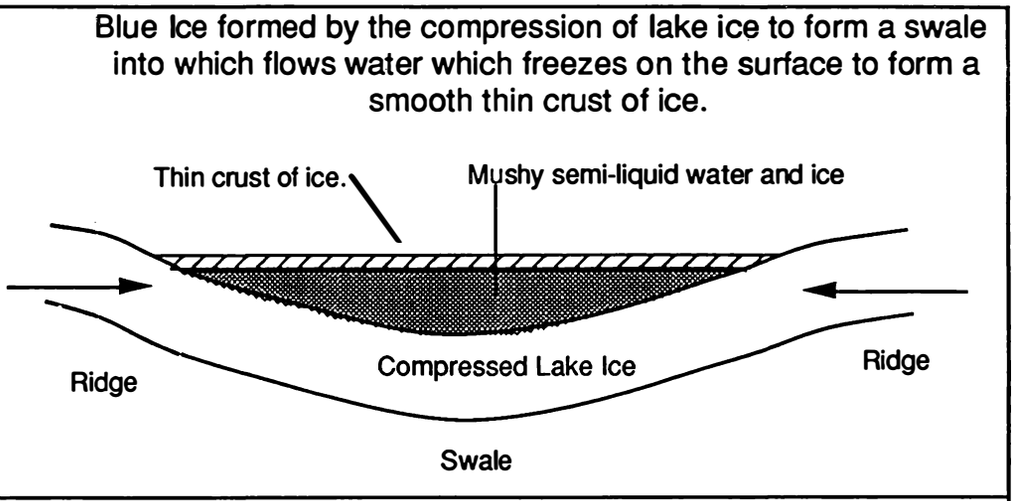

Figure 2.2 The formation of "blue ice" compressional features both surrounding the lake and between icebergs on Trough Lake.

A broad fan-shaped feature radiating from the glacier down the centre of the lake is clearly seen in aerial photographs. This is interpreted as a glacial melt water, out-wash zone where water, melting from the glacier, may flow over the surface of the lake ice (Plate 2.1). This feature bisects the ice ridges and shows some evidence of local channelised flow and is bounded on the western side by an extension of the rift that separates the triangular section of compressed lake ice from the bulk of the ice cover.

2.3 PYRAMID TROUGH

The valley floor for some distance south of the lake, is covered with a hummocky drift composed predominantly of coarse meta-sediments. This drift is similar in morphology and petrology to the debris covered domes on the lake surface at the southern end of the lake. The glacial drift covering the valley floor is considered to be the Ross Sea Drift of Denton and Hughes (1981), but is unusual in that it contains little basalt, the principle component of this drift through out the rest of the Koettlitz Glacier area, but is characterized by dolerite and granite (Blank, *et al*, 1963). While the basaltic sands found over most of the lake surface are typical of the Ross Sea Drift, the siliceous domes toward the southern end of the lake and surrounding the lake are not. There is no terrestrial evidence of the basaltic drift so common to the north with the exception of a number of basalt cones located in the valley floor, including three very prominent ones at the southern end of the lake (fig. 2.1).

Two large ridges at the southern end of the lake are interpreted as terminal moraines related to a previous advance of the Koettlitz Glacier up the valley from the north. One of these moraines forms the southern shoreline of the lake, and separates the lake from some ponds immediately to the south. These ponds are fed by a river from an impinging arm of the Koettlitz Glacier at the southern end of Pyramid Trough. The second moraine

Plate 2.11 A view from the southern shoreline of Trough Lake south towards The Almond in the background. The ridge in the immediate foreground is a terminal moraine forming the southern shoreline of the lake. The generally hummocky nature of the topography can be seen, as well as the basalt drift that dominates the western arm of the valley. The lateral moraine left by the retreating Koettlitz Glacier is apparent on the eastern margin of the valley (photo F. Judd).

separates the ponds from the alluvial fan formed by the stream flowing into them (fig. 1.3) (Plate 2.11).

A large lateral moraine runs up the eastern side of the valley (Plate 2.11) and is draped with Cenozoic basalts. This, together with the presence of basaltic cones on the valley sides, suggests that at least some of the volcanism post-dates the last advance of the Koettlitz Glacier up the valley.

An alluvial fan occupies the northeastern corner of the valley, where it supplies the lake with melt water from the margin of the Koettlitz Glacier around the edge of The Bulwark (Plate 2.12). This alluvial fan is composed primarily of basaltic sands and gravels derived from the englacial material supplied from the Koettlitz Glacier. Above this fan, on The Bulwark, is a paleo-alluvial fan attesting to a higher lake level and an advanced Koettlitz Glacier in the past. On the western side of the valley, a number of streams drain the Dromedary Platform and flow down into Pyramid Trough, where alluvial fans have formed (Plate 2.13). These streams appear to reach the ponds, and hence Trough Lake, only infrequently, as the alluvial fans were incrusted with evaporite deposits (Plate 2.14). Four previous high lake levels can be identified using these fans, the deposits on the Bulwark and the Ross Sea Drift at the southern end of the valley (Plate 2.2). These fans had been previously mapped as volcanic features (Blank *et al*, 1963).

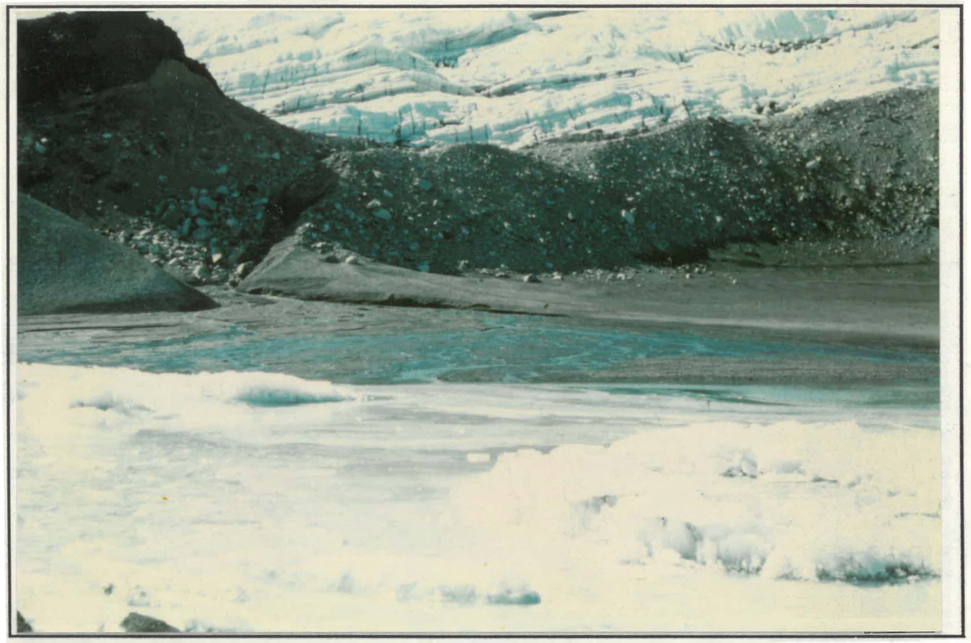

Plate 2.12 The alluvial fan formed by the stream that flows marginal to the Koettlitz Glacier at the northeastern corner of the lake. This is the modern counterpart of the feature immediately above it (Plate 2.3) on The Bulwark. The large moraine is the present lateral moraine of the glacier (background). The predominantly basaltic englacial material is clearly visible within the glacier.

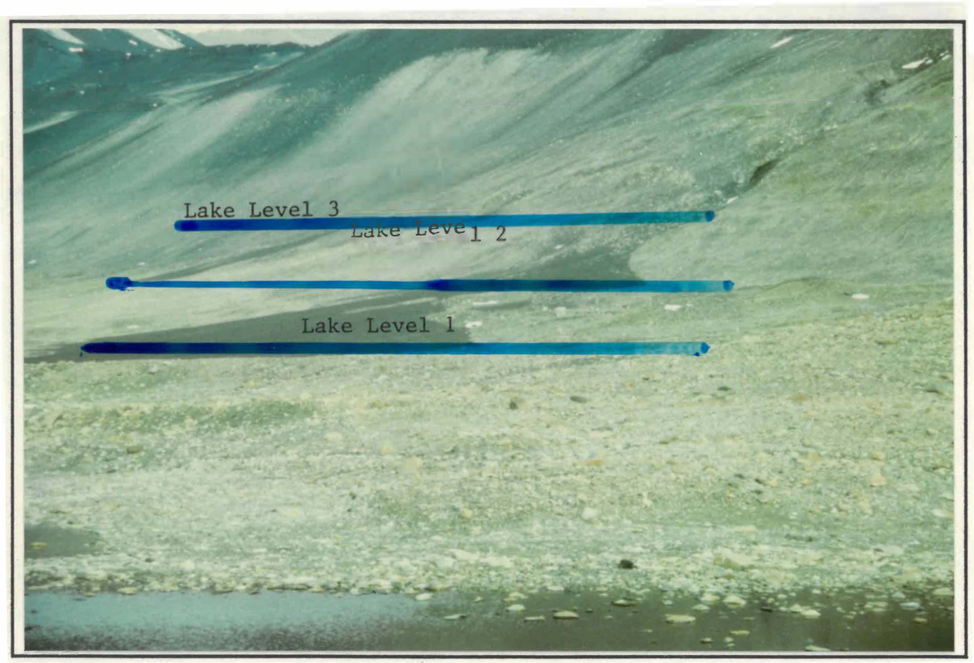

Plate 2.13 Successive alluvial fans developed by streams draining the Dromedary Glacier on the Dromedary Platform. The two levels represent past lake levels when the streams reached the lake. The top-most fan seen is associated with a lineament running above the top of the alluvial fan in the foreground. In addition many smaller lineaments can be seen between the major breaks. At present the alluvial fans are encrusted in evaporative salts (Plate 2.14) suggesting that these streams seldom reach the lake or the ponds to the south.

Plate 2.14 The evaporite salts that encrust the alluvial fans on the western margin of Pyramid Trough.

CHAPTER THREE

FIELD WORK, METHODS, AND SAMPLING PROCEDURES

3.1 FIELD WORK

Aerial photography of Pyramid Trough showed the presence of substantial quantities of surficial sediments on the ice cover of Trough Lake. The pattern of the sediments distribution suggested that they were derived from the Koettlitz Glacier were moving southwards away from the glacier front. It was apparent when this study was undertaken that the sediment cover coarsened progressively with distance from the ice front, and that not only was the lake ice transporting glacial sediments as suggested by Clayton-Greene *et al.* (1987), but with the loss of fine grain-sized sediments, sorting processes were occurring as well. Consequently the following work was undertaken:

(1) The bathymetry of the lake was established, to determine the broad shape, and dimensions of the lake. These characteristics are important with respect to water circulation, and hence the temperature profile, as well as the sedimentary processes occurring within the lake.

(2) The lake ice thickness and its variability was determined. This affects the sediments ability to migrate through the ice and into the water column below. Lake ice thickness is also believed to be closely related to the temperature profile of the lake.

(3) Light intensity below the ice cover and its variation through the water column was measured. This determines the light penetration into the waters, and therefore the possible heating of the lake, as well as determining the amount of suspended material in the lake water.

(4) Temperature profiling of the water column was conducted to determine possible circulation patterns as well as heating mechanisms within the lake. Heat flux is assumed to be important in determining the lake ice thickness, as is circulation of the lake water. The variation of temperature through the water column is also

important in determining the degree of circulation occurring, as well as the source of heat within the lake, and the degree to which it is extracted through the lake bed, the lake ice or the glacier.

(5) Water sampling down the water column was conducted to determine if chemical, and hence density, stratification exists within the lake. The possibility of density stratification within the lake, is likely to affect sediments falling through the water column. In addition, density stratification can influence the temperature profiles, as heat may be trapped in a dense slowly mixing brine as in Lake Vanda (House *et al.*, 1966).

(6) Surface sediment sampling was carried out to obtain samples for grain size analysis. This was to establish if any systematic variation in grain size characteristics over the lake surface existed, and also to establish the source and possible transport mechanisms of these sediments.

(7) Coring of lake bed sediment was also undertaken to determine if any spatial variation of lacustrine sediments existed within the lake, and their possible sources. In particular, the cores were examined for evidence of surficial sediments within the lacustrine sediments, to determine if sediment has melted through the overlying lake ice. Any stratigraphy apparent in cores extracted would also aid in determining the glacial history of the valley.

In addition to the work conducted on the lake bed and surface, a survey of the surrounding area was carried out to determine the general morphology and petrology of the moraines and tills present, as well as examining possible fluvial input into the lake. Evidence for past variation in lake levels was also sought to aid in establishing the glacial history of the valley.

Having conducted this work a model for sedimentation and the processes occurring within the lake was derived that could be applied to present and previous proglacial lakes in the McMurdo region.

3.2 FIELD METHODS

The field work was conducted during the month of January 1987. It was necessary to drill holes through the lake ice to facilitate bottom sampling and water temperature profiling. The holes were drilled with a 200 mm post-hole borer and auger extensions totaling 4.5 m in length. This method was successful for most of the holes drilled, although problems were experienced in drilling two holes (#10 and #11) where the ice

was exceptionally thick, and the auger extensions were insufficient to drill completely through the lake ice. Therefore the post hole borer was used to drill to the maximum depth it could reach, and a hand operated 100 mm S.I.P.R.E. ice corer with additional extensions was used to complete the holes.

Once the holes had been drilled and marked with flags for later surveying, the depth of the lake and ice thickness were measured. Temperature and light intensity profiling of the water column for selected sites was also carried out. Depth was measured with a polypropylene cord and a lead weight, a method found quite suitable due to the absence of excessive water movement under the ice. Ice thickness was measured from the hydrostatic water level (fig. 3.1) to the base of the lake ice. This was accomplished with a flat weight on a polypropylene cord that could be lodged under the base of the lake ice.

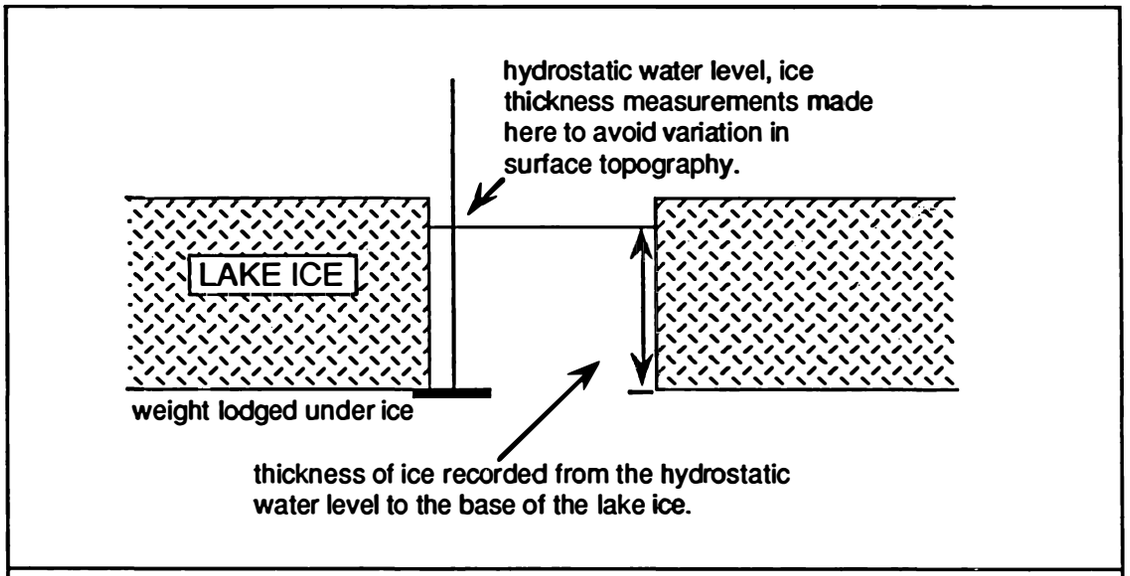

Figure 3.1 The method of recording lake ice thickness.

Temperature was measured using a copper-constantan thermocouple and a Hewlett Packard potentiometer, with power supplied by a petrol powered portable generator. Light intensity was measured using a photo-electric cell to such depth as was measurable, within the accuracy of the apparatus, (12-15 m).

In addition to the measurements made in the field, sediment samples were collected from various sites on the lake ice surface for later laboratory analysis. Sediment cores and bottom samples were also extracted from the lake bed at some sites. Water samples from selected holes were retrieved with the use of a bilge pump, and a graduated length of polyethelene tubing to determine the depth at which sampling was being carried out.

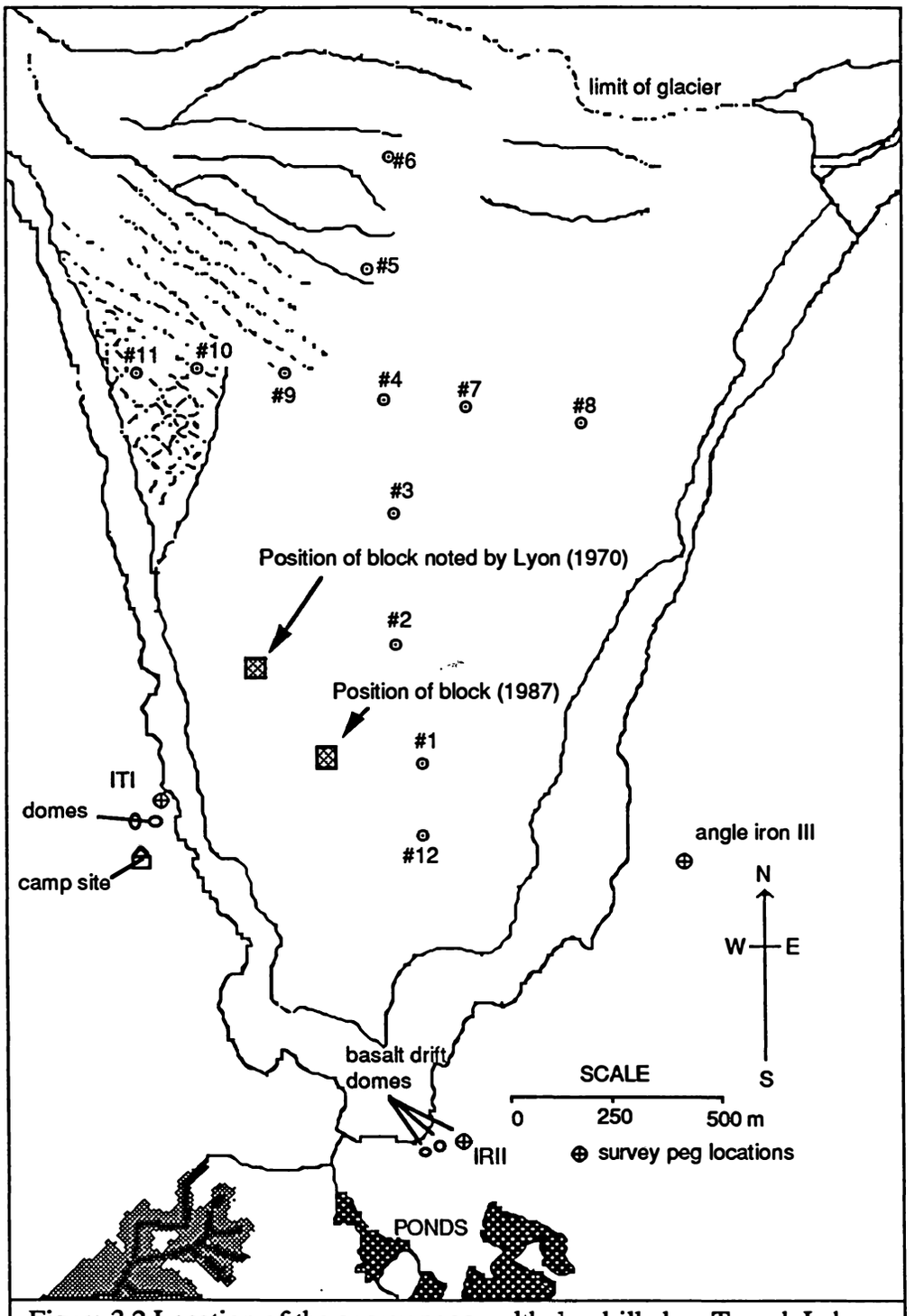

Figure 3.2 Location of the survey pegs and holes drilled on Trough Lake.

A survey was carried out to accurately locate the various holes drilled in the lake ice and their relative positions to three permanent markers driven into the ground surrounding the lake.

3.2.1 Hole Locations

The holes were bored along a north-south transect down the centre of the lake, and an east-west transect about two thirds of the way up the lake from the southern end (fig. 3.2). Problems were experienced with holes #10 and #11 due to the additional thickness of the ice at these points. The ice thickness was such that the auger froze into hole #11, rendering it impossible to be extracted. Consequently this hole was never completed: the location of this auger was surveyed and mapped so it may be useful in determining transport rates of the lake ice in the future.

Holes #1 to #4 form the bulk of the longitudinal transect, and are located in a zone of surficial drift. This drift of basaltic sand lies in ablation hollows that have formed as the drift, heated by the sun, melts the underlying ice. Holes #5 and #6 are in the zone of ice ridges being rafted within the lake ice. Both holes were drilled in lake ice which forms a flat floored "valley" between adjacent ridges. The last hole of this transect (hole #12) was drilled at the extreme southern end of the lake in the zone of hummocky deposits. This hole was drilled close to some large ice-cored domes of predominantly siliceous till.

The lateral transect starting with hole #8 in the extreme east and including holes #7, #4 and #9 are in the surface drift zone. The remaining two holes #10 and 11 were drilled in the wedge of thicker ice in the west.

It was noted while drilling the holes in the lake ice that lenses of basaltic sands were encountered in discrete layers at various depths, and that a number of such lenses may occur at various depths through the lake ice.

3.2.1.1 Survey of the Holes Drilled in the Lake Ice

The survey was conducted by Mr B. D. Anderson of the New Zealand Department of Lands and Survey, the Antarctic Surveyor for the 1986/87 season. No survey control exists in the area at present and due to the scale of the survey conducted one was not justified. Consequently three arbitrary points were selected to triangulate position with and a solar azimuth observed to provide orientation.

Plate 3.1 View north from the camp site of the large silicic drift domes on the shore of the lake the top of the right hand side one being the location of the reference point ITI used for the survey.

The three points used for the survey were:

(1) 0.1 m above the highest point on a prominent knoll at the lake edge immediately north of two large dome shaped mounds of silicic drift 100 m north of the camp site (Plate 3.1). The position of this reference point was fixed at 78° 16' 53" S, 163° 26' 01' E (scaled latitude and longitude) and this point (ITI) is used to locate the holes and the other reference points in metres north and east of here.

(2) Position IRII is 0.2 m above the highest point of the eastern most basaltic drift dome to the immediate south of the south-eastern corner of the lake. Its bearing is 153° 32' 0" from ITI at a distance of 1055.36 m.

(3) Position angle iron III is up 0.2 m in a cairn at the base of a slight gully about 10 m above the lake level on the eastern shore at a distance of 1168.45 m and a bearing of 117° 34' 40" from ITI.The positions of the holes in the lake ice, and the reference points with respect to ITI are recorded in Table 3.1 below.

POINT	DISTANCE NORTH OF ITI (m)	DISTANCE EAST OF ITI (m)
Hole 1	-96.74	589.32
Hole 2	159.09	651.50
Hole 3	430.65	721.54
Hole 4	717.25	787.83
Hole 5	999.48	865.78
Hole 6	1225.77	1007.61
Hole 7	601.05	969.87
Hole 8	487.80	1184.80
Hole 9	822.61	600.53
Hole 10	926.34	420.79
Hole 11	971.31	307.18
Hole 12	-316.90	530.61
ITI	0.00	0.00
IRII	-944.75	470.35
Angle Iron III	-540.96	1035.69

Table 3.1 Position of holes and reference points with respect to ITI, expressed in metres north and east.

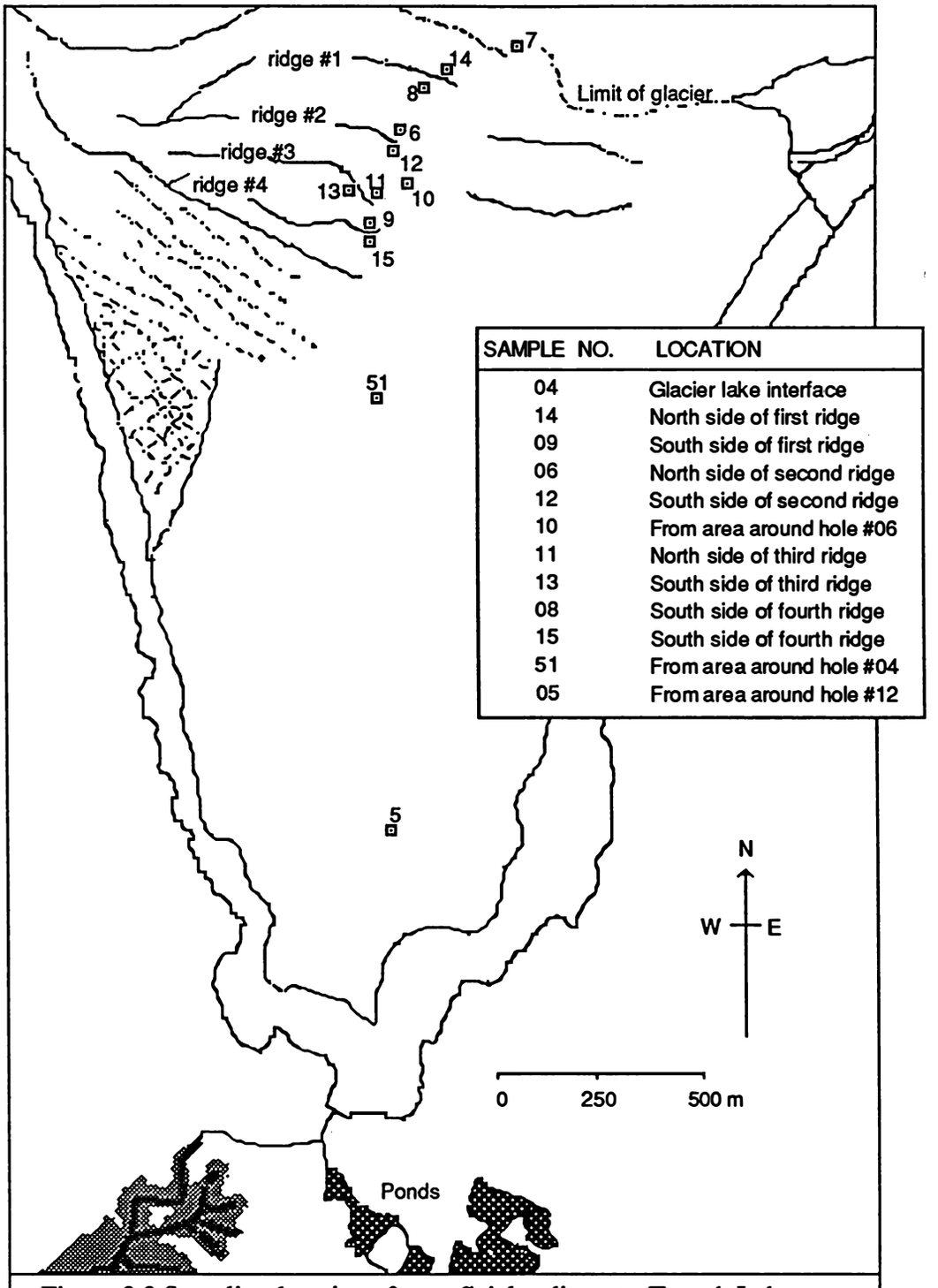

Figure 3.3 Sampling locations for surficial sediments, Trough Lake.

The distances and bearings of the various holes starting at hole #12 are recorded in Table 3.2 below:

POINT	BEARING WITH RESPECT TO PREVIOUS HOLE (° ' ")	DISTANCE WITH RESPECT TO PREVIOUS HOLE (m)
Hole 12		
Hole 1	14 56 00	227.85
Hole 2	13 39 40	263.28
Hole 3	14 27 40	280.45
Hole 4	13 01 20	294.16
Hole 5	15 26 20	292.80
Hole 6	32 04 40	267.06
Hole 4		
Hole 7	122 33 00	215.97
Hole 8	117 47 10	242.94
Hole 4		
Hole 9	299 21 40	214.90
Hole 10	299 59 20	207.52
Hole 11	291 36 00	122.19

Table 3.2 Calculated distances and bearings between the various holes drilled in the lake ice.

3.2.2 Sediment Sampling

3.2.2.1 Surface Sediments

Samples of sediment were collected from the glacier-lake interface, and then in a longitudinal transect down the lake toward the south where the more distal surface sediments occur as ice-cored domes of predominantly siliceous gravels and sands. Samples were collected from the glacier face, and the area adjacent to holes #06, #04 and #12 (fig. 3.3). The sediments collected from the area adjacent to holes #06 and #04 were in ablation hollows. The sample from around hole #12 was collected from one of the ice-cored domes in the region.

3.2.2.2 Sediment Cores

Coring of the lake bed was carried out using a modified piston corer. Restrictions on the length of the various components resulted due to transport requirements to and from Antarctica. The coring equipment consisted of a tripod, about 1 m in height, with a large pulley used to remove the core from the lake bed. The corer consisted of a length of plastic drainage pipe into which a piston could be inserted (fig. 3.4). The piston was attached to a stainless steel braided cable, which ran back to the surface over the pulley on the tripod. The bottom metre of this cable, immediately above the core barrel, was enclosed in a steel tube to act as a guide for the hammer which would drive the corer into the lake sediments. This hammer was connected to a cord which ran back to the surface

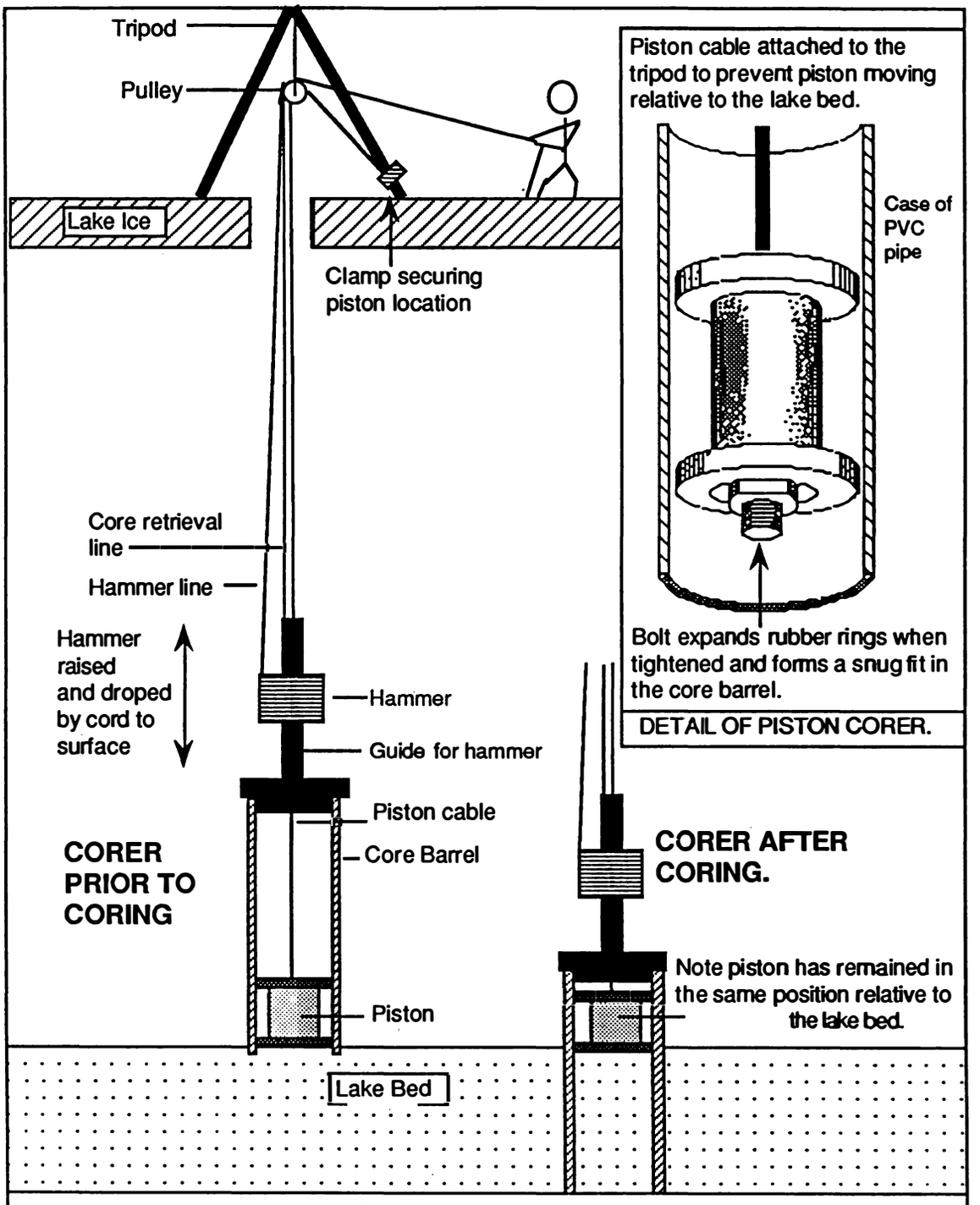

Figure 3.4 Operation of the piston corer used at Trough Lake.

via the pulley on the tripod. Finally the core barrel was connected to a second cable which ran back to the surface as well, and over the pulley. This second cable was used to retrieve the core barrel from the lake bed.

Cores were obtained as follows: the piston attached to the cable carrying the guide and hammer was placed in the core barrel and adjusted to fit snugly; the piston was then forced down to the bottom of the core barrel which was attached to the retrieval cable; the corer was lowered to the bottom of the lake; once the bottom was reached the piston cable could be tightened and clamped to the tripod to ensure that the corer was vertical, before driving the corer into the bottom of the lake; the hammer was then raised and lowered by the line attached to it and thus drove the corer into the sediments.

Retrieval was finally achieved by pulling on both the retrieval cable and the piston cable, so the core would not be sucked out of the core barrel.

Problems were experienced with the hammer, which, due to the size restrictions placed on the guide, effectively reduced the stroke and velocity with which the core case could be struck. This, together with the friction of the water column on the hammer and cable, due to the depth of the lake, reduced the effectiveness of the piston corer, making coring a very difficult procedure.

Coring of the lake bed was attempted through five of the holes drilled in the lake ice (#1, #2, #3, #4 and #12). However due to the extreme depth of Trough Lake and the hardness of the lake sediments complete cores were only retrieved from holes #4 and #12. Sediment samples were, however, obtained from the remaining holes (#1, #2 and #3).

CHAPTER FOUR

RESULTS

4.1 TEMPERATURE PROFILES

The temperature of the water column below holes #1, #6 and #10 was recorded in millivolts at 3 m intervals and subsequently converted to degrees centigrade (Table 4.1).

THERMOCOUPLE READINGS FROM TROUGH LAKE (8/01/87)

Thermocouple = copper/ constantan
-10°C = -0.38 mV
0°C = 0 mV
10°C = 0.38 mV
correlation formulae: T = 25.9679 mV - 0.2597
R =1 (for -20 ≤ T≤ 20°C)

DEPTH	HOLE NUMBER					
	#1		#6		#10	
(m)	(mV)	(°C)	(mV)	(°C)	(mV)	(°C)
0	0.016	0.26				
1			0.006	0.16	0.010	0.26
3	-0.006	-0.15	-0.002	-0.05		
6	0.008	0.20	-0.005	-0.13	-0.005	-0.13
9	0.017	0.44	-0.006	-0.16	0.004	0.10
12	0.017	0.44	-0.004	-0.11	0.009	0.23
15	0.022	0.56	-0.004	-0.11	0.015	0.38
18	0.015	0.38	-0.004	-0.11	0.018	0.46
21	0.015	0.38	-0.003	-0.13	0.017	0.44
24	0.015	0.38	-0.001	-0.03	0.016	0.41
30	0.013	0.33	-0.004	-0.11	0.022	0.56
33	0.012	0.30	-0.006	-0.16	0.021	0.54
36	0.012	0.30	-0.008	-0.21	0.021	0.54
39	0.012	0.30	-0.008	-0.21	0.021	0.54
42	0.009	0.23	-0.009	-0.24	0.019	0.49
45	0.015	0.38	-0.008	-0.21	0.019	0.49
48			-0.008	-0.21	0.019	0.49
51			-0.008	-0.21	0.009	0.23*
54			-0.008	-0.21	0.008	0.21*
57			-0.008	-0.21	0.016	0.41
60			-0.008	-0.21	0.016	0.41
63			-0.008	-0.21	0.018	0.46
66			-0.007	-0.18	0.018	0.46
69			-0.008	-0.21	0.019	0.49
72			-0.008	-0.21	0.018	0.46
75			-0.008	-0.21		
78			-0.007	-0.18		
81			-0.006	-0.16		
84			-0.005	-0.13	* Junction problems	
87			-0.004	-0.11	experienced	
90			-0.004	-0.11		

Table 4.1 Thermocouple and corresponding temperatures recorded at Trough Lake.

From time to time problems were experienced with the cold junction on the thermocouple and this gave spurious results where indicated (Table 4.1). It was also noted that while measuring the temperature profile for hole #1 that there was a comparatively large change in temperature between 12 and 18 m in depth. Consequently measurements were made over 1 m intervals to validate the temperatures recorded in Table 4.1 (Table 4.2).

DEPTH (m)	READING (mV)	TEMPERATURE (°C)
12	0.017	0.48
13	0.017	0.44
14	0.019	0.49
15	0.019	0.49
16	0.018	0.46
17	0.017	0.44
18	0.015	0.38

Table 4.2 Temperature results from hole #1 between 12 and 18 m depth.

4.2 BATHYMETRY AND LAKE ICE THICKNESS RESULTS

For both bathymetry and lake ice thickness, measurements were made from the hydrostatic water level (fig. 3.1). This is done to remove variation in ice thickness over the lake and provides a datum from which to measures variations in these two parameters. This is particularly important for the measurement of ice thickness as surface topography of the lake ice may vary considerably and consequently produce a scattering of results not indicating the relatively homogeneous nature of the ice thickness. The measurements recorded for bathymetry and ice thickness for all holes completed are recorded in Table 4.3 below:

Hole No	Depth (m)	Ice Below Water Level (m)	Ice Above Water Level (m)
1	39.05	3.84	0.45
2	52.15	3.93	0.35
3	54.29	3.99	0.31
4	76.23	3.05	0
5	78.91	3.37	0.37
6	93.20	3.90	0.32
7	71.25	3.30	0
8	53.18	3.32	0.33
9	81.84	3.87	0.41
10	72.32	6.11	0.33
12	36.61	3.75	0.70

Table 4.3 Bathymetry and ice thickness measurements for Trough Lake.

4.3 LIGHT PENETRATION

The readings for light penetration through the lake ice are recorded in Table 4.4. These readings were made on a partly cloudy day which led to fluctuating lighting conditions. As a result the initial reference reading for the three sites examined tends to vary depending on the overhead conditions. Despite this, light readings were accurate, confirmation being achieved by checking the initial reading after completing the profile.

The readings on their own are not comparable and therefore they were expressed as a percentage of the initial reading for each hole to overcome the problem of different overhead conditions at the various sites.

	HOLE No.					
DEPTH	#1		#6		#10	
(m)	(mV)	(%)	(mV)	(%)	(mV)	(%)
0	630	100.0	474	100.0	970	100.0
3	40	6.3	21	4.4	162	16.7
6	9	1.4	6	1.3	50	5.2
9	19	3.0	3	0.6	27	2.8
12	9	1.4	1	0.2	7	0.7
15					2	0.2

Table 4.4 Light penetration readings through the water column, both absolute and as a percentage of the initial surface reading

4.4 WATER SAMPLING

The aim of the water sampling program was to determine if there is any variation in water chemistry with depth as in some Antarctic lakes (eg. L. Bonney and L. Vanda) that may indicate chemical or thermal stratification, as well as the degree of mixing within the lake. Samples of water were retrieved from the lake through holes #1, #6 and #10 at 12 m intervals, and labeled with reference numbers for future chemical analysis. The program was largely successful with the exception of hole #6, which was closest to the glacier. If the temperature profile results for this hole are examined (Table 4.1) it will be noted that at depth the water temperature is actually below 0°C; the freezing point being depressed by the weight, and hence pressure, of the water above the point being measured. This combined with the very cold day on which sampling was conducted (it was snowing in Pyramid Trough), meant that the water was freezing in the tube while being pumped to the surface. Consequently a full set of samples were never obtained from the water column at hole #6.

The samples collected, their associated identification numbers, depth, and location are recorded in Table 4.5.

Depth of Sample (m)	Hole #1 Sample No.	Hole #6 Sample No.	Hole #10 Sample No.
0	TS/87/20	TS/87/30	
12	TS/87/21	TS/87/31	
24	TS/87/22	TS/87/32	TS/87/40
36	TS/87/23	Sample Froze	TS/87/41
40	TS/87/24*		
48			TS/87/42
60			TS/87/43
72	*bottom water sample.		TS/87/44*

Table 4.5 Water sample locations, depth of sampling and identification numbers

In addition to the samples collected through the water column water samples were collected from the stream flowing into Trough Lake from the south (Pyramid Trough) (stream), the brine from the evaporite deposits on the western margin of Pyramid Trough (brine), the core water from core from hole #3 (TS/87/50) and from Lake Porkchop a small non-contact glacial lake below The Amphitheatre in Roaring Valley some 8 km west of Trough Lake (lake).

SAMPLE No.	pH (ppm)	K^+ (ppm)	Na^+ (ppm)	Ca^{2+} (ppm)	Mg^{2+} (ppm)	Cl^- (ppm)	HCO_3^- (ppm)	SO_4^{2-} (ppm)
20	7.82	1.71	11.6	5.28	1.10	30.8	35	6.14
21	7.90	1.62	12.0	5.05	1.14	30.8	23	6.37
22	7.93	1.64	11.8	5.40	1.14	29.1	37	6.84
23	7.81	1.63	11.9	5.51	1.12	27.4	37	6.60
24	8.55	4.84	19.2	11.60	2.70	27.4	87	6.84
30	7.30	0.65	3.2	2.07	0.38	14.0	11	4.75
31	7.88	1.66	11.6	5.51	1.18	30.8	37	5.44
32	7.89	1.62	11.9	5.63	1.19	30.8	23	9.62
40	7.93	1.80	12.3	5.97	1.12	30.8	36	6.37
41	7.85	1.66	11.9	5.51	1.14	34.2	36	4.05
42	7.84	1.63	11.9	5.63	1.18	30.1	35	3.36
43	7.73	1.88	11.6	5.17	1.08	30.1	36	3.59
44	8.55	3.10	13.2	5.63	1.64	35.9	53	8.69
50	8.38	3.12	11.4	4.36	1.61	23.9	49	9.62
stream	7.97	1.97	8.7	9.99	1.11	25.7	40	13.01
lake	7.57	2.47	10.3	7.58	1.71	46.2	35	4.98
brine	7.83	375	1818	429	281	20.5	162	2057

Table 4.6 Water analysis results of the samples collected from Trough Lake and the surrounding area.

The water samples were subsequently analysed in the laboratory for the concentrations of cations and anions. The pH was measured prior to filtering the water for analysis. Sodium and potassium were analysed by flame photometry, calcium and magnesium by atomic absorption spectroscopy, chloride by chloride electrode, bicarbonate by "gran" plot, and sulphate by the turbidimetric method. The results are recorded in Table 4.6.

4.5 ANALYSIS OF SURFICIAL SEDIMENTS

The sediment samples collected from the surface of Trough Lake were dried, and sub-samples of at least 400 g were sieved at 0.25 Ø intervals. The cumulative sieve weights were entered into the university's computer for textural analysis. The textural parameters derived by the Folk and Ward (1956) graphical method are summarized in Table 4.7 below:

Sample I.D.	Sampling Site Location	GRAPHICAL METHOD (FOLK & WARD 1956) M_z	M_d	Mode	C	D_{35}	D_{65}	S.D.	S_k	K_G
07	glacier	-0.45	-0.46	-0.25	-2.74	-0.81	-0.05	0.98	-0.04	0.94
14	nth/1	+0.21	+0.30	+0.50	-1.84	-0.02	+0.55	0.77	-0.17	1.01
08	sth/1	-0.57	-0.56	-0.50	-4.71	-0.92	-0.17	1.36	-0.22	1.69
06	nth/2	+0.16	+0.22	+0.50	-4.14	-0.14	+0.52	0.84	-0.12	1.00
12	sth/2	-0.78	-0.83	-0.50	-4.71	-1.15	-0.51	1.27	-0.15	1.89
10	hole#06	-2.99	-2.73	-2.00	-5.41	-3.40	-2.21	1.38	-0.18	0.84
11	nth/3	-0.41	-0.47	-0.50	-2.10	-0.73	-0.12	0.78	+0.11	0.97
13	sth/3	-1.03	-1.08	-1.00	-3.69	-1.36	-0.79	0.86	+0.10	1.28
09	nth/4	-0.12	-0.19	-0.50	-2.01	-0.60	+0.29	1.00	+0.11	0.86
15	sth/4	-1.36	-1.40	-1.50	-4.65	-1.62	-1.16	0.72	+0.07	1.31
51	hole#04	-1.01	-1.28	-1.50	-3.17	-1.54	-0.92	1.05	+0.42	1.27
05	hole#12	-3.80	-3.97	-4.50	-5.45	-4.40	-3.55	1.22	+0.30	1.12

nth/1 = northern side of ridge number 1 Sth/1 = southern side of ridge number 1

Table 4.7 Summary of textural parameters for surficial sediments derived by the Folk and Ward (1956) graphical method.

4.6 ANALYSIS OF CORES

Core samples were obtained from five of the holes in the lake (#1, #2, #3, #4 and #12), of which only the cores from holes #4 and #12 were complete. Sediment samples from holes #1, #2 and #3 were retrieved, but not as complete cores. Core #3 was unusual in that it consisted entirely of basaltic sand, similar in appearance to that on the surface of the lake.

4.6.1 Core Descriptions

4.6.1.1 Core #12

The core was obtained from the extreme northern end of the lake, in the vicinity of the inlet stream, at a depth of some 37 m. Three distinct zones were distinguished in the core (Fig. 4.1 and Plate 4.1). The uppermost was 12 cm thick, and consisted of lacustrine silt grading into sand with depth. The sand size ranged from granule through to very fine sand.

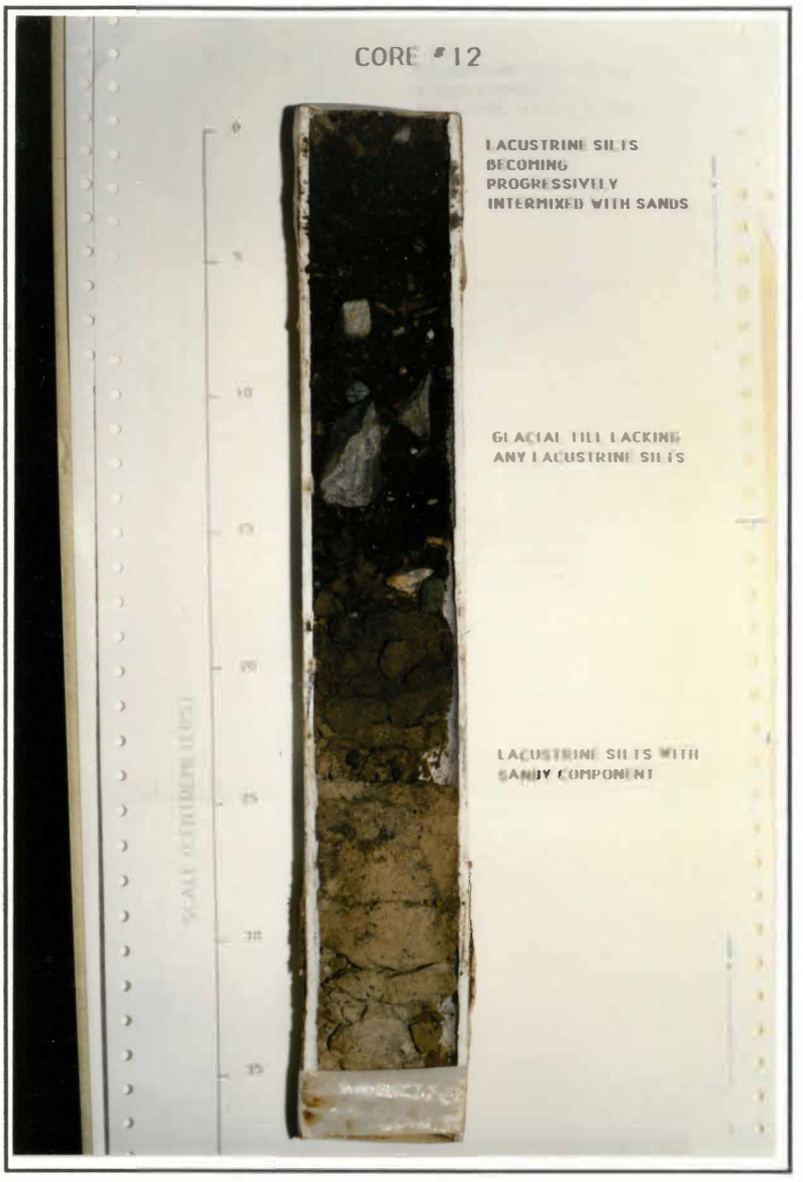

Plate 4.1 Photograph of the core from hole #12 showing the two zones of lacustrine sedimentation with a diamicton between.

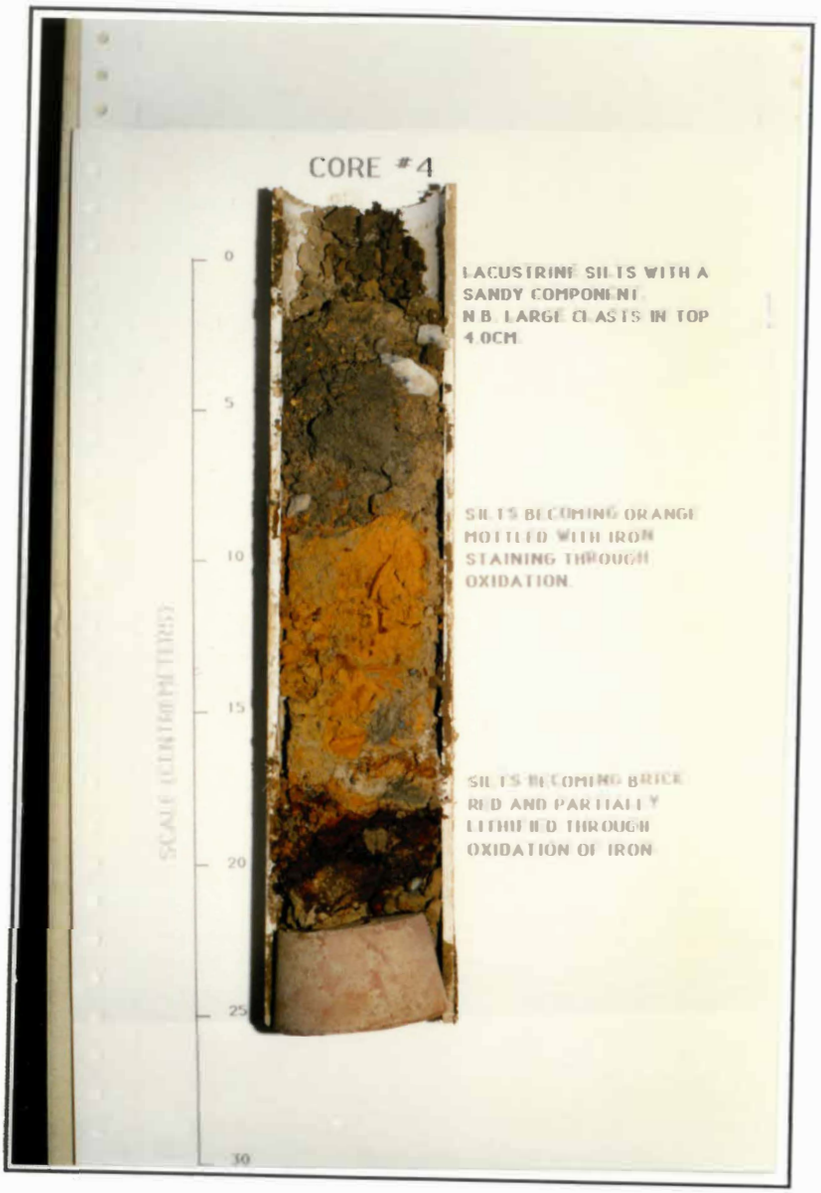

Plate 4.2 Photograph of the core from hole #4, showing the zones of oxidation in lacustrine silts. The larger clasts are visible in the top 10 cm.

The boundary between the the first and second zone was gradational, the second zone being characterized by a lack of silt and a more chaotic grain size distribution. The largest clast within this zone measured 6 cm in length and was very angular. Therefore, this zone represented either a diamicton, or glacial till. A sharp contact occurred at the base of this zone at a depth of 25 cm, where the sediments were lacustrine silts with scattered sand.

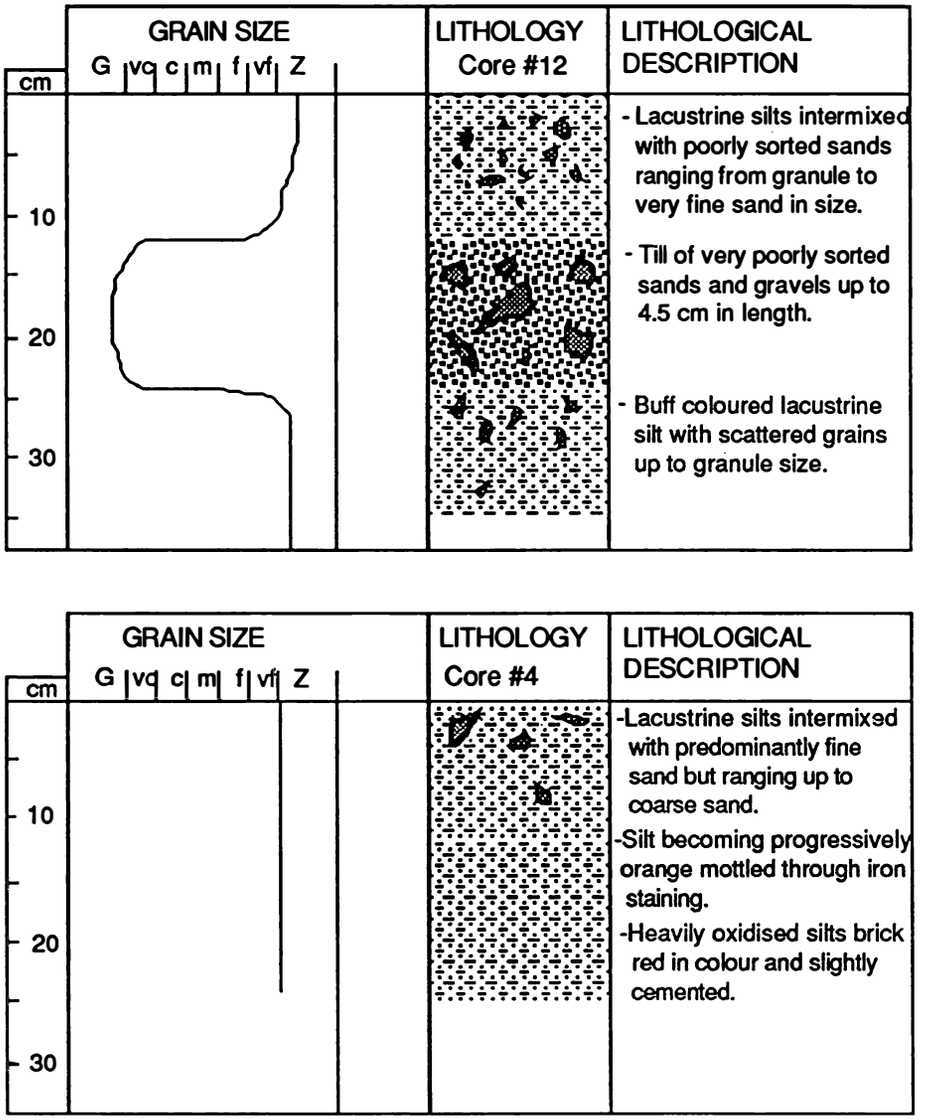

Figure 4.1 Core logs for cores 4 and 12 from Trough Lake.

4.6.1.2 Core #4

This core (Fig. 4.1 and Plate 4.2) consisted predominantly of lacustrine silts, intermixed with some fine sand, and the occasional pebble-sized clast, in the top 3 cm. At a depth of 15 cm the core became orange-mottled, with iron oxidation. The mottling increases to a depth of 25 cm, where the core is brick red and slightly cemented by iron oxides. This oxidation occurred after coring.

4.6.2 Sediment Analysis

Samples from the top of each core, as well as the sediment samples from the other holes (with the exception of hole #3) were disaggregated with an ultra-sonic probe. This was sufficient to break down the sediment into discrete grains, due to the lack of clays in an environment dominated by physical as opposed to chemical weathering. The sediments were split into sand and mud fractions. The very small sample weights of the sand fraction were dry sieved at 0.5 Ø intervals down to 4 Ø. The mud fraction was analysed by pipette analysis to determine the grain size distribution down to 10 Ø. It is worth noting that without exception, all the sand fractions were dominantly basaltic suggesting that they have their source in the Koettlitz Glacier, rather than the surrounding predominantly silicious drifts and moraines.

The following sample weights were used for the dry sieving and their associated errors (Table 4.8), calculated from the cumulative weights (see Appendix 1 for spreadsheet and calculations).

Core Number	Sand		Mud		Sample	
	Weight (g)	Error (%)	Weight (g)	Error (%)	Weight (g)	Error (%)
1	1.910	4.10	4.923	1.37	6.832	0.22
2	0.719	10.47	11.596	1.01	12.315	0.40
4	9.319	3.54	7.356	1.08	16.675	3.06
12	0.993	8.51	9.595	0.85	10.588	0.05

Table 4.8 Weights and associated errors of sand and mud fraction together with the total sample used for core grain size analysis.

While the errors for the sieve analysis may appear high, especially for cores 2 and 12, this can be attributed to the small sample size associated with the very low percentage of sand in the cores. The percentage of sand in the top of the cores was as follows:

-core #1 30.0%
-core #2 5.8%
-core #4 55.9%
-core #12 9.4%

Core #3, as mentioned, is unusual in that it consists almost entirely of basaltic sands. Some small clasts of silt were apparent in the sample, but these were isolated and rare. These clasts may represent the top of an underlying mud sequence. Due to the larger grain size this core could be analysed by the same graphical method as the surface sediments (Folk and Ward, 1956). The statistical data derived is recorded below (Table 4.9):

Sample I.D.	Sampling Site Location	GRAPHICAL METHOD (FOLK & WARD 1956) M_z	M_d	Mode	C	D_{35}	D_{65}	S_k	S.D.	K_G
	hole#03	1.68	1.65	1.75	-1.70	1.44	1.92	0.03	+0.77	1.16
51	hole#04	-1.01	-1.28	-1.50	-3.17	-1.54	-0.92	+0.42	1.05	1.27
05	hole#12	-3.80	-3.97	-4.50	-5.45	-4.40	-3.55	+0.30	1.22	1.12

Table 4.9 Summary of textural parameters for the lake sediment sample from hole #3 and the surficial sediment samples either side of hole #3, derived by the Folk and Ward (1956) graphical method.

CHAPTER FIVE

DISCUSSION OF RESULTS

5.1 TEMPERATURE RESULTS

Most available literature on temperature profiles in proglacial lakes is based on lakes not perennially ice covered. As a result, such articles concentrate on the changes from winter to summer temperature profiles. In high latitudes, during winter, the lake surface is covered by ice, and solar heating is at a minimum. This results in an essentially vertical temperature profile (Ashely *et al.*, 1985). In theory, with the melting of the ice cover, and the increase in solar radiation during spring, this profile can be expected to change and take on a hyperbola-like shape. However this is not the case as a rule, due to other factors affecting the lake:

(1) Cooling of the water surface -by evaporation,
-by back radiation and sensible heat loss (conductive and sensible heat loss at the air/water boundary);
-convection currents near the surface; and
-changes in the amount of radiation (daily and weather).

(2) Wind generated turbulent motion results in mixing and downward transfer of heat (Ashely *et al.*, 1985).

The result of this is a turbulent warm surface zone that is thermally heated and has a relatively uniform temperature called the epilimnion, and an undisturbed cold bottom layer called the hypolimnion. These two zones are separated by a zone characterized by rapid temperature change called the metalimnion.

The situation in lakes within the McMurdo Oasis is quite different, however, as all but the shallowest of these are perennially ice covered. So that in Trough Lake, most of these effects are eliminated, or at least reduced. Wind mixing of surface waters is eliminated, as is cooling by evaporation although cooling of the ice surface by sublimation persists. This heat loss however, is only inefficiently transferred to the rest of the lake, being limited by conduction through the ice cover. The radiation effect is dramatically reduced by the ice cover; at Trough Lake the incident light penetrating through the ice was about 6%.

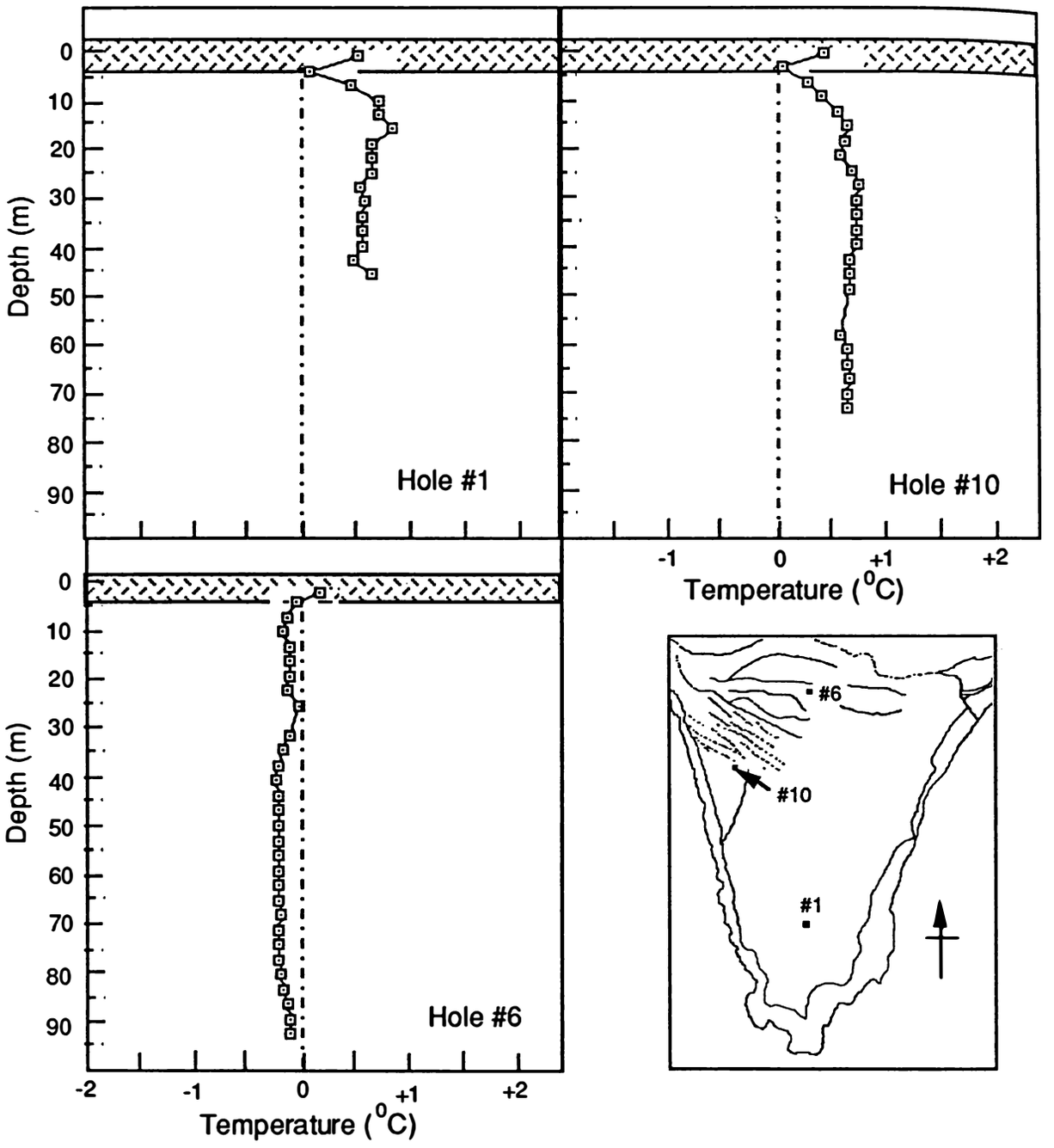

Figure 5.1 Temperature profiles at holes #1, #6, and #10 with their locations on Trough Lake

Heat fluxes into and from the water of a perennially ice covered lake, such as Trough Lake can be achieved by the following mechanisms:

(1) Flow of waters into and out of the lake, resulting in the transfer of sensible heat. In general, melt water flowing over lithic surfaces will be a little above freezing point due to absorption of solar radiation by the surfaces, and as such will tend to raise the temperature of the lake. The outflowing waters on the other hand are likely to exhibit mean lake temperatures;

(2) Inflows over ice (e.g. the Koettlitz Glacier) will be very close to freezing point implying a reduction in lake temperature;

(3) Conduction of heat through the ice to the atmosphere will be limited by the thickness of the ice cover and the temperature difference, but due to the mean annual temperature of ~-20° C will result in a heat loss;

(4) Ablation of ice from the surface to the dry atmosphere will result in a heat loss which, at equilibrium, will be partly negated by the freezing water onto the base of the ice cover. But as most ablation heat will exchange with the atmosphere, and most of the fusion effect will be released to the lake, the relative importance of these two processes is difficult to assess;

(5) Incoming solar radiation will be absorbed by the ice, solid material within the ice, the lake water, and the sediment at the bottom of the lake. Despite the abundance of clastic material observed on the surface of Trough Lake, comparable light intensities were observed in Trough Lake to those recorded in Lake Vanda (Wilson, 1981), which has a clastic free ice cover but they were lower than those recorded by Goldman et al.(date) However, the opacity of the waters in Trough Lake is apparently much higher, reducing the heat inputs to the sediment and bottom waters except in shallow waters;

(6) Exchange of heat between the lake (~0° C) and the glacier (mean temperature estimated at ~-20° C) will result in a heat loss, as will heat used to melt glacial ice in contact with the lake; and

(7) Minor heat exchanges will also occur between the lake and the underlying sediments, as well as directly to the atmosphere via the moat ice that melts out seasonally. These fluxes are probably insignificant when compared to those above.

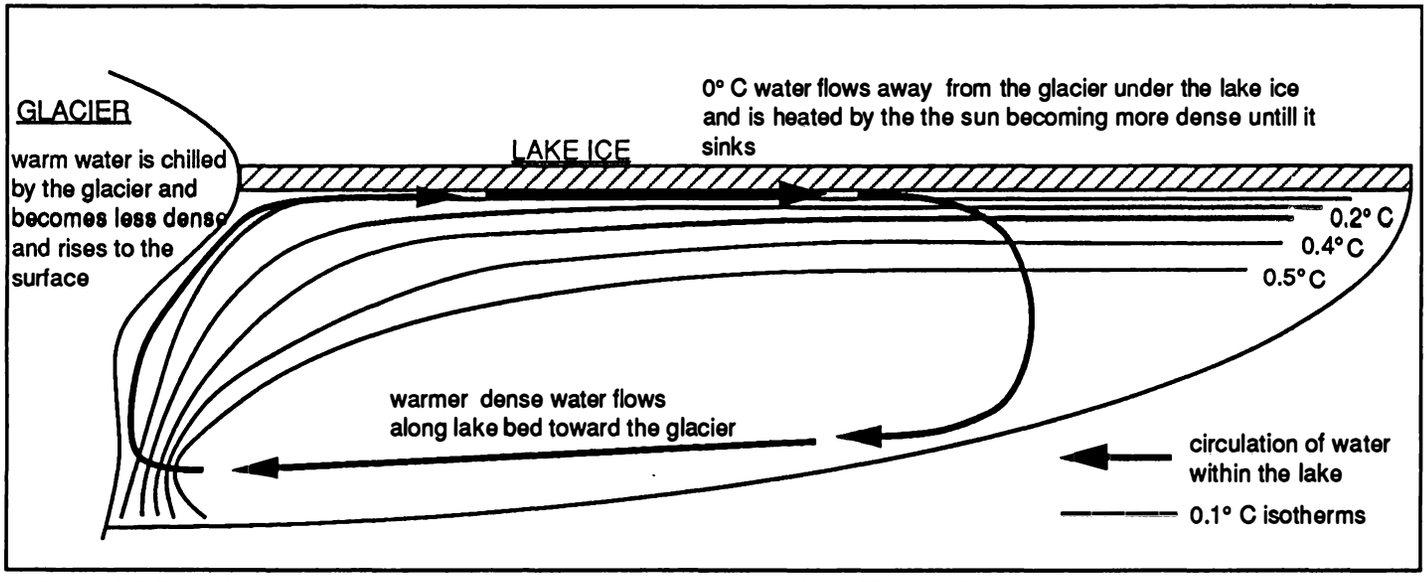

Figure 5.2 Postulated temperature structure and convection cell for Trough Lake.

The water in contact with the perennial ice cover (fig. 5.1) is very close to (0° C) and increases in temperature with depth at stations 1 and 10 (distal from the glacier), probably as a result of absorption of solar radiation and the sinking of the denser warm waters. Adjacent to the glacier (station 4) temperatures remained slightly below 0° C throughout the water column, and in fact froze if brought to the surface. Here the effects of conduction of heat to the glacier and melting of glacial ice combine to completely remove the excess heat supplied by solar radiation.

It is likely that convection is occurring, with the solar heated waters over most of the lake sinking as the temperature rose above 0° C, but cooling and rising in contact with the glacier. In this way, solar heat is collected over a large area and is brought to a small lake/glacier contact. This will result in accelerated melting of the glacier, and stabilization of the lake water temperature to within a few degrees of the freezing point of water. The same very small temperature range is observed in Lake Wilson (Hendy, *pers. comm.*) and the west lobe of Lake Bonney (Hoare *et al.*, 1964), both of which are in contact with glacier ice, although to a smaller extent than Trough Lake.

Figure 5.2 shows the anticipated thermal structure of Trough Lake, with a convection cell adjacent to the ice front, and vertical isotherms proximal and horizontal isotherms distal to the ice front. This is similar to the suggested temperature structure of Icelandic ice contact lakes (Ashley and Smith, 1985), but temperatures are much closer to 0° C (fig. 5.3).

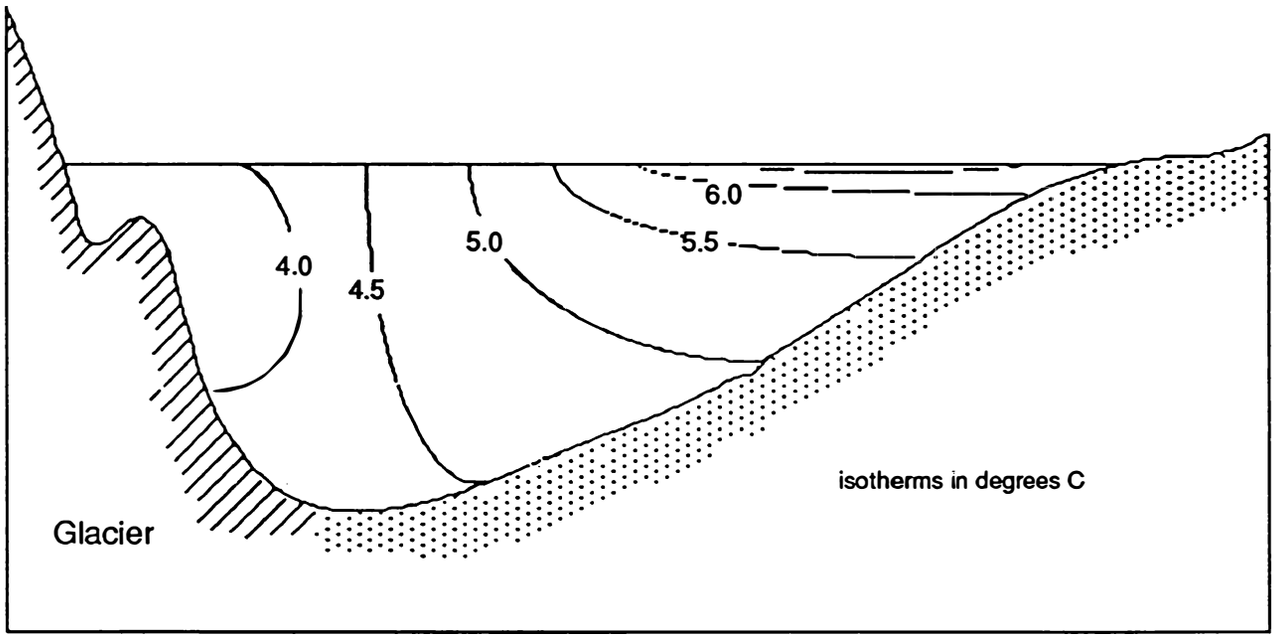

Figure 5.3 An Icelandic ice contact lake showing the thermal effects of the glaciers proximity (after Ashley and Smith, 1985).

Therefore, while Trough Lake is solar heated (if it was not, it would be a solid block of ice), its characteristics are quite different to lakes which do not have a glacier contact.

Workers such as Wilson (1967/b), House *et al.*, (1966) and Hoare *et al.*, (1964) have shown that Lakes Fryxell, Vanda and Bonney follow closely the theoretical thermal profile as predicted by the equation:

$$T = \frac{Q_o e^{-\alpha x}}{k\alpha - Dx + F}$$

where T = Temperature

Q_o = energy reaching the depth x=0

$\alpha = \frac{0.693}{x_{1/2}}$ where $x_{1\backslash 2}$ is the distance in which the radiation intensity is reduced to half of the value at Q_o.

k = the thermal conductivity of water

D and F are both constants

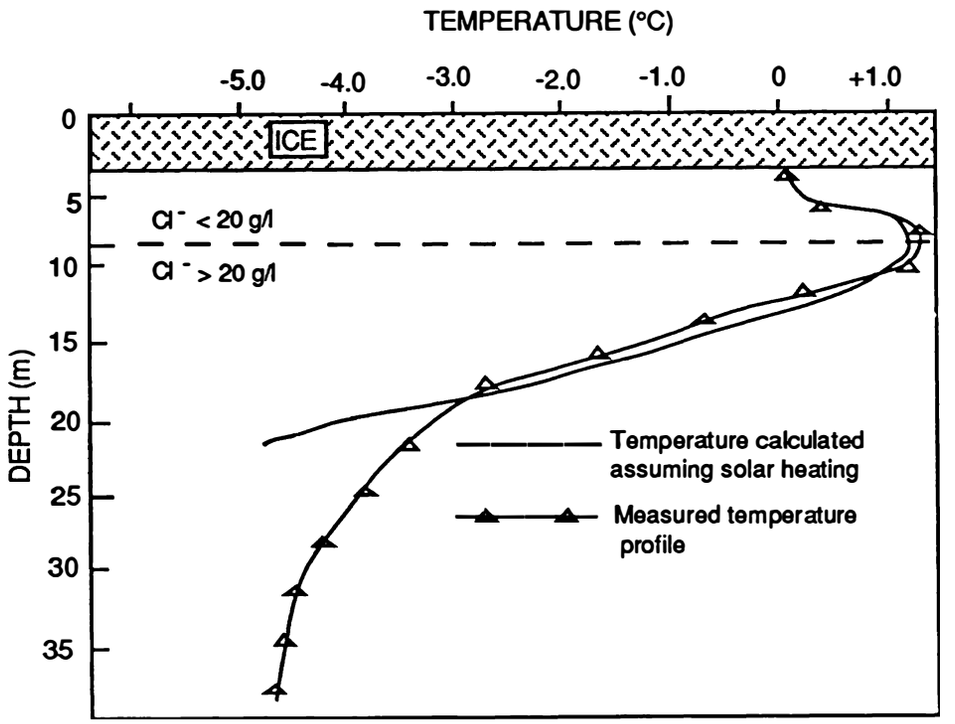

Figure 5.4 Temperature profile for the western lobe of Lake Bonney and that predicted assuming solar heating (Hoare *et al.*, 1964).

This occurs in Lake Bonney where the west lobe (fig. 5.4), which is in contact with the glacier, and the eastern lobe which is not, follow very closely the temperature profile predicted on the basis of solar heating. The variation in temperature observed from the theoretical values may be as a result of the western lobe cooling slightly and the eastern heating up, a factor associated with the strong density stratification of both lobes due to high NaCl concentrations

(Hoare *et al.*, 1964). This close agreement with predicted values only appears to apply in the top 15 m of the water column, due to the inability of light of sufficient intensity to directly heat the water below this level, as well as the density stratification of the lake restricting circulation. Hence the solar heating of the lake only manifests itself in the top 20 m of the water column, depending on water clarity and assuming little mixing of waters.

In the case of Trough Lake the effect of solar heating is sufficient to maintain a liquid state, but does not manifest itself in the thermal profile to any degree. The over-riding influence is that of the glacier and its ability to cool the surrounding waters. This results in the formation of a convection cell that keeps the lake waters well mixed and consequently masks the expected temperature profile.

5.2 ICE THICKNESS AND LIGHT PENETRATION

The ice thickness below the water level is relatively homogeneous, except for the triangular section in the west (about 6 m thick), being about 4 m thick. McKay *et al.* (1985) considered the thickness of perennially frozen lakes and presented a model to explain ice thickness (fig. 5.5). They identified four energy sources and sinks for a perennially ice covered lake:

-Solar radiation -reflected (albedo)
-conducted through the ice into the water
-Atmospheric, ablation (sensible heat) and latent heat of evaporation
-Geothermal heat
-Fluvial input-streams
-glacier
-Conduction of heat through the ice cover by freezing on of new ice to the base (sensible heat) and the latent heat of freezing.

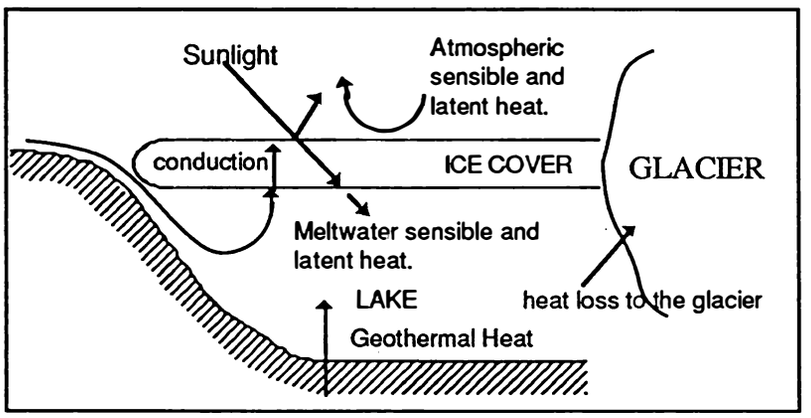

Figure 5.5 Energy sources and sinks for perennially ice-covered lakes

However all these variables are likely to be the same throughout the lake surface, and certainly should not change as abruptly as indicated by the change in ice thickness between holes #9 and #10 (Table 4.3). The most likely answer to this paradox is that the extra thickness is due to the force exerted by the glacier. This is manifested in the unusual topography of the area in question (fig. 2.1). It is also apparent, by the a large transcurrent crack in the lake ice between the two holes (fig. 2.1), that this section of lake ice is not moving toward the south at the same rate as the bulk of the lake ice. It is worth noting that the temperature profile under the thicker ice (hole #10) does not indicate any unusual temperature characteristics such as a different convection cell operating. Therefore this eliminates such possibilities as a cause of the thicker ice.

The amount of light penetrating even this over-thickened section of ice is very similar to the other sites examined. It must be noted that the ice thickness here is 6 m and hence the second reading at 3 m in Table 4.4 must be ignored. The readings at the base of the lake ice are all between 4% and 6%, values that agree well with those recorded at Lake Vanda (~5% [Wilson 1981]).

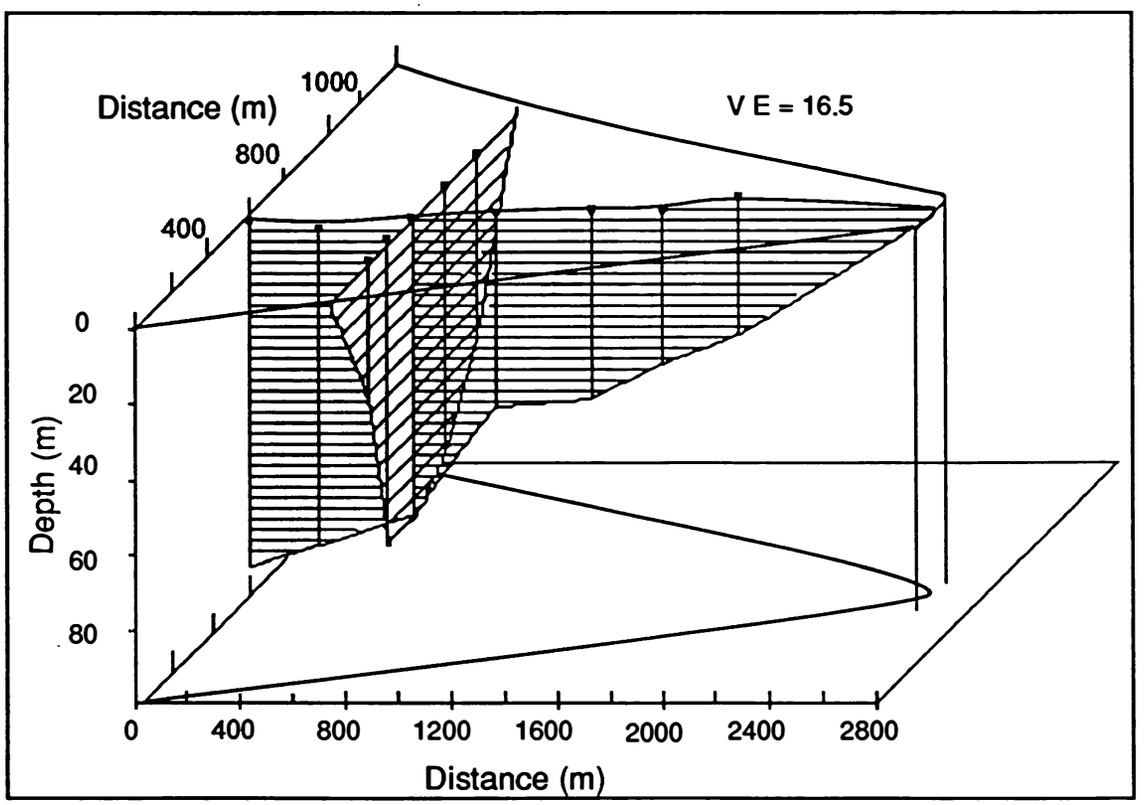

Figure 5.6 Bathymetry of Trough Lake as indicated by depth soundings.

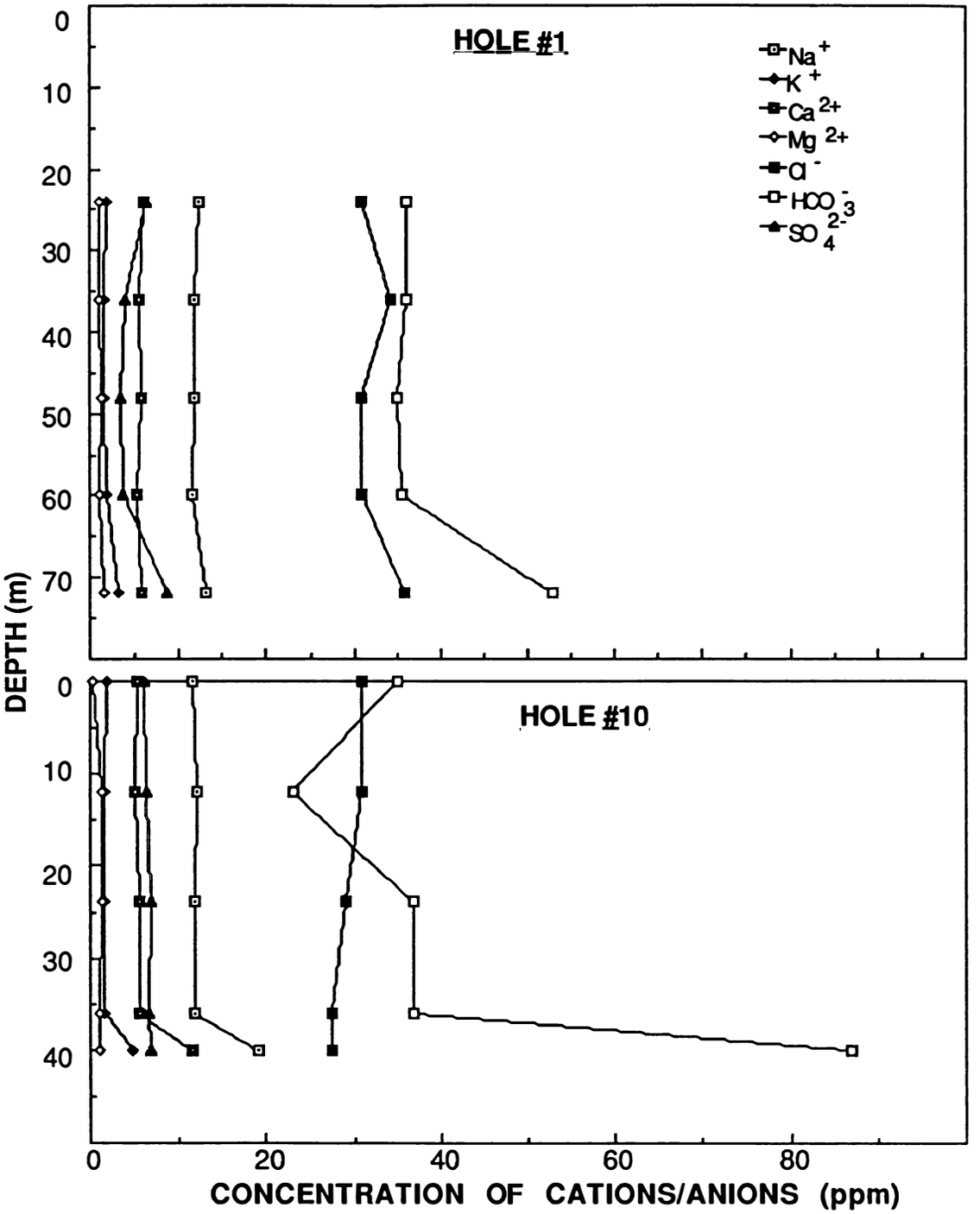

Figure. 5.7 Variation in the concentration of some anions and cations through the water column at holes #1 and #10 on Trough Lake. The increase in concentration for the bottom samples is attributed to contamination by entrained sediments present in the containers prior to analysis.

5.3 BATHYMETRY

The bathymetry results show that the lake occupies a "U" shaped valley deepening toward the north (fig. 5.6). The lake is deep, compared to others in the area reaching a recorded maximum of 93 m. The flow pattern on the surface of the Koettlitz Glacier indicates that Walcott Bay is a basin separated from the bulk of the glacier by a topographic high between The Bulwark and Heald Island.

5.4 WATER CHEMISTRY

The variation in concentration of the various cations and anions through the water column (fig. 5.7) is very slight, with the water column being characterized by essentially vertical profiles. The increase in the concentration of most ions analysed toward the bottom of the lake, is attributed to some lake bottom sediments contaminating the water after sampling and prior to analysis. This is also supported by the pH profiles (fig. 5.7) which show an increase in pH at the bottom of the lake. Any fluctuation in results between the surface and the bottom can be attributed to normal experimental error. The vertical profiles match the temperature profiles, and confirm that the lake is well mixed, there being no evidence of either temperature or chemical stratification.

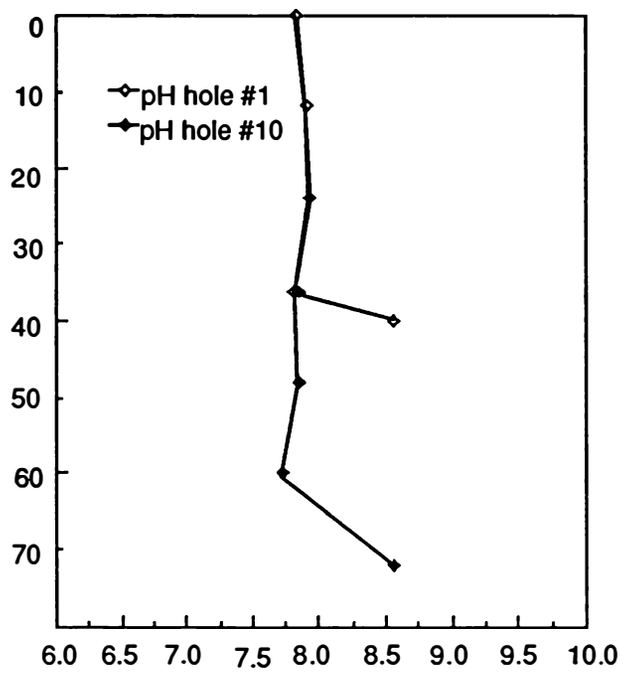

Figure. 5.8 pH versus depth for the water column through holes 1 and 12.

The surface water sample from hole #6 (TS/87/30) is consistently anomalous and therefore is believed to be contaminated in some manner, either prior or subsequently to sampling. As a result the values obtained are ignored. The core water sample from hole #3 (TS/87/50) is very similar in composition to the other bottom water samples and does not show any evidence of chemical precipitation on the lake bottom, or within the sediments. The results for the stream water flowing into the southern end of Trough Lake are very similar to those of the lake water itself, with any increase in concentration likely to be due to the stream flowing over evaporite deposits, such as those on the western side of Pyramid Trough. The water sampled from Lake Porkchop is very similar to that from Trough Lake, and the higher value recorded for chloride may be attributed to local geological differences.

5.5 SURFICIAL SEDIMENTS

5.5.1 Presentation of Results

The data from Table 4.7 were plotted against distance from the assumed sediment source the glacier face. In all the plots, the data from around hole #06 were anomalous, so the results for this sample are examined separately. The mean, mode and median data all show the same trends of coarsening grain size away from the glacier Therefore only the mean grain sizes are plotted in Figure 5.9.

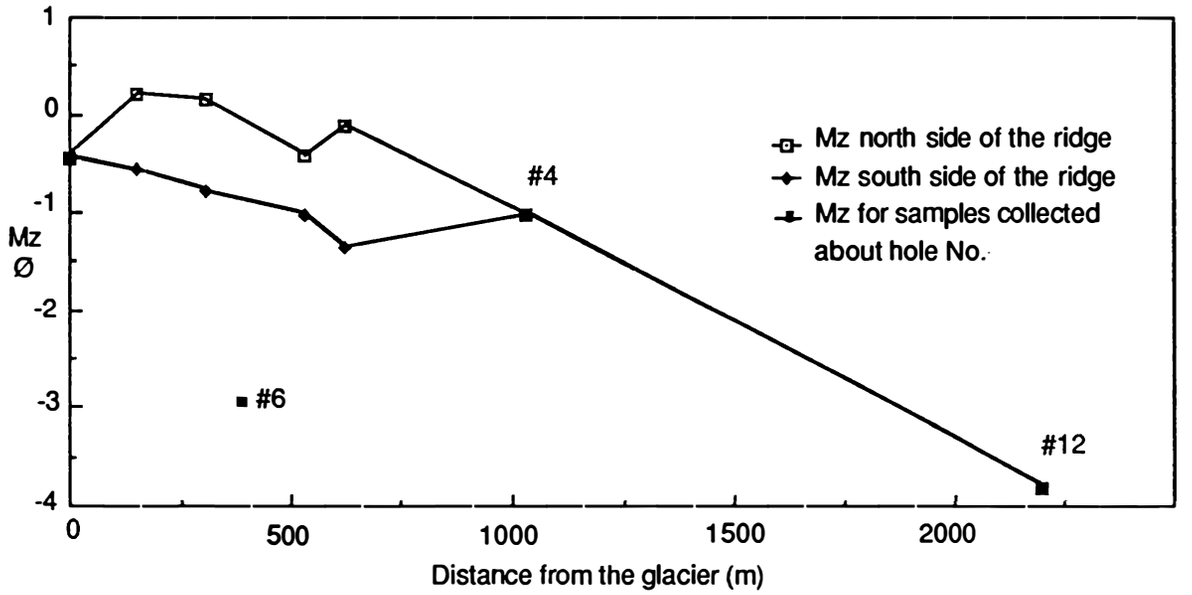

Figure 5.9 Distance from the glacier versus mean grain size of the surficial sediments.

It was considered when plotting the coarsest 35% and 65% of the grain sizes that if, as is suggested by the mean grain size results, fines are being removed from the system, that the finest 35% and 65% (F35 and F65) would be more appropriate and better represent

the trends occurring. The resulting graphs (fig. 5.10) confirm the trend toward coarser grain sizes as is shown in Figure 5.9.

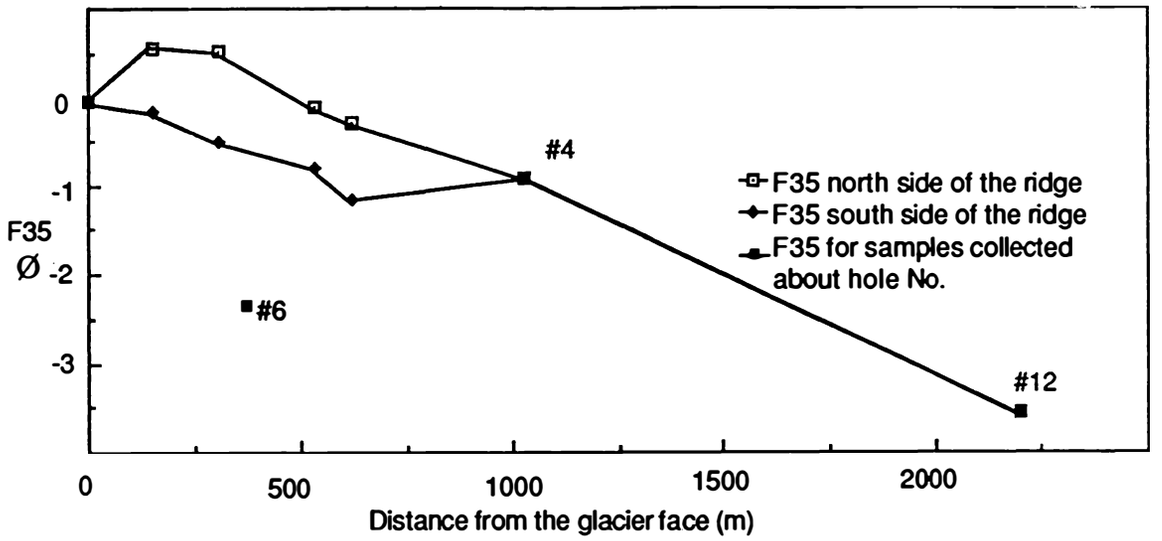

Figure 5.10 Distance from the glacier face versus the finest 35% of the surficial sediments.

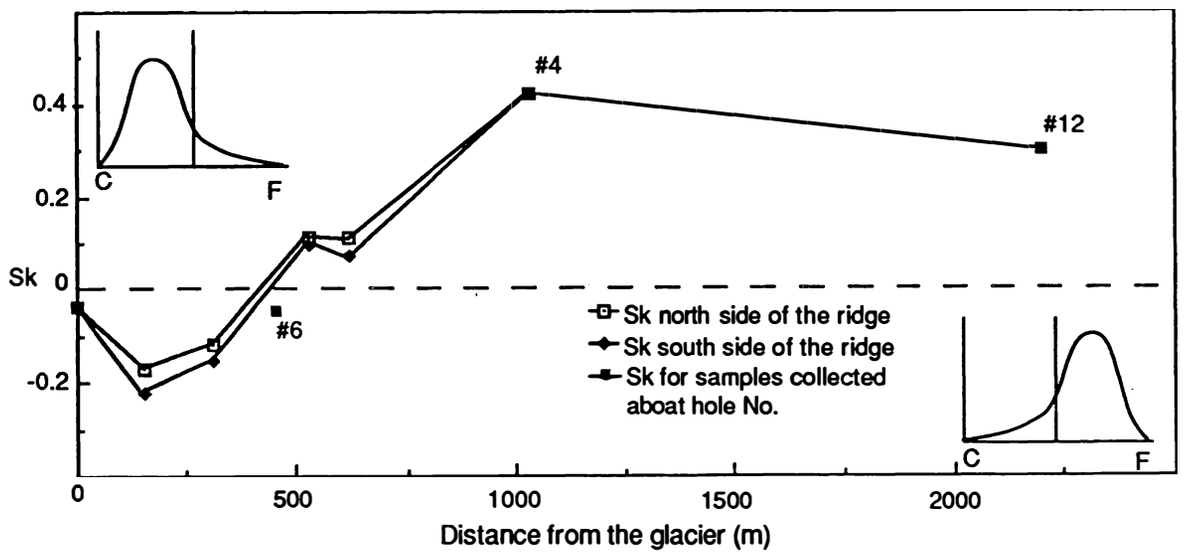

Figure 5.11 Skewness of the surficial sediments versus distance from the glacier. The inserts show the effect of positive and negative skewness either side of the dotted line.

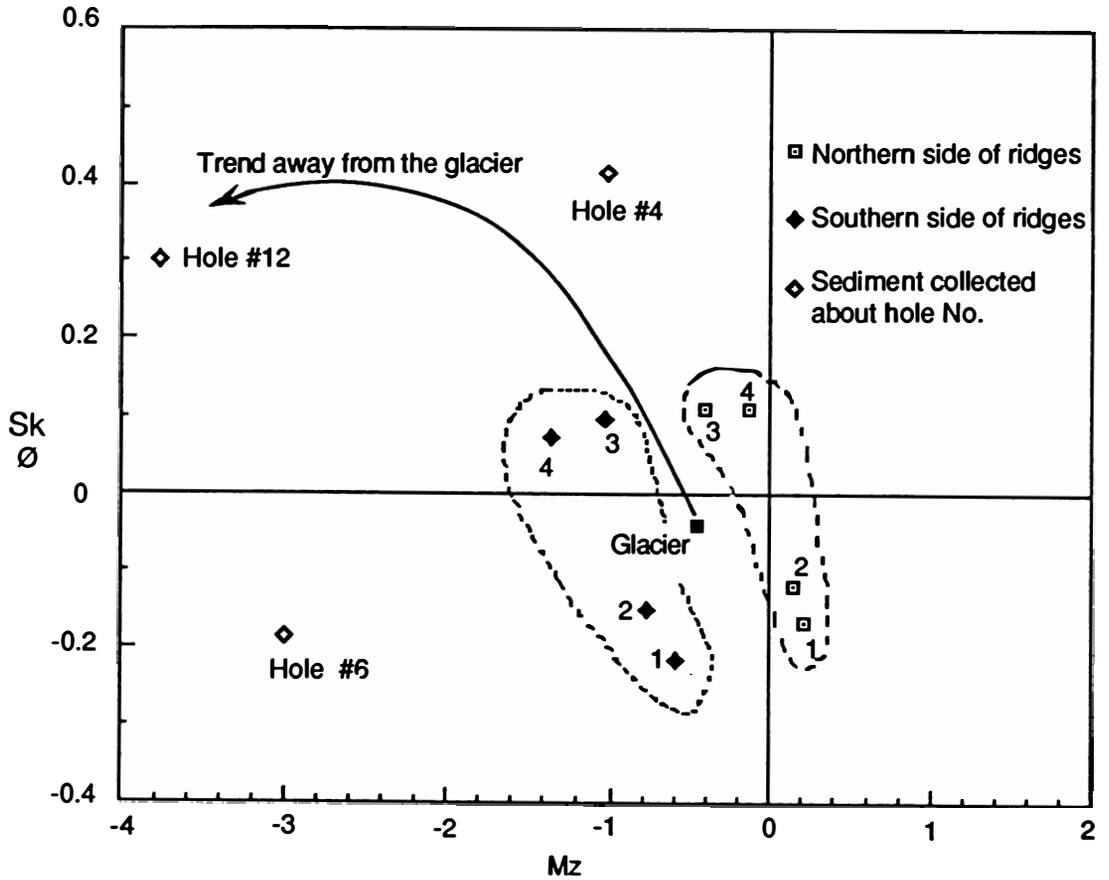

Figure 5.12 Mean grain size versus skewness for surficial sediments.

Plate 5.1 The large block raised on a pedestal of ice noted by Lyon in 1970 and subsequently by event K021 in 1987. The relative position of this feature gives an approximation of the rate of movement of the lake ice away from the glacier.

The plot for skewness (fig. 5.11) exhibits an initial tendency to be coarse skewed (negative value) due to the concentration of fines at the glacier face. However with distance from the glacier and removal of fines this changes to a positive value and hence fine skewness due to the relative concentration of the coarser grain sizes (see inserts in fig. 5.11)

Based on the plots produced, there is a clear separation between the northern and southern sides of the glacial ridges yet a general coarsening trend is apparent. This is illustrated graphically in Figure 5.12 where mean grain size is plotted against skewness following the approach of Moiala and Webster, (1968). The differentiation of opposite sides of the ridges is represented here by two distinct populations occurring either side of the value for the glacier face. These populations are essentially parallel and show trends toward positive skewness (i.e. becoming fine skewed due to concentration of the coarse fraction) and coarser grain sizes.

This variation between northern and southern sides of the ice ridges can be attributed to wind or some other factor affecting opposite sides to a greater or lesser extent. The parallel trend however must be due to a common factor such as the removal of fines through the ice cover or melt water washing fines away.

5.5.2 Discussion

The movement of the lake ice away from the glacier has been confirmed by establishing the relative position of a large block raised on a pedestal of ice over a 17 year period (plate 5.1). This feature was located by G. L. Lyon in 1970 and marked on his field map (Appendix 3). Subsequently in the summer of 1986-87 it was located by event K021 and found to have moved a distance of about 300 m (fig. 3.2) to the south. This equates to a yearly movement of about 18 m.

Two strong trends are apparent over the lake surface, the coarsening of grain sizes present and the variations either side of the glacial ice ridges. To explain this, one or more of the following mechanisms must be operating on the surface of Trough Lake:

- -removal of fines by melt water streams flowing from the melting ice ridges and or glacier.
- -removal of fines by the strong southerly katabatic winds that blow from the East Antarctic Ice Sheet, and to a lesser extent, northerly winds from the McMurdo Ice Sheet and the tongue of the Koettlitz Glacier.
- -removal of fines by sediment melting the underlying lake ice and moving through under gravity.

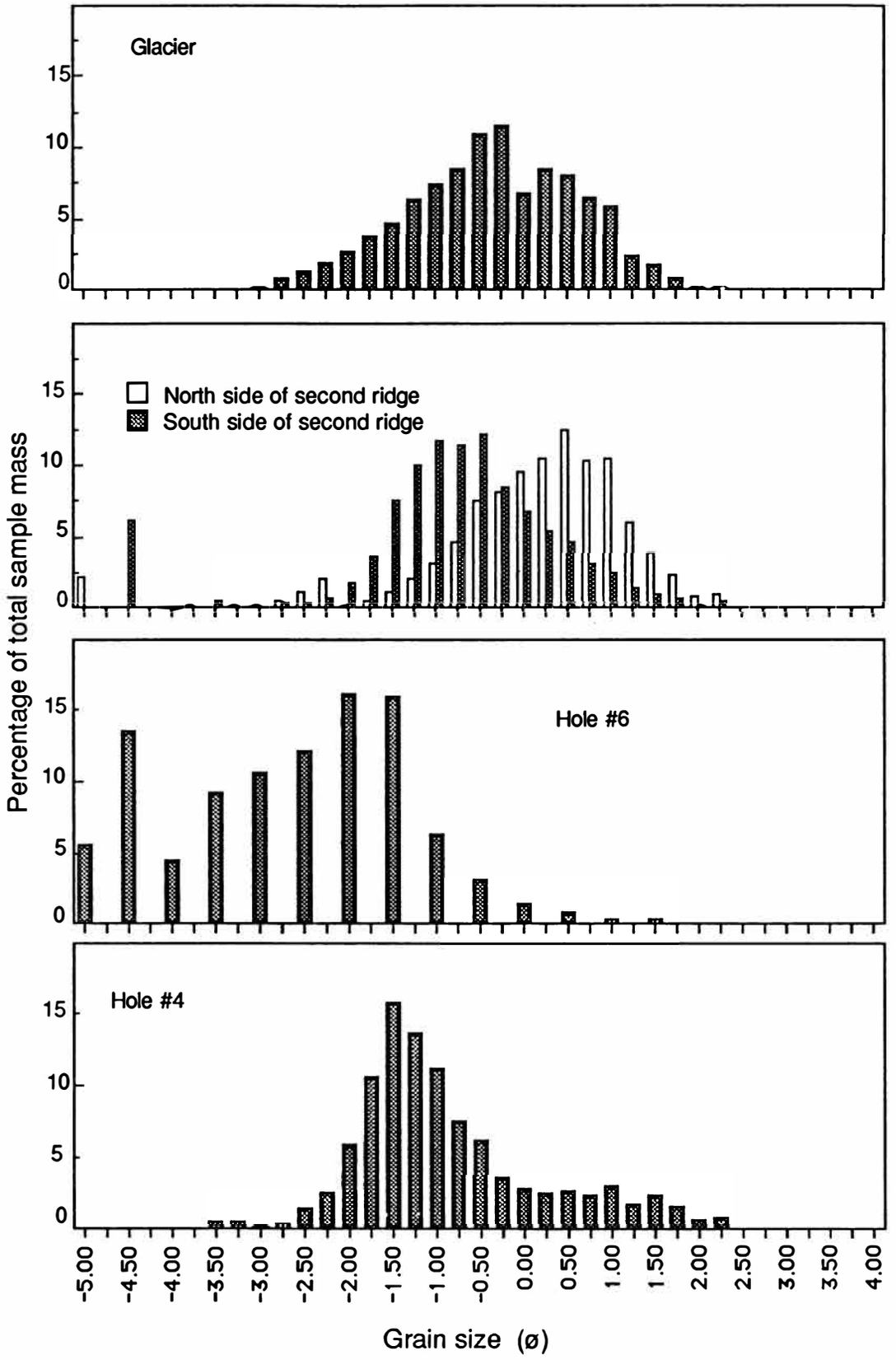

Figure 5.13 Grain size distribution histograms for the surficial sediments collected around the glacier, hole #4, hole #6 and both northern and southern sides of the second ridge from the glacier.

Fluvial activity can be eliminated as it is unlikely to affect the entire lake surface since melt water was confined to channelised streams close to the glacier face, and the associated sediments are likely to be concentrated around these streams. Fluvial flow removing fines would also imply that the fines must be deposited some where and no evidence of this was observed. This leaves only aeolian dispersion of the sediment or extraction through the ice cover.

The variation either side of the ridges is likely to be the result of aeolian processes. Due to the shape of the valley, winds only blow north up the valley from the McMurdo Ice Shelf, or south down the valley from the East Antarctic Ice Sheet. These southerly winds are katabatic and consequently very strong (see 1.12 Dry Valley Climate) and will affect the southern side of the ridges more than the northern. Weaker winds blow from the north and therefore would affect the northern side of the ridge more than the southern. This is evident by the generally finer sediment on the northern sides of the ridges.

The overall trend of coarsening sediment toward the south is explained by the progressive loss of sediment through the ice cover with time. The rate at which this process occurs is related to grain size, and tends to concentrate the coarser fraction on the lake surface while removing the fines. This is considered to be the mechanism, rather than aeolian processes, as the trends on opposite sides of the ridges are similar indicating similar processes.

5.5.3 Results From Hole #06.

The apparently anomalous results from the sediment surrounding hole #6 is due to multiple sediment sources. This is apparent from the grain size distribution histograms (fig. 5.13). The hole #6 sample is the only bimodal distribution, indicating a dual population of sediments from different sources. The sample also appears unusually coarse. This 6 sample was taken from a broad glacial out-wash zone running down the centre of the lake. Consequently this sediment contains a fluvial transported component from the glacier, as well as the normal ice rafted component.

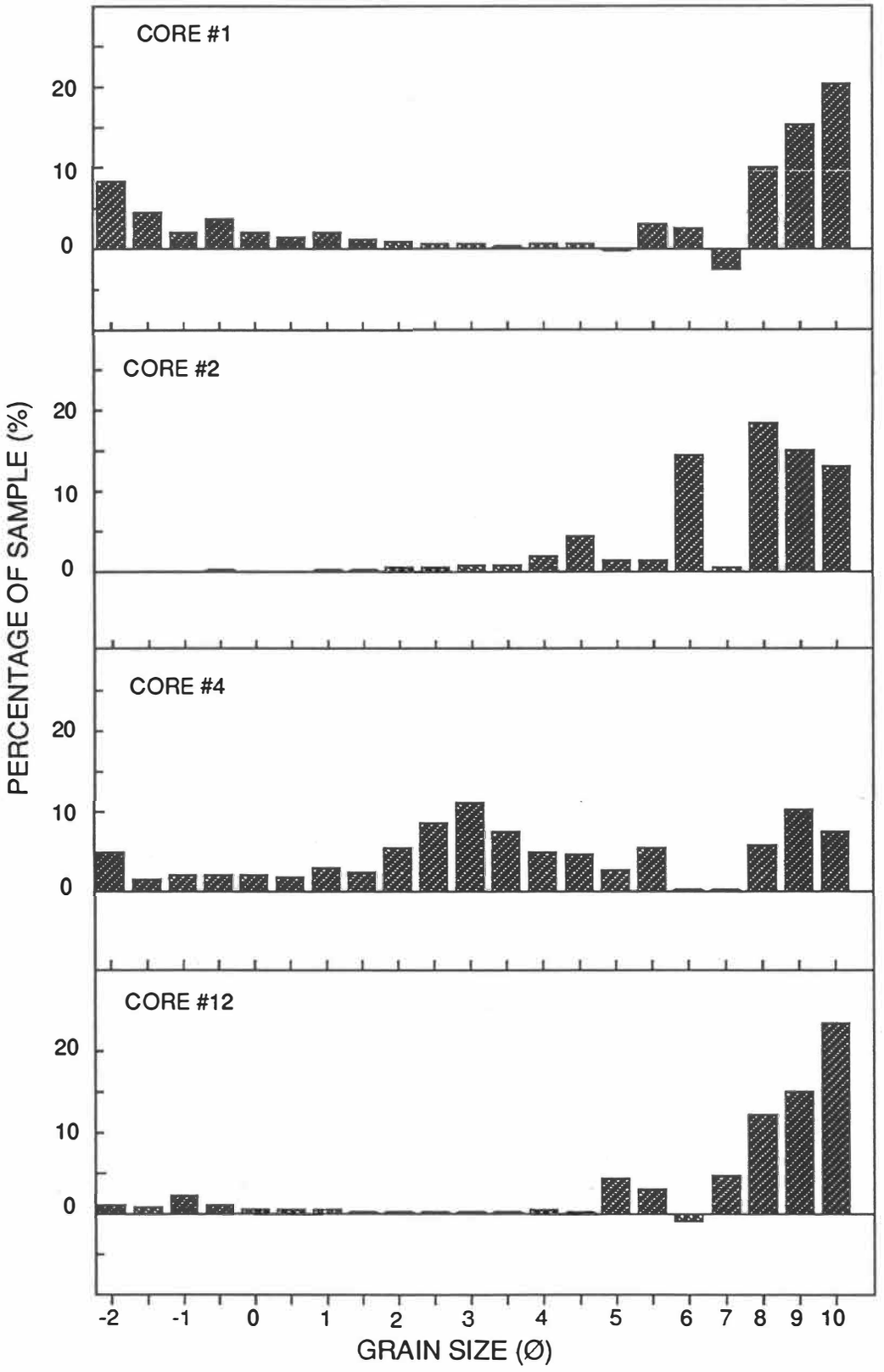

Figure 5.14 Grain size distribution for the samples from the top of cores 1, 2, 4 and 12

5.6 CORE SEDIMENTS

5.6.1 Cores 1, 2, 4 and 12

Histograms of the percentage of sediment for each grain size were plotted to examine the possibility of more than one sediment population (fig. 5.14), indicating a multiple sediment source. It was decided to ignore sediment above 0.5 Ø, as, due to the small sample size, one or two grains could disproportionately affect the results.

When these histograms were plotted, a homogeneous background level of sedimentation spanning the entire spectrum of grain sizes is evident. Above this a peak rises between 7 and 10 Ø for cores 1, 2 and 12. However core #4, the closest to the glacier, shows two distinct peaks. One at 10 Ø, as for the other cores, and an additional one at 3 Ø. This indicates two sources of sediment, the normal lacustrine sedimentation of mud, and an additional source of sand not accounted for by normal lacustrine processes.

As the sand fraction in all cores including core #4 was intermixed with the lacustrine silts this indicates contemporaneous sedimentation and not instantaneous sedimentation as in core #3. Therefore, as core #4 was taken from the middle of the lake a substantial distance beyond the sides of the valley, fluvial input or interference from the glacier (the sample site was beyond the glacial ice ridges eliminating melting of these as a sediment source), the sand fraction must be coming through the overlying lake ice.

The lack of a bimodal sediment size distribution in all cores but core #4 suggests that either the sediment has moved completely through the ice prior to reaching hole #3 or it is trapped within the ice unable to move any further due to insufficient solar energy or too large a grain size to melt the surrounding ice.

The diamicton observed in the core from hole #12 at the southern end of the lake is believed to be the result of dumping off the end of the lake ice. The lake ice can be considered a conveyor belt moving sediment from the glacier to the opposite end of the lake so these ice rafted sediments must be deposited off the end of the ice at some point. The fact that the till overlies lacustrine silt indicates that a lower lake level has existed in the past. Also the presence of underlying silt suggests that the till was dumped by lacustrine processes since, if the silts were exposed to the atmosphere, the strong winds of the area would have removed them.

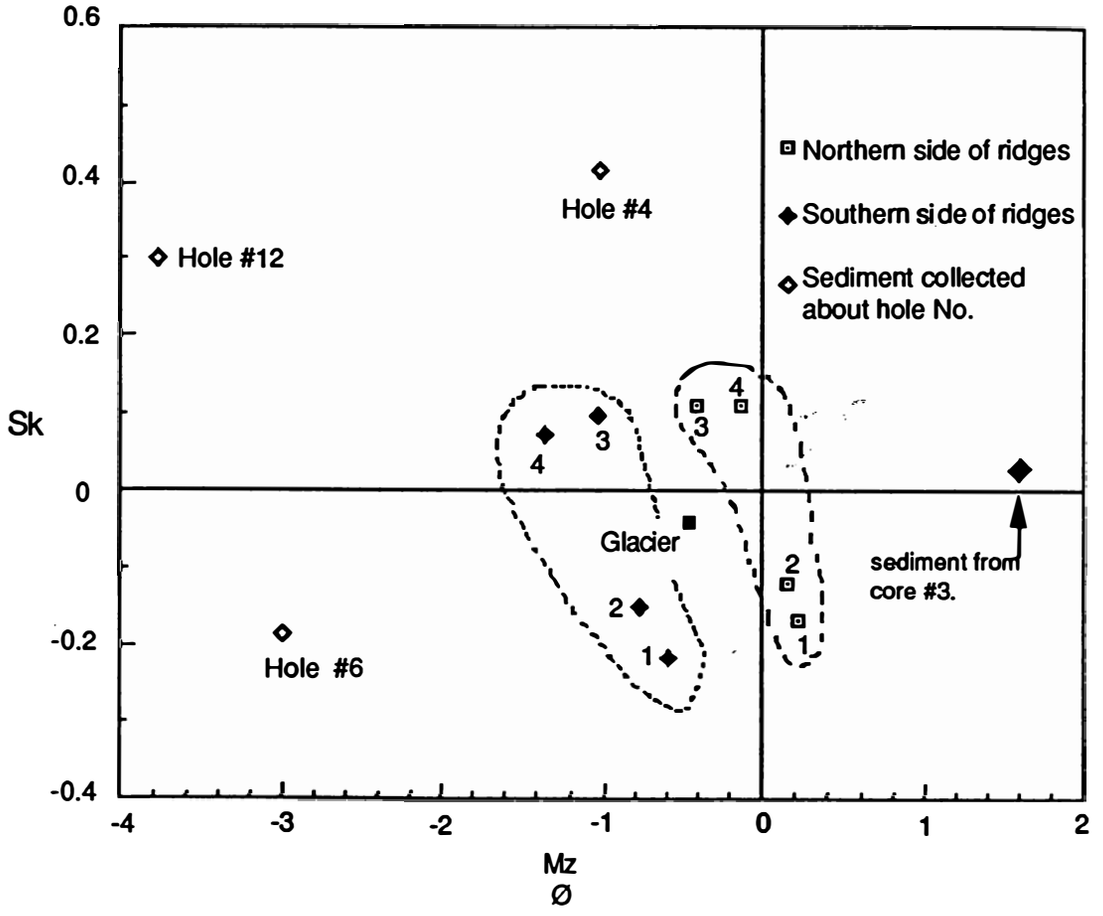

Figure 5.15 Mean grain size versus skewness for the surficial sediments, indicating the relative position of lake sediments obtained from hole #3

5.6.2 Core #3

The most likely explanation for the occurrence of these coarse sediments in core #3 is that they represent surface sediments which have fallen through a crack in the lake ice. The possibility of fluvial input could be ruled out due to the remoteness of the site from any streams and the absence of evidence for fluvially derived sediments in core #12, which was retrieved closer to the only stream in the vicinity. To establish whether or not the sediment was derived from surface sediments its textural parameters were plotted on the same graph as the surface sediments (fig. 5.15).

Very little resemblance to the surface samples was evident, the sediment being much finer than even the glacial source. Skewness was much less than that of the surrounding surface sediments, indicating that additional sorting had occurred prior to deposition on the lake bed. The obvious differences between this core sample and the surrounding surface sediments eliminates a crack through the ice, allowing surface sediments to fall through, as a possible source. It is apparent, however, from the petrology of the sample, that it has been derived from the glacial source, as have all the surface sediments.

The grain size of this sediment is substantially coarser than the sand fraction of the core obtained from the hole next closest to the glacier, hole #4 (see appendix 2 for textural, parameters), the sediments source must be one of the following:

(1) A lense of sand that has melted through the ice and been deposited on the lake bed as a unit.
(2) A lense of sand close to the base of the lake ice that has been exposed to the lake waters by a crack, allowing deposition as a discrete unit on the lake bed.

Although the sediment is slightly coarser than the sand fraction from core #4, this is what would be expected as with distance from the glacier progressively coarser sediments migrate through the ice. Despite this it would appear unlikely, although not impossible, for it to have been deposited by the first mechanism, as the core represents a discrete unit of sediment, and shows no evidence of contemporaneous sedimentation of lacustrine silts and muds which could be expected. Therefore it is concluded that this sample represents an instantaneous deposition of sand by exposure of a deep lense of material within the lake ice via a crack .

CHAPTER SIX

MECHANISMS FOR SEDIMENTATION IN PROGLACIAL LAKES

6.1 DISCUSSION OF SAND/ICE INTERACTION MECHANISMS

Simmons *et al.* (1986) have proposed a model for sediment migration through the ice cover of perennially frozen lakes. They concluded that sand particles migrate through ice by absorbing solar radiation, and re-emitting it as heat which melts the surrounding ice. The particles then migrate downwards, through the ice, under the influence of gravity. This process is analogous to the migration of algae through ice in Antarctic lakes. The algae absorb solar energy, convert this into heat which creates a pool of liquid water. They then migrate upwards surrounded by this pool buoyed on gases (the product of photosynthesis) trapped under the algal mats (Plate 2.10).

Simmons *et al.* proposed an empirical relationship, relating grain size to the possibility of sediment movement through the ice. This relationship is referred to as "the spherically symmetrical equation," and is given by:

$$F(1-\varpi)\pi r^2 = 4\pi r k \Delta T \quad \text{.....Eqn 6.1}$$

where: F = the vertically averaged radiation field in the ice cover (Wm^{-2})

ϖ = the single scattering albedo of the grain ($\varpi \cong 0.2$)

r = the radius of the sand grain (m).

k = the thermal conductivity of the ice (at -1°C, k~ 2.3 $W K^{-1} m^{-1}$)

ΔT = the temperature difference between the ice and the sand grain ($\Delta T \geq 1°C$).

Measurements by Palisano and Simmons (1986) determined the maximum radiation (at noon on the summer solstice), as being given by the relationship:

$$F \cong 1.5 S_o e^{-kz} \quad \text{.....Eqn.6.2}$$

where S_o = the incident solar flux (at solstice noon $S_o \sim 500\ W\ m^{-2}$)

z = the depth into the ice the sand grain is (m)

k = the absorption coefficient of the ice including scattering ($k \cong 0.9\ m^{-1}$)

These equations can be combined to give the equation:

$$r = \frac{1}{65.22e^{-0.9z}} \quad \text{.....Eqn.6.3}$$

or making the depth to which the sand grain will sink the subject:

$$z = \frac{\ln \frac{1}{65.22r}}{-0.9} \quad \text{.....Eqn. 6.4}$$

Using equation 6.4, for the various grain radii (r) a maximum depth that a particle can sink (z) can be calculated. From this data a graph of grain size, against maximum depth to which the particle can sink, can be plotted (fig. 6.1).

From this a minimum grain diameter of 30.67 mm capable of melting ice at the lake surface can be derived. This implies that, according to Simmons *et al.*, only sediments with a grain size of greater than 30.67 mm can migrate through the lake ice, and the grain size determines the depth to which the grains can reach. Simmons *et al.* calculated that for a clast to reach a depth of 2 m the clast must have a diameter of at least 93 mm.

While at Trough Lake many such clasts were observed on the lake ice, however none were encountered while drilling holes in the lake ice. The material encountered within the ice was fine basaltic sands similar to that at the glacier/lake interface, and tended to be concentrated in successive lenses at a variety of depths. Simmons *et al.* have noted the occurrence of smaller grain sizes within the ice and concluded that fluvial activity on the lake ice concentrated sand in surface ponds melted out during summer, where, once enough sand accumulated it could achieve a large enough mass to melt through the ice as the larger clasts are suggested to.

If this mechanism was to be effective the heat transfer from grain to grain would need to be very efficient, as underlying grains are unlikely to have direct exposure to sunlight, and hence a deposit of sand could not have the same or similar thermal properties as a large intact block. It is more likely that the sand will insulate underlying ice and reduce ablation of the underlying ice as the large surface area is likely to be an efficient heat sink. This is due to the high void ratio characteristic of the loosely packed sands (Selby, 1982) which allows cool air to flow through the sediments while reducing grain to grain contact to a minimum and therefore minimizing heat flow. This situation was observed at the base of many icebergs on Trough Lake, where a sheet of sand trapped against the side of icebergs, protected underlying lake ice from the sun and formed a slope, the steepness of which is determined by the internal friction angle of the sediment (Plate 2.7). Due to the

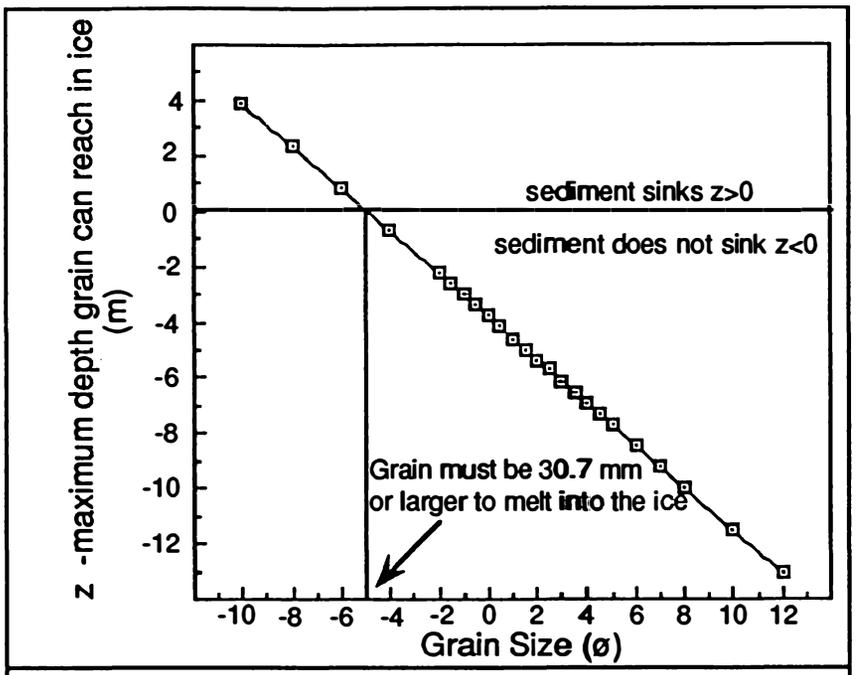

Figure 6.1 The relationship of grain size (2r) to the maximum depth to which the grain will sink (z) as predicted by equation 3.

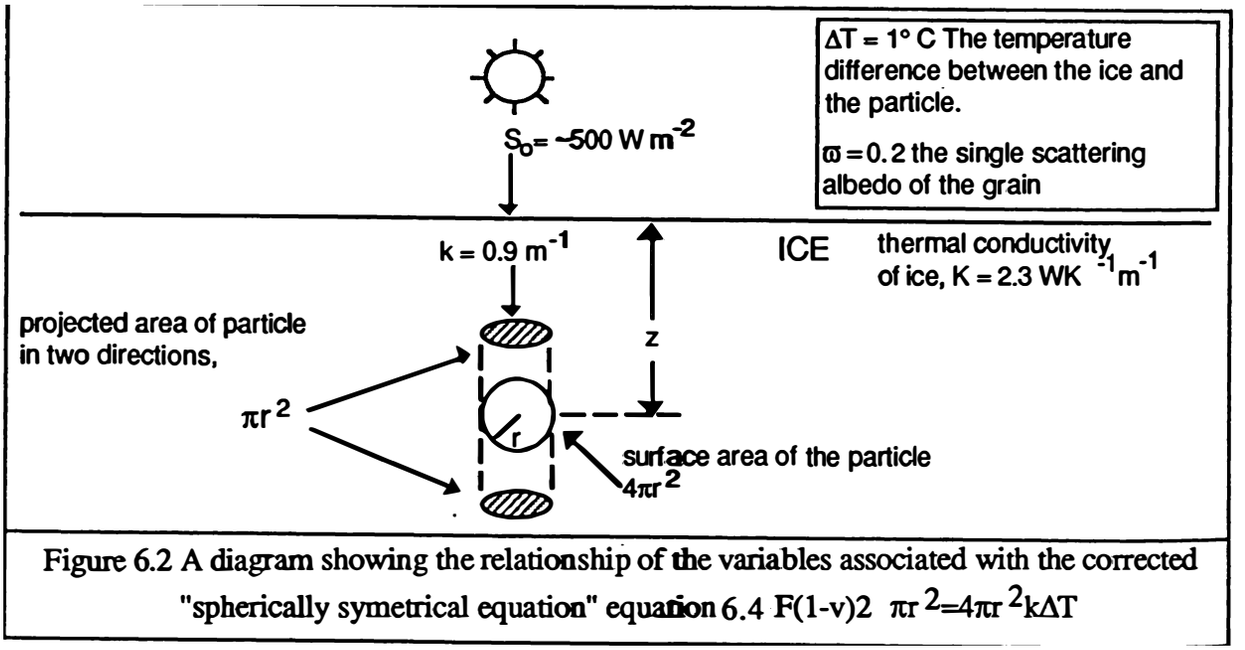

Figure 6.2 A diagram showing the relationship of the variables associated with the corrected "spherically symetrical equation" equation 6.4 $F(1-v)2\ \pi r^2 = 4\pi r^2 k\Delta T$

high ablation rates in the Dry Valleys this friction angle is unaffected by ice cementation, the individual grains being unattached to the ice core (Plate 2.9).

Nedell *et al.* (1987) observed sand sized particles on the bed of Lake Hoare, and on the basis of the work conducted by Simmons *et al.* decided that, for the sand to reach the lake bed another mechanism must be employed. They concluded that sand deposited in the lake ice during partial melting of the ice during summer at a depth of 0.5 m. Subsequently sand can migrate through water filled vertical gas channels to a depth of 2.5 m where these channels cease. Below this point the sand can only reach the bottom of the lake by vertical cracks within the ice. This mechanism eliminates the need of sand to absorb solar energy and melt surrounding ice to migrate through the lake ice cover.

Wharton *et al.* (1989) set sediment traps within Lake Hoare at sites near the glacier/lake interface and proved that sand moves through the lake ice. When the divers were placing the sediment traps under the lake ice they observed mounds of sand on the lake bed indicating a point source of sediment. While this confirms Nedell *et al.*'s theory that sand reaches the lake bed by falling through cracks in the ice it does not necessarily imply this is the only mechanism by which sand can migrate. Robert Wharton has subsequently confirmed that the sediment traps employed were placed under cracks within the lake ice (Hendy *pers. comm.*) and consequently are likely to trap only sediment accumulating by this mechanism.

The equation 6.1 in simple terms states that the heat from the sun warming the particle is equal to the heat lost by the particle by thermal conductivity. It is apparent that two corrections are required for this equation to hold true.

(1) The surface area of a sphere is $4\pi r^2$ and not $4\pi r$ as given.
(2) The projected surface area of the particle, given by πr^2 in the first part of equation 6.1 must be considered in both directions, up and down, requiring multiplication by two (fig. 6.2).

Therefore equation 6.1 should read as follows:

$$F(1-\varpi)2\pi r^2 = 4\pi r^2 K\Delta T \quad \text{.....Eqn. 6.5}$$

Using Simmons *et al.* 's values, the equation 6.5 may be rewritten as follows:

$$F \times 0.8 = 2\Delta T \times K \quad \text{.....Eqn. 6.6}$$

Equation 6.6 implies that the movement of sediment through ice is not dependent on grain size (πr^2 cancels out on both sides). If this is taken one step further, the maximum

thickness of ice that a grain may melt through can be calculated using Simmons *et al.* 's values:
Assuming $\Delta T \cong 1°$ C and using equation 6.2:

$$F = 1.5 \times 500 \times e^{-kz}$$

$$\text{Therefore} \quad 0.8 \times 1.5 \times 500 \times e^{-kz} = 2.1 \times 2.3$$

$$\text{or} \quad e^{-kz} = 7.7 \times 10^{-3}$$

$$kz = 4.8$$

$$z = 5.4 \text{ m}$$

To summarize, two important points have emerged from this analysis:

(1) The movement of sediment through ice by radiating absorbed heat is independent of grain size.
(2) The maximum ice thickness through which a particle can melt is 5.4 m.

While this model has looked at the possibility of sediment movement, it has not considered the rate at which this movement occurs, and this may be related to grain size. Larger sediment sizes will take longer to heat up sufficiently to melt surrounding ice, since, as grain size increases, the volume of the grain, and hence the mass to be heated, increases to the power of $\frac{3}{2}$ with respect to the surface area exposed to radiation. Therefore it will take longer to heat up a larger grain sufficiently to melt ice, and they may never obtain sufficient radiation to reach the point where they can melt ice due to the periodic nature of the radiation (either seasonal or climatic). Hence, with the introduction of temporal variables, it is apparent that the finer the sediment is, the more rapidly it will begin its migration through the ice and emerge into the underlying lake waters.

In addition, the continued ablation from the surface of the perennial lake ice and freezing to the base, introduces an upwards ice velocity (30-60 cm per yr.) which the downwards migration of the particle must exceed to achieve any net downward migration. The observations of large clasts supported on ice pedestals, coarse gravel and cobbles on the surface, coarse sand in lenses within the ice, and the absence of fine sands suggests that this balance is achieved on Trough Lake, with clasts of diameters of ~1-10 cm.

6.2 LABORATORY LAKE MODELING EXPERIMENT

6.2.1 Introduction.

To test the mechanisms implied for the movement of sediment through lake ice a model of an Antarctic lake was set up in a freezer.

Plate 6.1 The experiment as it was set up in the freezer on day 1. Note the distribution of sediments on the surface of the ice. There is a general scattering of material of various grain sizes over the surface with five concentrations of the same material deposited to represent concentration in ablation hollows, or as lenses within the ice.

Plate 6.2 By day 7, ice-cored domes have formed under the concentrations of sediment as ablation here is much slower than on the unprotected ice. The larger clasts are beginning to be elevated on pedestals of ice due to the protection offered by the overlying clast.

Blocks of ice 40 by 20 cm and 5 cm thick were made. It was not possible to form these ice blocks by pouring the appropriate amount of water into a container, as the resulting ice blistered and formed an irregular cracked surface, due to expansion during freezing. To counter this, the water was poured into the container in successive layers of about 0.5 cm, and to reduce thermal shock to the already frozen layers, the water used was chilled to 4°C.

To simulate the lake, a saturated salt solution was used to prevent freezing of the water, and the blocks of ice were floated on this. However this was unsuccessful as the brine warmed up under the ice while the heat lamp that was used to simulate the sun was on, melting the ice from below. In addition, as the brine was near saturation, it tended to dissolve the overlying ice. A portable freezer unit was used to keep the brine cooler and thus reduce the melting which occurred, however sufficiently sensitive control of the unit could not be maintained to keep the brine liquid.

Floating the ice on a liquid was eventually abandoned, and the block of ice was placed on four polystyrene block insulators, to prevent the supports melting the ice (fig. 6.3). This arrangement was placed under a 250 W heat lamp connected to a variable rheostat so that the heat could be controlled. The heat lamp was run at 170 V and at a height of 30 cm above the ice throughout the experiment. At this temperature melting of the ice did not occur, although sublimation did due to the very dry air in the freezer.

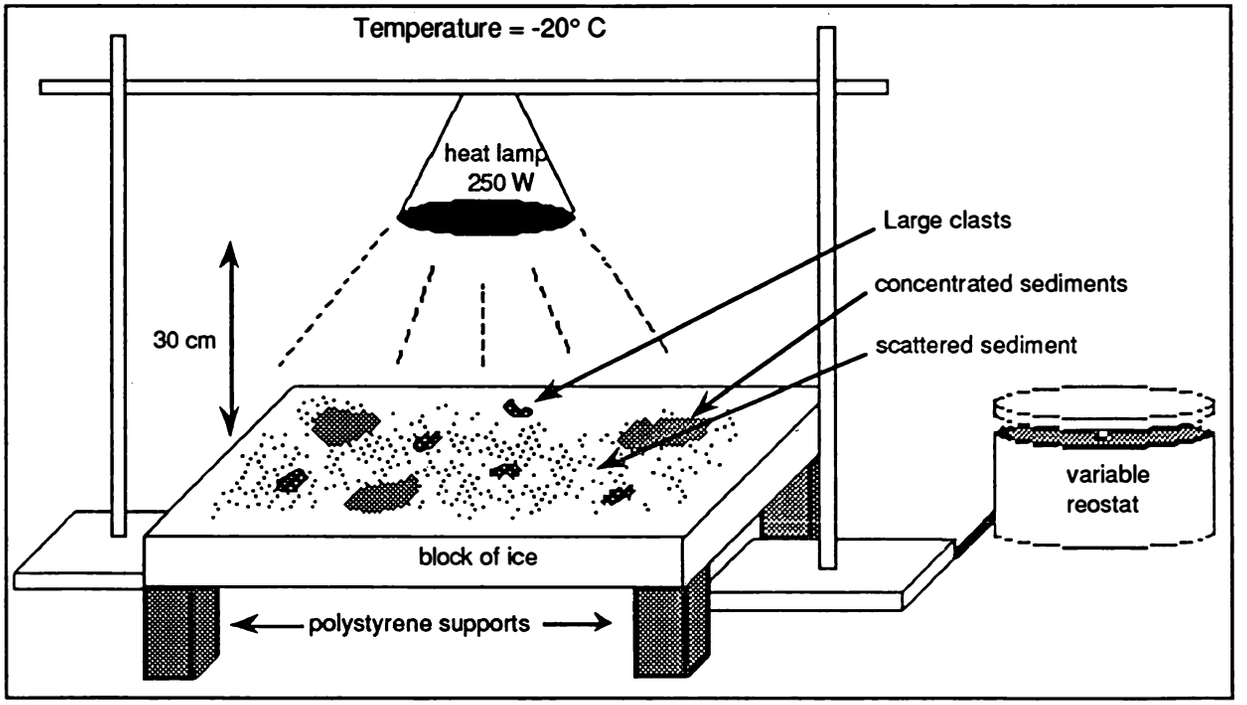

Figure 6.3 The lake model used to simulate sediment/ice interactions at Trough Lake.

Plate 6.3 By day 9 the ice-cored domes have become quite prominent and the finest sediments scattered over the ice surface have begun to move through the ice, very slowly at first, but once cocooned in ice, very rapidly. The larger clasts are very prominent on the ice surface and have shown no evidence of moving through the ice.

Plate 6.4 A side profile of the experiment at day 12 showing the profile of the ice-cored domes formed. The larger clasts are clearly visible elevated above the surface level, especially in the centre foreground. The finer sediments are below the ice surface level by this time and beginning to move through the ice.

Finally sediment from the glacier face was spread thinly over the surface of the ice, and in some areas quite thickly to represent concentrations of sediment that may form ice-cored domes (Plate 6.1).

6.2.2 Observations

The experiment was run for a period of 15 days (Plates 6.1 to 6.6) before the ice became too thin through sublimation to support the sediment. Initially no evidence of the sediment moving through the ice was observed, as the thinly spread sediment tended to sit on the surface which was gradually lowering due to sublimation. The larger grains, however were lifted up by pedestals of ice forming beneath them (Plate 6.3). This was due to the sheltering provided by these grains, protecting the ice which consequently could not sublime at the same rate as the surrounding unprotected ice. In an extreme example of this, the areas covered in concentrated sediment, intended to represent the formation of domes, quickly formed ice-cored domes within four days as the sediment protected the underlying ice (Plate 6.2).

After ten days, the finer grain sizes (medium sand or finer) began to move through the ice (plates 6.3 and 6.4), and once encased in ice moved very rapidly downward (approximately 1 cm per day).

6.2.3 Conclusions

From this experiment it has been shown that the ability of sediment to migrate through ice is size related, but not directly, as suggested by Simmons *et al.* (1984). Instead an inverse relationship exists with the fine sediments moving before any of the larger. The minimum size capable of moving through the ice suggested by Simmons *et al.* of 3 cm was found to be incorrect, since sediment of this size tended to be raised on pedestals at the ice surface due to protection offered to the ice by the grain.

Ice-cored domes were simulated by the concentration of sediment which protected the ice below, resulting in the rapid formation of dome-like features on the surface of the ice. It would appear that the ice-cored domes characteristic of many lakes in Antarctica, represent concentrations of sediment which by protecting underlying ice form domes the shape and angle of which are determined by the static friction angle of the sediments (Plate 6.5).The static friction angle can be justifiably used as a guide for the slope likely to be achieved, in the same way it is used to determine the stable slope of talus slopes. The angle of a talus slope is related to the angle of residual shear ($\emptyset_r$), a relationship that holds true provided the kinetic energy of the rock falls is not high. In general, for low energy

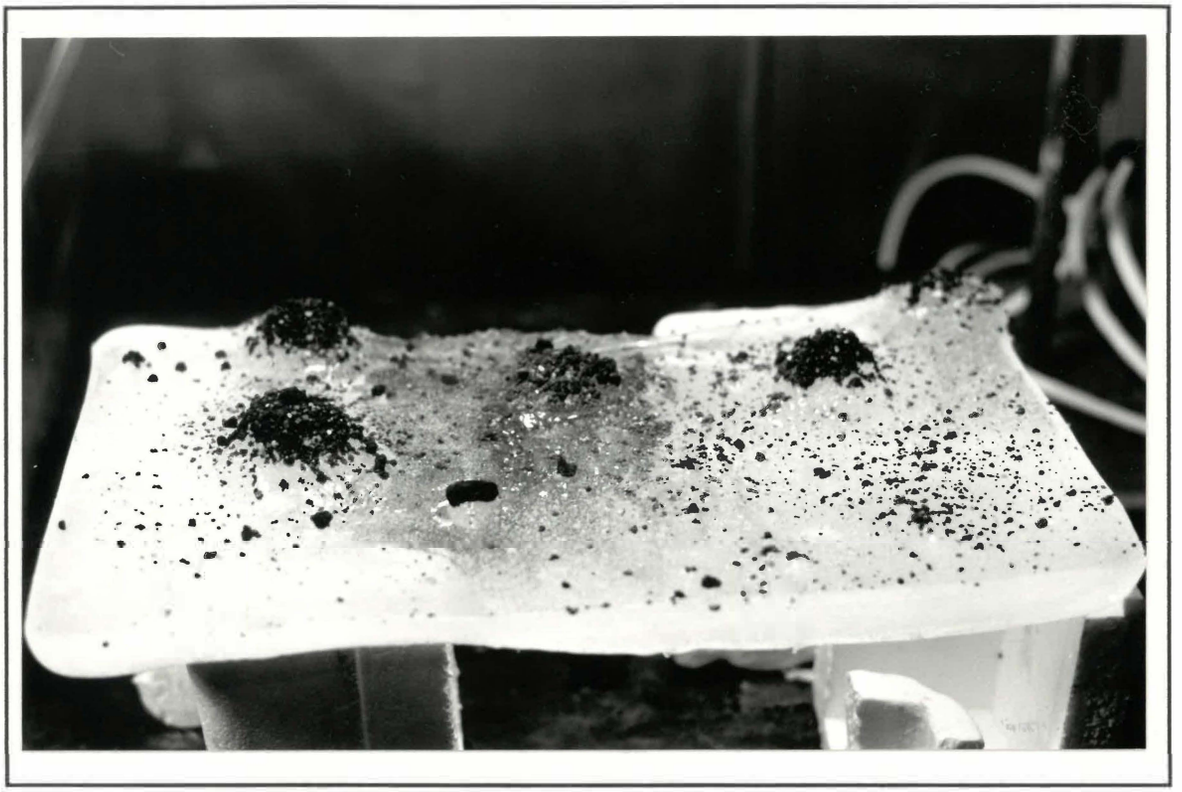

Plate 6.5 The ice surface near the end of the experiment on day 13. The ice-cored domes are still very prominent, as are the larger clasts raised on pedestals of ice. The finer sediment has either started to move through the ice, or is sitting below the ice surface in hollows formed by the sediment as it warms up and melts the underlying ice. The clear ice in the centre of the block is not due to melting but to the thinness of the ice through sublimation.

situations, such as on the lake surface, $\emptyset_r$ can be considered to be equal to the static angle of friction ($\emptyset$) (Selby, 1982).

The friction angle for a sandy gravel, which comprises most lake surface sediments considered, ranges from 32-41° depending on the initial void ratio (Selby, 1982). The higher the void ratio of the sediment, the lower the friction angle is. Therefore, with predominantly basaltic sands and gravels, the void ratio is expected to be quite high resulting in a static friction angle of about 35° (Plate 2.8). The effect of ice cementing the sediment in place is negligible, due to the high sublimation rates for the area, the sediment on such ice-cored domes is loose and uncemented (Plate 2.9). The friction angle of mixed talus as determined by Selby (1982) is 37°, a value that agrees with that for sandy gravel and the slopes observed on the ice-cored domes on Antarctic lakes.

The fine sediment observed to move through the ice, appeared to require a long period of heating, prior to melting through the ice. Once through the surface, the sediment moved at a rapid rate. The reason for this is that the proportion of the grains surface area in contact with the ice is very small initially. Once the ice begins to melt the proportion of the grain in contact with the ice increases improving the efficiency of heat transfer. When the grain is completely covered by ice it is in a closed system and although ice is a poorer insulator than air, because the air is moving, and therefore redistributing any heat generated by the grain, ice acts as an insulator improving heat transfer efficiency.

6.3 THE MODEL

Having looked at Trough Lake in some detail, a model for the deposition of sediments within the lake can be devised (fig. 6.4).

6.3.1 Lake Ice Features

At the lake/glacier contact, icebergs of glacial ice are calved off periodically and float in the lake beyond the glacier. Lake ice forms around these icebergs, and by repetitive calving, pressure is exerted on the lake ice which moves away from the glacier, with the entrained glacial icebergs imbedded within the lake ice. The regular occurrence of iceberg ridges down the lake suggests that calving must occur at regular intervals.

Over a period of time, as the icebergs move away from the glacier they ablate and release englacial material either onto the surface of the lake ice, or into the lake waters to be deposited at regular intervals as discrete mounds of sand on the lake bed. This continues until the glacial ice has been replaced by the lake ice through sublimation and melting at

the surface, and freezing on of water below. As the glacial ice above the lake ice surface ablates the englacial material is exposed, and forms steep-sided cones of debris on either side of the ridge (Plate 2.7) similar in appearance to talus slopes. These cones are usually ice-cored, the blanket of sediment protecting the underlying ice from the dry atmosphere, and thus preventing ablation.

The different sediment characteristics observed on either side of the ridges are due to the winds that blow either from the south down the valley or from the north up the valley. The katabatic southerly winds from the East Antarctic Ice Sheet are much stronger than the northerlies blowing from the McMurdo Ice Shelf and the tongue of the Koettlitz Glacier. As a result fines on the southern side of the ridges are removed and deposited in the lee on the northern side of the ridge during the strong southerlies. The reverse occurs during lighter northerly winds, but to a lesser extent.

With distance from the glacier, the ridges become smaller due to the longer period for which they have been exposed to the dry atmosphere. As a result the ridges take on a more subdued relief which does not provide the protection and shelter to the surface sediments offered by the large ice ridges. As the ridges disappear and are replaced by lake ice, the surface sediments begin to melt through the lake ice by absorbing solar energy and emitting heat. The sediments are not likely to migrate through the glacial ice as it is opaque and therefore the solar radiation cannot penetrate as far as through the clear lake ice. This results in the formation of the second zone of sediment on the lake ice characterized by ablation hollows with entrained sediments. Any large blocks in the area are lifted above the ice surface on pedestals of ice protected from sublimation by the rock.

Sublimation is related to the surface area exposed to the atmosphere, and when a large block is placed on top of the ice it reduces the sublimation at this point. As a result, the balance between sublimation and freezing on of water at the base of the lake ice is upset. As freezing to the base is occurring at a greater rate than sublimation at the surface the block is raised up on a pedestal of ice. This will continue until the sublimation rate for the exposed pedestal is equal to the freezing on below. Therefore, the larger the block, the greater the loss of subliming surface area, and the higher the ice pedestal can become until a balance is re-established (Plate 5.1)

The sediment trapped in the ablation hollows will melt through the lake ice at a rate inversely proportional to grain size, the smallest sediments moving the fastest. With time, aeolian and/or fluvially derived sediment can be trapped in the ablation hollows, and this too will move through the lake ice. The rate of sediment movement is related to the amount of solar energy reaching it. Therefore, at some point, the rate of movement will

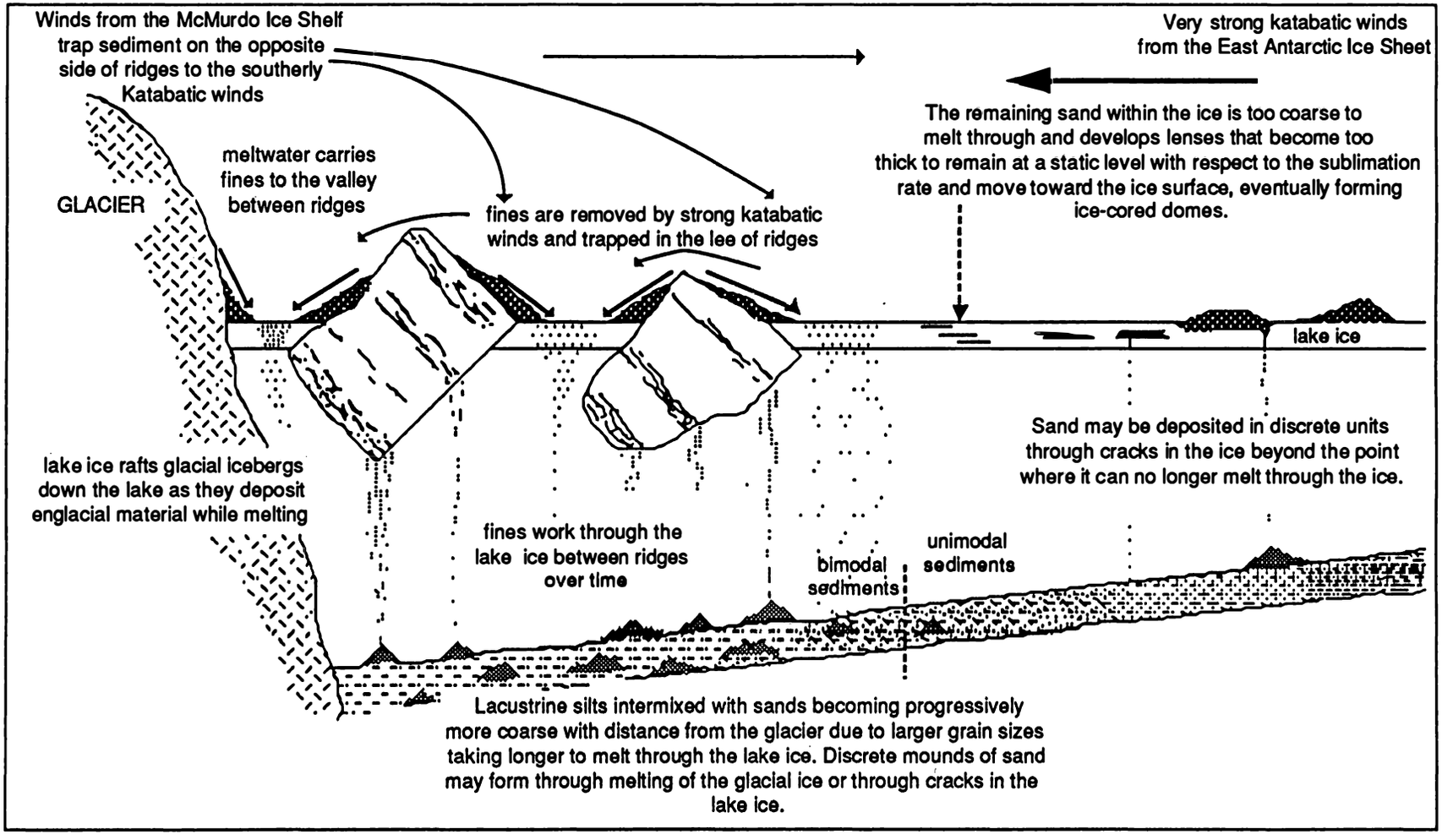

Figure 6.4 The model for sand/ice interactions and sedimentation within a pro-glacial, perenially ice covered, proglacial lake based on Trough Lake, McMurdo Sound , Antarctica.

decrease to the point where, due to decreasing solar radiation with depth, it is equal to the upward rate of ice migration due to sublimation and freezing of lake water (fig. 1.1). When the downward movement of sediment is equal to the upward movement of ice, lenses of similar sized sediment form within the lake ice. As this occurs successive lenses of sediment develop, either through additional sediments becoming trapped in the ablation hollows, or the various fractions of the glacial derived sediments that are separated into layers due to their relative migration rates within the ice. These lenses further restrict the light's ability to reach the lower lenses of sediment which will no longer be able to maintain their relative position within the ice with respect to the sublimation rate. Consequently sediments begin to move upward, until they telescope together forming even more dense blankets of sediment in the ice, which migrate upward at ever quicker rates.

The result of this is the eventual re-emergence of the sediment at the surface of the lake ice in the form of a low mound of sediment. As the sediment toward the centre of such a mound protects the underlying ice to a greater extent than that at the edges, the centre will continue to move upward forming an ice-cored dome characteristic of the third surface sediment zone (Plate 2.8). The slope of this dome will be determined by the friction angle of the sediment, and therefore achieves a maximum of about 35° before the sediment rolls away re-exposing the ice core to the atmosphere. When this happens ablation of the core lowers the angle of the ridge until more sediment is bought up from below to replace that lost, or if there is no sediment below, an equilibrium between the slope angle and the sublimation rate is achieved. The result of this activity over a longer period of time can be observed at Lake Miers (fig. 1.2), where the lake is no longer attached to the glacier and therefore the ice rafted debris is static. Over time, through continued exposure of the ice core domes to the atmosphere, the domes have been subdivided into smaller ones as the centres ablate leaving two smaller domes. As the lake has no sediment supply from a glacier most of the material within the ice will be deposited on the surface through sublimation, resulting in the entire lake surface being covered in apparently chaotic ice-cored domes.

With time these domes on a proglacial attached lake, such as Trough Lake, will be dumped off the lake ice, as drift. This can be observed in the case of the core from hole #12 at the southern end of the lake where a lense of glacial drift occurs between two layers of lacustrine silt indicating dumping of surface sediments during a period where the lake level was lower than present. In addition ice-rafted domes, related to previous lake level highs are scattered around the floor of Pyramid Trough.

6.3.3 Lake Bed Features

Discrete mounds of sediment form on the lake bed due to melting of the icebergs. This can only occur while the icebergs are present, hence beyond the first surface sediment zone, this type of sedimentation of former englacial material can no longer occur. In addition to deposition via glacial ice melting, similar discrete packages of sediment may be deposited through cracks in the lake ice. These cracks open up periodically due to the pressure exerted on the lake ice by the glacier. Through these cracks sediment either within the ice, or on the ice surface, may fall to form discrete mounds of sediment on the lake bed. As these cracks form in similar places in the ice each season (C. Hendy *pers comm.*) and the lake ice is moving away from the glacier, a series of mounds will be deposited down the lake by any one crack. These mounds may cover or be covered by silts due to the normal lacustrine sedimentation, and any other sand mound that forms as the result of a crack forming in a similar position in the lake ice relative to the lake bed at a latter date.

Sediment will migrate downward within the lake ice at a rate relative to its grain size and grains fine enough to melt all the way through the lake ice will be deposited on the lake bed. since this occurs at a rate relative to grain size, the finer sediment will melt through the ice the quickest, and therefore be deposited closest to the glacier. The result is a lake bed covered in bimodal sediments of lacustrine silt, and, with increasing distance from the glacier, progressively coarsening sands. Within, or on top of this, will be mounds of much coarser material deposited either by icebergs, or through cracks in the ice. At some point the sediment within the ice will be too coarse to melt all the way through, and will therefore be trapped within the ice. Further from the glacier than this point only unimodal sands will occur. This point is about 1 km south of the glacier on Trough Lake (fig. 3.2).

CHAPTER SEVEN

CONCLUSIONS

7.1 TROUGH LAKE: A MODEL FOR PROGLACIAL SEDIMENTATION IN POLAR REGIONS

Trough Lake has been used in this study as a model for proglacial lake sedimentation in polar regions, answering a number of questions on how deep proglacial lakes operate. With this information a working model for sedimentation occurring within such systems has been derived, and therefore facies models for former proglacial lakes in the McMurdo Sound area of Antarctica can be postulated. This is of particular relevance when examining evidence for proglacial lakes that formed by the Ross Ice Sheet of Denton *et al* (1984) during past glacial events (eg.Glacial Lake Trowbridge in the Miers Valley [Péwé, 1960; Clayton-Greene, 1986] Glacial Lake Washburn in the Taylor Valley [Péwé, 1960; Stuvier *et al.*, date] Glacial Lake Muller in the Davis Valley.[Péwé, 1960] and Glacial Lake Howard in the Garwood Valley [Péwé, 1960]).

A number of important points have been raised, the first of which is the relationship between the lake ice and the glacier. It is apparent that the glacier and the lake ice are in intimate contact, establishing a continuity between the two types of ice. This, together with confirmation that the lake ice is moving (on Trough Lake at about 18 m per annum) away from the glacier, front necessitates speculation on how this is achieved.

Initially, there is the pressure exerted by the glacier as it flows into the lake forcing the lake ice ahead of it. This mechanism, however, cannot explain the addition of lake ice to the ice sheet as is indicated by the movement of drift on the surface.

During the winter, when the moat ice is frozen and anchoring the lake ice, the applied pressure of the glacier is taken up in the comparatively thin lake ice as compressional folds. When the moat ice melts out during summer, the lake ice relaxes and movement of the whole ice sheet takes place. The forward-moving ice is replaced by icebergs that calve from the glacier snout, which in turn are ultimately replaced by lake ice as their upper surfaces are removed by ablation and lake ice freezes on beneath.

Calving of icebergs is facilitated initially by fissures and then crevasses, and eventually discrete icebergs form orthoganal to the accelerated flow into the lake. Lake water can flow into any space thus created below water level. The surface of this lake water

immediately freezes, except for very brief periods in midsummer when the air temperatures exceed melting point. Since the lake ice always provides some resistance against which the icebergs must move, movement will take place while contact remains between glacier and iceberg.

The cracks formed in the glacial ice act as melt water stream channels and accumulate sediment, comprising former supra- and englacial material which is blown or washed into them as melting of the glacial ice occurs. This is rafted onto the lake as the icebergs are calved from the snout of the glacier. Additional sediment is accumulated as the icebergs ablate leaving englacial material behind. This results in ridges of glacial ice, with their lower slopes protected by sediments draped over them, as found in the first surficial sediment zone described in Chapter 2.

An important feature of the manner in which these icebergs melt, is their ability to bring englacial material to the lake surface from below the water level. This is achieved by ablating ice from the surface at a much greater rate than melting of the glacial ice from below. This is due to the very cold water in the lake, particularly close to the glacier, that has little ability to melt the ice. In fact it is likely that lake water is freezing onto the icebergs in a similar manner to its freezing onto the base of the lake ice.

The lack of glacial ice melting below the water level is aided by the reverse convection cell operating within the lake (fig. 5.2), with relatively warm dense waters flowing toward the glacier at depth, where they cool and rise toward the surface. The cool water (at about 0°C) then moves away toward the end of the lake below the lake ice. The result of this convection cell is a very well mixed lake, with little variation in temperature or chemistry throughout.

As the lake ice and associated sediments move away from the glacier, the sediments are reworked by the melting of glacial ice, or aeolian processes, that spread them over the lake surface. The prevailing southerly winds tend to concentrated the fines around the glacier in the shelter provided by the glacial ice ridges. In addition, it has been demonstrated that the very small grain sizes can migrate through the lake ice, at a rate inversely proportional to their grain size, by absorbing solar energy and re-emitting it as heat. Therefore sorting of the sediments is occurring with increasing distance from the glacier, with the fines being removed from the system through the lake ice, leaving behind a progressively coarsening drift.

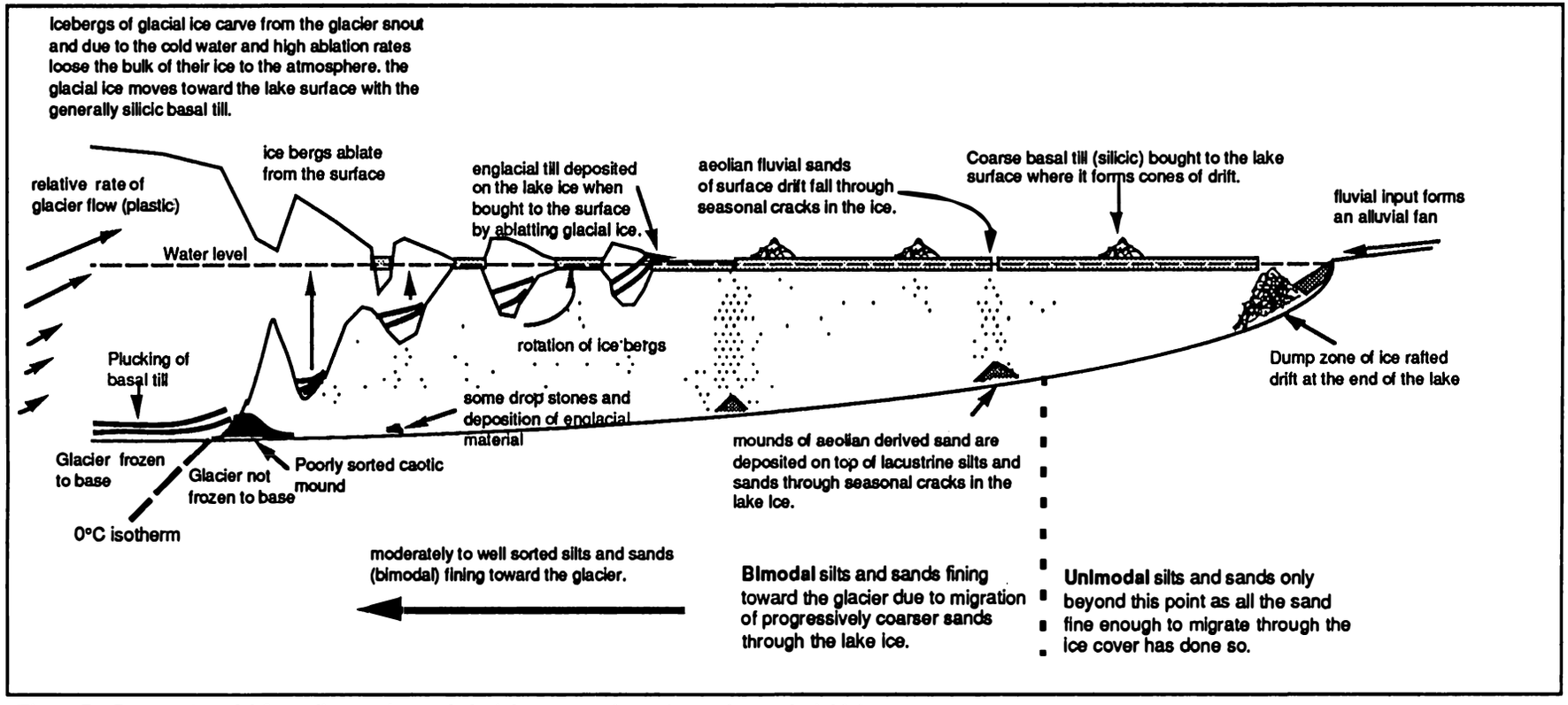

Figure 7.1 Proposed model for sedimentation and glacial processes in an Antarctic proglacial lake.

Although the finer grains can melt through the lake ice, the coarser material may only be able to melt part way, forming stratified lenses of graded material within the ice. As this sediment melts into the ice, ablation hollows form, and these create additional traps for aeolian, as well as fluvial sediments, that add more material to the system than would be available from the icebergs alone.

Once enough material has accumulated within the ice, interception of the solar radiation by overlying sediments means that the downward movement of the lenses of debris will no longer be able to keep pace with ablation of the surface and freezing to the base of the ice. Hence they begin to move toward the surface. This results in a "concertina" effect with successive lenses higher up the ice column being combined into one layer. Eventually, if enough lenses are superimposed, the sediment acts as if it were a single clast and protects the underlying ice from ablation. As a result this ice will continue to be uplifted as freezing to the base continues, until the ice surface is reached and the covering debris begin to slide off the edges causing the ice core to be exposed. Constant reworking of the material results in the domes and ridges that can be seen on the surface of many lakes in the McMurdo Sound region (e.g. Lake Miers [Clayton-Greene, 1986 and Clayton-Greene et *al.*, 1987]).

It was observed that drift on the surface of Trough Lake differed in lithology depending on location. Close to the glacier, especially toward the east of the lake, the drift was predominantly basaltic. Close to the western interface between the glacier and the lake, there was markedly less drift, except for aeolian sands in sheltered locations, but clasts of silicic rocks up to boulder size were present. With increasing distance from the glacier the abundance of silicic clasts, especially of cobble and gravel size increased. Rocks of this composition form the basement for much of the Koettlitz Glacier catchment and locally form the basement of Pyramid Trough. This material was too large to melt through the ice cover, yet it did appear to be concentrated in discrete units. The only place similar material could be observed was surrounding the lake as a silicic drift, although some silicic material was to be found on the lake ice. It is concluded therefore that this material had its origin at the base of the glacier where it was pushed in front of the advancing glacier. Where a cold based glacier flows onto an unfrozen surface, such as a lake filled valley, it will freeze onto it's base and this will allow plucking of material into the glacier as basal till. Englacial till will require a source much further from the glacier's terminus, as sufficient distance is needed to allow more ice to be mixed beneath the till. As the icebergs calve from the glacier snout some of this material will be dropped into the lake as drop stones, but much will be lifted up with the glacial ice (fig 7.1) where it is transported toward the surface as ablation removes the glacial ice above water level.

As this material is too coarse to be able to move downward by absorption of solar energy, it migrates upward through the ice, and upon meeting surficial sediments moving down becomes intermixed and moves upward as a unit as described above, thus forming the dominant surficial drift to the west and south of the lake.

7.2 IMPLICATIONS FOR POLAR PROGLACIAL FACIES.

With this information a model for facies analysis of the sediments left by former proglacial lakes can be devised.

At the maximum extent of the glacier there will be a ridge of intermixed lacustrine silts and glacial material that was shoved in front of the glacier where the glacier, was not frozen to its base. This material may retain some of the stratigraphy of the former lake bed, but it will be chaotic and not necessarily in stratigraphic order.

Beyond this ridge, marking the maximum advance of the glacier, the former lacustrine sediments will have been removed by the strong winds of the area unless they have been protected by overlying coarse material from one of the following sources (fig 7.2):

-drop stones from the melting glacial icebergs
-material falling through cracks in the lake ice
-dump zones of ice rafted material from the extremes of the lake
-let down of ice rafted material with draining of the lake.

Drop stones will be characterized by impact features in the lacustrine sediments and, where present, the algae within them. This zone will be restricted to the maximum advance of the glacial ice ridges within the lake ice.

Material falling through cracks in the ice is likely to be well sorted and finer, and therefore less likely to show impact features. Mounds of sand covering lacustrine sediments and algae will occur as ridges scattered over the valley floor. Simmons *et al*. (1986) while diving in Lake Hoare, noted the occurrence of these features beneath cracks in the lake ice. As the lake ice is moving away from the glacier so will the associated cracks, implying that old deposits may have younger ones precede them as new cracks form when older ones are lost at the extremities of the lake. This results in the age of these ridges exhibiting a random distribution with no sensible chronological order.

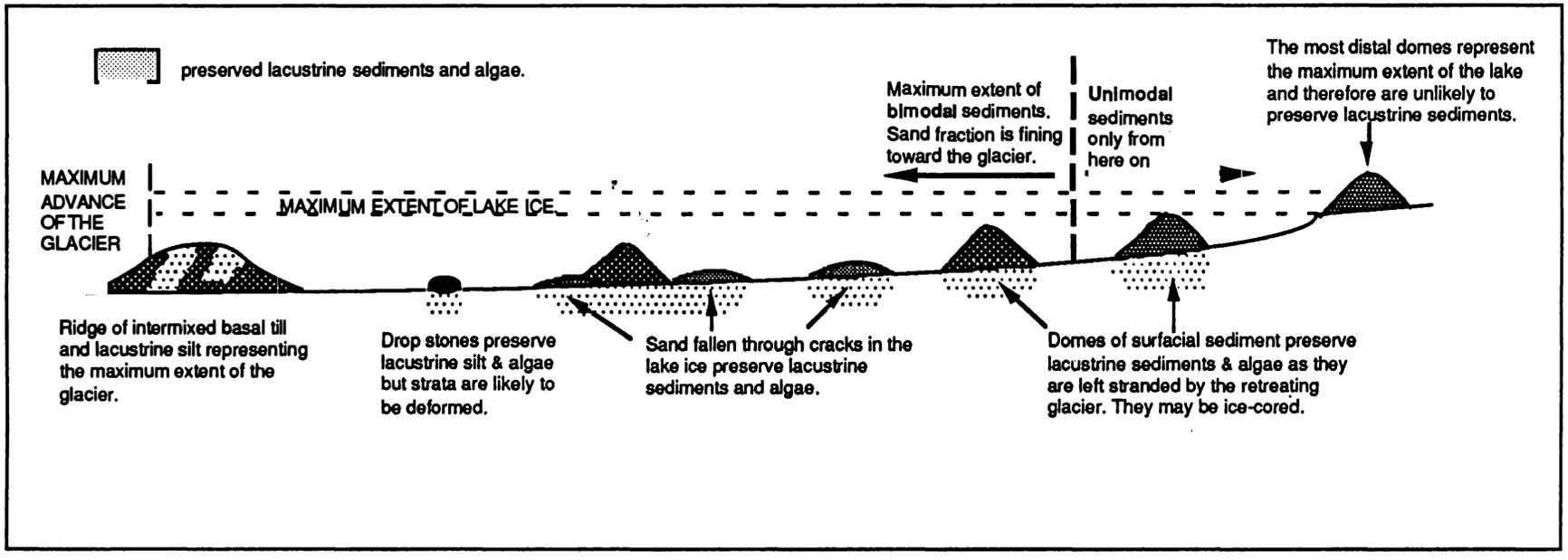

Figure 7.2 Facies model for former proglacial lacustrine environments in polar regions. Lacustrine sediments are only preserved where protected by coarse material .

The ice cored domes on the lake surface will cover underlying lacustrine sediments as they are dumped from the extremes of the glacier, or left stranded by a retreating lake on the withdrawal of the glacier (Clayton-Greene *et al.*, 1987). Depending on age and thickness of the protecting drift, these domes may or may not be ice-cored. Where preserved, these lacustrine sediments will show a bimodal grain size distribution, up to the maximum extent of the zone within the lake ice that sand can melt through.

Toward the glacier, the bimodal sediments will become finer as the time taken for sand to migrate through the ice is size related. Beyond the maximum extent of the bimodal zone the lacustrine sediments will be unimodal. Thus it is apparent, that grain size distribution analysis of proglacial lacustrine sediments, and their associated drift, can be very useful in determining the size and structure of former Antarctic proglacial lakes.

In addition to the sediments deposited by the lake there will be some material locked within the lake ice that, on retreat of the glacier, will be released as a drift of sands that are likely to be too fine to remain in an area where the winds are strong.

REFERENCES

Anderton, P. W. and Fendwick, J. K. 1976. Hydrological research Dry Valleys, Antarctica, 1973-74. *Annual Report 37, N. Z. Ministry of Works and Development,* Christchurch, 42 p.

Angino, E. E. and Armitage, K. B. 1963. A geochenical study of lakes Bonney and Vanda, Victoria Land, Antarctica. *J. Geol.*, 71(1). p. 89-95.

Armitage, K. B. and House, H. B. 1962. A liminological reconnaissance in the area of McMurdo Sound, Antarctica, *Liminol. Oceanogr.*, 7(1), p. 36-41.

Ashley, G. M., Shaw, J. and Smith, N. D., (eds) 1985. Glacial Sedimentary Environments.Society of Paleontologists and Mineralogasts, Tulsa, OK. (SEPM Short Course No. 16) p. 170.

Bell, R. A. I., 1967. Lake Miers, South Victoria Land, Amtarctica. *New Zealand Journal of Geology and Geophysics,* v. 10(2), p. 540-556.

Blank, H. R., Cooper, R. A., Wheeler, R. H. and Willis, I. A. G., 1963. Geology of the Koettlitz-Blue Glacier Region, Southern Victoria Land, Antarctica. Transactions of the Royal Society of New Zealand, Geology, v. 2(5), p. 79-100.

Bradley, J. and Palmer, D.F., 1967. Ice-cored Moraines and Ice Diapirs, Lake Miers, Victoria Land, Antarctica. *New Zealand Journal of Geology and Geophysics,* v. 10(2), p.599-623.

Bull, C., 1966. Climatological Observations in Icce-free Areas of Southern Victoria Land, Antarctica. In J. Morton (Ed.), *Studies in Antarctic Meterology.* Antarctic Research Series No. 9, American Geophysical Union. p.177-194.

Cartwright, K. and Harris, H. J. H. 1981. Hydrology of the Dry Valley Region, Antarctica. In L. D. McGinnis (Ed.). *Dry Valley Drilling Project.* Antarctic Research Seris, American Geophysical Union p.193-214.

Clayton-Greene, J. M., 1986. *Proglacial Sedimentation of Late Wisconsin Age in Miers Valley, Antarctica.* An unpublished M. Sc. thesis, University of Waikato. 130 p.

Clayton-Greene, J. M. Hendy, C. H. and Denton, G. H., 1987. The origin of drift mounds in Miers Valley, Antarctica. *Antarctic Journal of the U. S.* 1987 review. p. 59-61.

Charlesworth, J. K., 1957. *The Quaternary Era- vol 1.* Edward Arnold, London 591 p.

Chinn, T. J. H., 1983. Hydrology and Climate in the Ross Sea Area. *Journal of the Royal Society of New Zealand.* v.11, p. 373-386.

Decker, E. R., and Bucher, G. J., 1982. Geothermal Studies in the Ross Island - Dry Valley Region- review paper. In C. Craddock (ed.) *Antarctic Geoscierce-vol 1.*, University of Wisconsin Press, Madison. p. 884-894.

Denton, G. H. and Huges, T. S., 1981. *The Last Great Ice Sheets.* Wiley- interscience, New York. 484 p.

Denton, G. H., Prentice, M. L., Kellogg, D. E. and Kellogg, T. B. 1984. Late Tertiary history of the Antarctic ice sheet: Evidence from the Dry Valleys. *Geology* v. 12, p. 263-267.

Folk, R. L. and Ward, W. C., 1956. A Study in the Significance of Grain Size Parameters. *Journal of Sedimentary Petrology,* v. 27, p. 3-26.

Goldich, S. S., Treves, S. B., Suhr, N. H. amd Stuckless, J. S., 1975. Geochemistry of the Cenozoic Volcanic Rocks of Ross Island and Vicinity, Antarctica. *Jounal of Geology,* v. 83(4), p. 415-435.

Goldman, C. R., Mason, D. T. and Hobbie J. E. 1967. Two Antarctic Desert Lakes. *Liminol. Oceanogr.* v. 12 p. 295-310.

Gumbley, J. W., 1975. *A Sedimentological Study of Three Saline Lakes in the Dry Valleys of Victoria Land, Antarctica.* An Unpublished M.Sc Thesis, University of Waikato. 140 p.

Henderson, R. A. Prebble, W. H., Hoare, R. A., Popplewell, K. B., House, D. A. and Wilson, A. T., 1966. An Ablation Rate For Lake Fryxell, Victoria Land, Antarctica. *Journal of Glaciology* v. 6(43) p. 129-133.

Hendy, C. H., Selby, M. J. and Wilson, A. T., 1972. Deep Lake , Cape Barne Antarctica. *Liminology and Oceanography.* v. 17(3), p. 356-362.

Hoare, R. A., Popplewell, K. B., House, D. A., Henderson, R. A., Prebble, W. H., and Wilson, A. T., 1964. Lake Bonney, Taylor Valley, Antarctica: A Natural Solar Energy Trap. *Nature.* v. 202, p. 886-888

Hoare, R. A., Popplewell, K. B., House, D. A., Henderson, R. A., Prebble, W. H., and Wilson, A. T., 1965. Solar heating of lake Fryxell, a permantly ice-covered Antarctic lake. *J. Geophys. Res.*, 70, p. 1555-1558.

House, D. A., Hoare, R. A., Popplewell, K. B., Henderson, R. A., Prebble, W. H., and Wilson, A. T., 1966. Chemistry in Antarctica. *Journal of Chemical Education.* v. 43 p. 502-505.

Judd, F. M., 1986.*The Cronology of the Ross II Glaciation an Antarctic Glaciation of Illinoian Age*. Unpublished M.Sc Thesis, University of Waikato. 227 p.

Laurence, M. J. F., 1982. *Origin and Occurrence of Antarctic Lacustrine Carbonates, with Special Reference to Lake Fryxell, Taylor Valley, Antarctica.* Unpublished M. Sc. thesis, University of Waikato. 246 p.

Lyon, G. L., 1979. Some Aspects of the Ice Topography of Trough Lake, Southern Victoria Land, Antarctica (note). *New Zealand Journal of Geology and Geophysics.* v. 22(2), p.281-284.

MacDonald, G. A.and Katsura, T., 1964. Chemical Composition of Hawaiian Lava. *Journal of Petrology* v. 1 p. 172-177.

McIver, R. R. and Gevers, T. W., 1970, Volcanic Vents Below the Royal Society Range, Cental Victoria Land. *Trans. Geol. Soc. South Africa* v. 73 p. 65-88.

McKay, C. P., Clow, G. D., Wharton, R. A. and Squyers, S. W. 1985. Thickness of Ice on Perennially Frozen Lakes. *Nature*, v. 313(14), p. 561-562.

Moiola, R. J., and Weiser, D., 1968. Textural Parameters: an evaluation. *Journal of Sedimentary Petrology*, v. 38, p. 45-53.

Neall, V. E. and Smith, I. E., 1967. The McMurdo Oasis *Tuatara* v. 15 p 152-164

Nedell, S. S., Anderson, D. W. Squyres, S. W. and Love, G. 1987. Sedimentation in ice-covered Lake Hoare, Antarctica. *Sedimentology* v. 34 p. 1093-1106.

Nichols, R. L. 1963. Origin of chemical stratification in Lake Vanda, South Victoria Land. Polar Record. v. 11, p.751-752.

Péwé, T. L., 1960. Multiple Glaciations in the McMurdo Sound Region Antarctica, -A Progress Report. *Journal of Geology.* v. 68 p. 498-515.

Ragotzkie, R. A. and Likens, G. E. , 1964. The Heat Balance of Two Antarctic Lakes. *Liminology and Oceanography*. v. 9 p. 412-425.

Rhodes, J. J., Armstrong, R. L. and Warren S. G., 1987. Mode of Formation of "Ablation Hollows" Controlled by Dirt Content of Snow. *J. Glaciology* v. 33(114), p. 135-139.

Selby, M. J. 1982. *Hillslopes Materials and Processes*. Oxford, Oxford University Press 264 p.

Simmons, G. M. (Jr.), Wharton, R. A., McKay, C. P., Nedell, S. and Clow, G. 1986. Sand/ice interactions and sediment deposition in predominantly ice-covered Antarctic lakes. *Antarct. Journ. U. S.* v. 21(#5), p. 217-220.

Stuvier, M., Denton, G. H. Hughes, T. J. and Fastook, J. L. 1981. The History of the Marine Ice Sheet in West Antarctica During the Last Glaciation: A Working Hypothesis. In G. H. Denton and T. S. Huges (Eds.), *The Last Great Ice Sheets*. Wiley-interscience, New York. p. 319-436.

Thompson, D. C., Craig, R. M. F. and Bromley, A. M., 1971, Climate and Surface Heat Balance in an Antarctic Dry Valley. *New Zealand Journal of Science,* v. 14 p. 245-251.

Wharton, R. A. (Jr.), Simmons, G. M. and McKay, C. P. 1989. Perennially ice-covered Lake Hoare, Antarctica: Physical Environment, Biology, and Sedimentation. *Hydrobiologia* v. 172, p. 305-320.

Wilson, A. T., 1967/a. The Lakes of the McMurdo Dry Valleys. *Tuatara,* v. 15 p. 152-164.

Wilson, A. T., 1967/b. Trace Element Content of Antarctic Lakes. *Nature*. v. 213, p. 167-168.

Wilson, A. T., 1981. A Review of the Geochemistry and Lake Physics of the Antarctic Dry Areas. In L. D. McGinnis (Ed.). *Dry Valley Drilling Project*. Antarctic Research Seris, American Geophysical Union p.185-192.

Wilson, A.T. Hendy, C. H., Healy, T. R., Grumbley, J. W., Field, A. B. and Reynolds, C. P., 1974. Dry Valley Lake Sediments: a Record of Cenozoic Climatic Events. *Antarctic Journal of the United States. Antarctic Journal of the United States.*. 9 p. 134-135.

Wright, A. C. 1978. A Reconnaissance Study of the McMurdo volcanics north-west of the Koettlitz Glacier. *N. Z. Antarctic Record*, v. 1 (#2), p. 10-15.

APPENDIX ONE

SPREAD SHEET FOR GRAIN SIZE DISTRIBUTION ANALYSIS.

APPENDIX ONE -SPREAD SHEET USED TO CALCULATE CORE GRAIN SIZE DISTRIBUTION PARAMETERS

	A	B	C	D	E	F	G	H
1							PHI SIZE	SAMPLE %
2			SAND WGHT=	=F20			-2.0	=F6
3			WGHT BKR=		% ERROR=	=((D18/D2)-1)*100	-1.5	=F7
4							-1.0	=F8
5	PHI SIZE	BKR + SAND	WT SAND	CUM WT	CUM%	%	-0.5	=F9
6	-2.0		=B6-D3	=SUM(C6)	=D6/F22*100	=C6/F22*100	0	=F10
7	-1.5		=B7-D3	=SUM(C6:C7)	=D7/F22*100	=C7/F22*100	0.5	=F11
8	-1.0		=B8-D3	=SUM(C6:C8)	=D8/F22*100	=C8/F22*100	1.0	=F12
9	-0.5		=B9-D3	=SUM(C6:C9)	=D9/F22*100	=C9/F22*100	1.5	=F13
10	0.0		=B10-D3	=SUM(C6:C10)	=D10/F22*100	=C10/F22*100	2.0	=F14
11	0.5		=B11-D3	=SUM(C6:C11)	=D11/F22*100	=C11/F22*100	2.5	=F15
12	1.0		=B12-D3	=SUM(C6:C12)	=D12/F22*100	=C12/F22*100	3.0	=F16
13	1.5		=B13-D3	=SUM(C6:C13)	=D13/F22*100	=C13/F22*100	3.5	=F17
14	2.0		=B14-D3	=SUM(C6:C14)	=D14/F22*100	=C14/F22*100	4.0	=F18
15	2.5		=B15-D3	=SUM(C6:C15)	=D15/F22*100	=C15/F22*100	4.5	=H26
16	3.0		=B16-D3	=SUM(C6:C16)	=D16/F22*100	=C16/F22*100	5.0	=H27
17	3.5		=B17-D3	=SUM(C6:C17)	=D17/F22*100	=C17/F22*100	5.5	=H28
18	4.0		=B18-D3	=SUM(C6:C18)	=(D18/F22*100+F25)/2	=H25	6.0	=H29
19					MUD ERROR (%)=	$\left(\frac{F21}{D20-F20}-1\right)\times 100$	7.0	=H30
20			SAMPLE (g)		SAND (S) =		8.0	=H31
21			CALGON (g)=		+MUD (F)=	=D25*50-1	9.0	=H32
22					TOTAL=	=F21+F20	10.0	=H33
23								
24	BEAKER No.	WTS S&B	WT BKR	SAMPLE WT	WT*50	CUM%	PHI SIZE	SAMPLE %
25				=B25-C25	=50*D25-D21	=100-(E26/F22)*100	4.0	=E18-E17
26				=B26-C26	=50*D26-D21	=100-(E26/F22)*100	4.5	=F26-F25
27				=B27-C27	=50*D27-D21	=100-(E27/F22)*100	5.0	=F27-F26
28				=B28-C28	=50*D28-D21	=100-(E28/F22)*100	5.5	=F28-F27
29				=B29-C29	=50*D29-D21	=100-(E29/F22)*100	6.0	=F29-F28
30				=B30-C30	=50*D30-D21	=100-(E30/F22)*100	7.0	=F30-F29
31				=B31-C31	=50*D31-D21	=100-(E31/F22)*100	8.0	=F31-F30
32				=B32-C32	=50*D32-D21	=100-(E32/F22)*100	9.0	=F32-F31
33				=B33-C33	=50*D33-D21	=100-(E33/F22)*100	10.0	=F33-F32

SAMPLE ERROR (%)= $\left(\frac{(D18-F21)}{F20}-1\right)\times 100$

APPENDIX TWO

GRAIN SIZE DISTRIBUTION RESULTS FROM THE UNIVERSITY OF WAIKATO'S RAPID SEDIMENT ANALYSIS PROGRAM RSA 5.5 A.

Particle Size Analysis
sediment collected from station 12

Sample Identification: TS/87/05

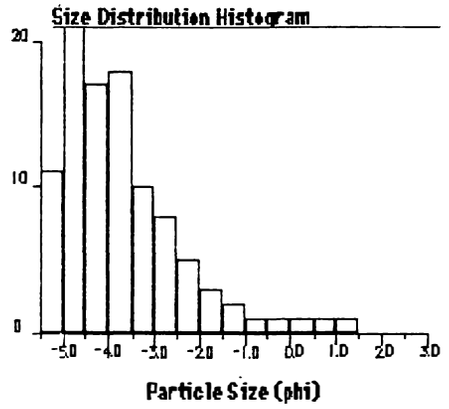

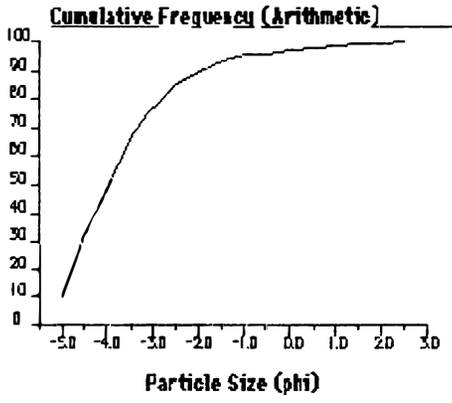

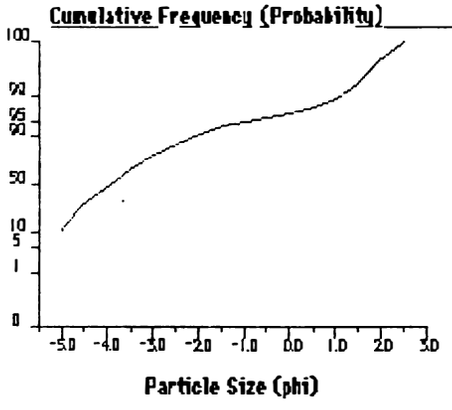

Particle Size (phi) Results Summary

Textural Size Classes

Gravel= 95.02% Sand= 4.98% Silt= 0.00% Clay= 0.00%

Gravel bearing detrital sediment

Gravel

Moment Method Parameters

Mean= -3.69 Sorting= 1.36 Skewness= 1.58 Kurtosis= 6.12

Graphical Method Parameters (Folk & Ward, 1957)

Mean= -3.80 Sorting= 1.18 Skewness= 0.35 Kurtosis= 1.05

Median= -3.97 C= -5.00 D35= -4.40 D65= -3.55

Textural Description

Poorly sorted, Strongly fine skewed, Mesokurtic

Data Summary

Size (phi)	Size (mm)	Cumulative Weight (g)	Interval Frequency (%)	Cumulative Frequency (%)
-5.00	3.20e+1	407.44	10.79	10.79
-4.50	2.26e+1	1194.12	20.83	31.62
-4.00	1.60e+1	1846.15	17.26	48.88
-3.50	1.13e+1	2525.04	17.98	66.86
-3.00	8.00e+0	2911.44	10.23	77.09
-2.50	5.66e+0	3213.18	7.99	85.08
-2.00	4.00e+0	3404.77	5.07	90.15
-1.50	2.83e+0	3531.26	3.35	93.50
-1.00	2.00e+0	3588.44	1.51	95.02
-0.50	1.41e+0	3628.05	1.05	96.06
0.00	1.00e+0	3659.68	0.84	96.90
0.50	7.07e-1	3691.89	0.85	97.75
1.00	5.00e-1	3724.12	0.85	98.61
1.50	3.54e-1	3749.93	0.68	99.29
2.00	2.50e-1	3765.05	0.40	99.69
2.50	1.77e-1	3776.69	0.31	100.00

Total Weight = 3776.69 g

University of Waikato
Rapid Sediment Analyser
Operating System Version 5.5

Particle Size Analysis

sediment collected from north side of ridge 2

Sample Identification: TS/87/06

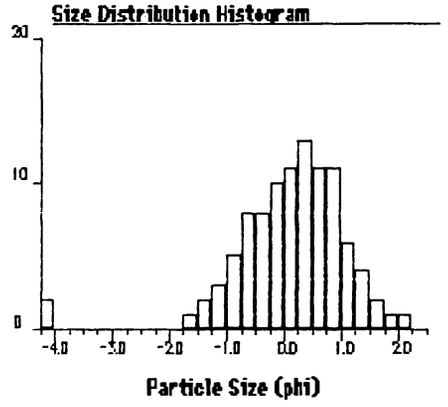

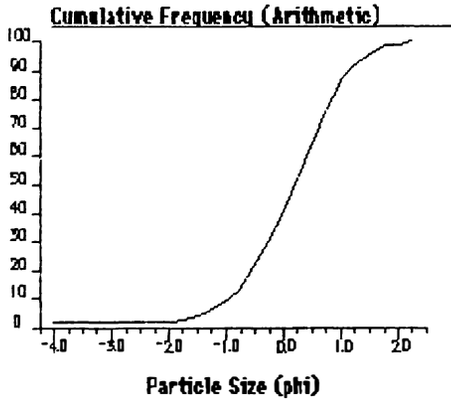

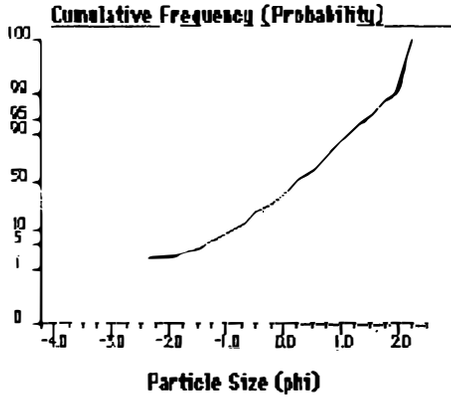

University of Waikato
Rapid Sediment Analyser
Operating System Version 5.5

Particle Size (phi) Results Summary

Textural Size Classes

Gravel= 9.43% Sand= 90.57% Silt= 0.00% Clay= 0.00%

Gravel bearing detrital sediment

Slightly Gravelly Sand

Moment Method Parameters

Mean= 0.10 Sorting= 1.01 Skewness= -1.54 Kurtosis= 7.76

Graphical Method Parameters (Folk & Ward, 1957)

Mean= 0.16 Sorting= 0.84 Skewness= -0.12 Kurtosis= 1.00

Median= 0.22 C= -4.00 D35= -0.14 D65= 0.52

Textural Description

Moderately sorted, Coarse skewed, Mesokurtic

Data Summary

Size (phi)	Size (mm)	Cumulative Weight (g)	Interval Frequency (%)	Cumulative Frequency (%)
-4.00	1.60e+1	14.47	2.18	2.18
-3.75	1.35e+1	14.47	0.00	2.18
-3.50	1.13e+1	14.47	0.00	2.18
-3.25	9.51e+0	14.47	0.00	2.18
-3.00	8.00e+0	14.47	0.00	2.18
-2.75	6.73e+0	15.20	0.11	2.29
-2.50	5.66e+0	15.41	0.03	2.32
-2.25	4.76e+0	16.20	0.12	2.44
-2.00	4.00e+0	17.03	0.13	2.57
-1.75	3.36e+0	20.24	0.48	3.05
-1.50	2.83e+0	27.40	1.08	4.13
-1.25	2.38e+0	41.45	2.12	6.25
-1.00	2.00e+0	62.57	3.18	9.43
-0.75	1.68e+0	94.09	4.75	14.18
-0.50	1.41e+0	146.05	7.83	22.02
-0.25	1.19e+0	202.41	8.50	30.51
0.00	1.00e+0	267.63	9.83	40.34
0.25	8.41e-1	340.03	10.91	51.26
0.50	7.07e-1	425.53	12.89	64.14
0.75	5.95e-1	496.67	10.72	74.87
1.00	5.00e-1	568.80	10.87	85.74
1.25	4.20e-1	610.63	6.31	92.05
1.50	3.54e-1	636.97	3.97	96.02
1.75	2.97e-1	652.60	2.36	98.37
2.00	2.50e-1	657.51	0.74	99.11
2.25	2.10e-1	663.40	0.89	100.00

Total Weight = 663.40 g

Particle Size Analysis
sediment collected from glacier face

Sample Identification: TS/87/07

Size Distribution Histogram

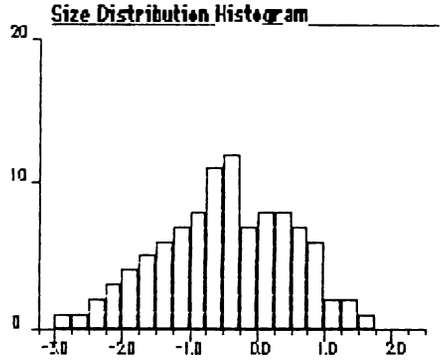

Cumulative Frequency (Arithmetic)

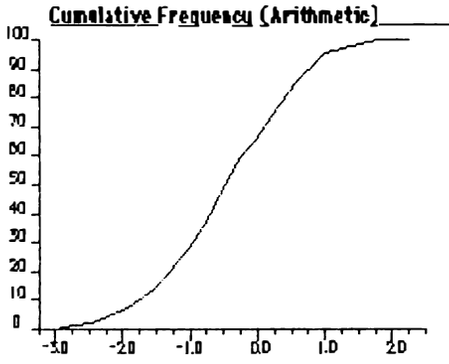

Cumulative Frequency (Probability)

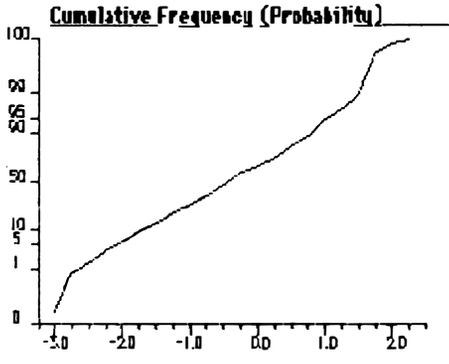

Particle Size (phi) Results Summary

Textural Size Classes

Gravel= 28.64% Sand= 71.36% Silt= 0.00% Clay= 0.00%

Gravel bearing detrital sediment

Gravelly Sand

Moment Method Parameters

Mean= -0.47 Sorting= 0.96 Skewness= -0.17 Kurtosis= 2.61

Graphical Method Parameters (Folk & Ward, 1957)

Mean= -0.45 Sorting= 0.98 Skewness= -0.04 Kurtosis= 0.94

Median= -0.46 C= -2.74 D35= -0.81 D65= -0.05

Textural Description

Moderately sorted, Near symmetrical, Mesokurtic

Data Summary

Size (phi)	Size (mm)	Cumulative Weight (g)	Interval Frequency (%)	Cumulative Frequency (%)
-3.00	8.00e+0	1.22	0.24	0.24
-2.75	6.73e+0	4.89	0.71	0.95
-2.50	5.66e+0	11.08	1.20	2.15
-2.25	4.76e+0	20.28	1.78	3.93
-2.00	4.00e+0	34.02	2.66	6.59
-1.75	3.36e+0	52.99	3.68	10.27
-1.50	2.83e+0	76.90	4.63	14.90
-1.25	2.38e+0	109.54	6.33	21.23
-1.00	2.00e+0	147.78	7.41	28.64
-0.75	1.68e+0	191.60	8.49	37.13
-0.50	1.41e+0	247.71	10.87	48.00
-0.25	1.19e+0	307.37	11.56	59.57
0.00	1.00e+0	342.53	6.81	66.38
0.25	8.41e-1	385.86	8.40	74.78
0.50	7.07e-1	426.77	7.93	82.70
0.75	5.95e-1	460.40	6.52	89.22
1.00	5.00e-1	490.23	5.78	95.00
1.25	4.20e-1	502.32	2.34	97.35
1.50	3.54e-1	510.82	1.65	98.99
1.75	2.97e-1	514.66	0.74	99.74
2.00	2.50e-1	515.38	0.14	99.88
2.25	2.10e-1	516.02	0.12	100.00

Total Weight = 516.02 g

University of Waikato
Rapid Sediment Analyser
Operating System Version 5.5

Particle Size Analysis
sediment collected from south side of ridge 1

Sample Identification: TS/87/08

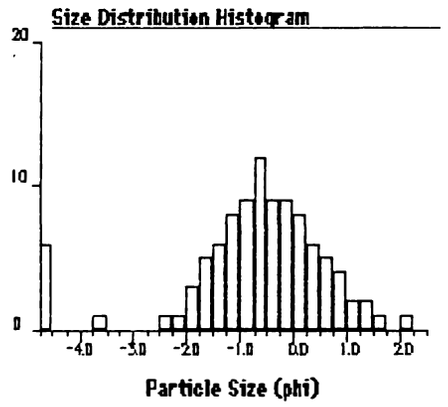

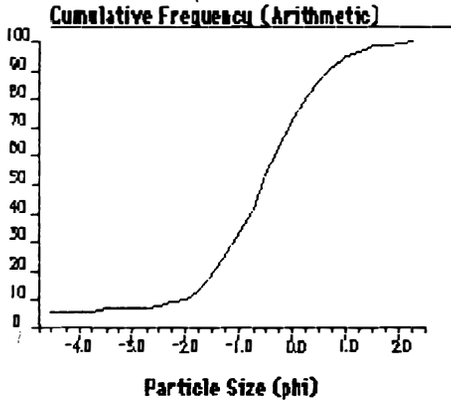

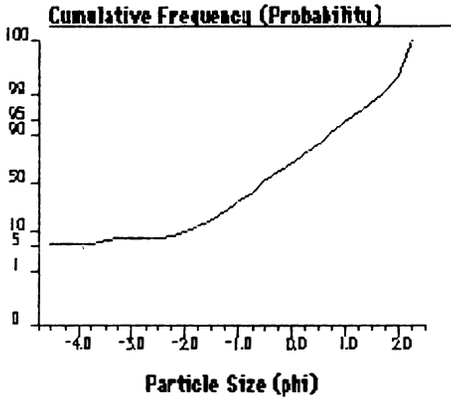

University of Waikato
Rapid Sediment Analyser
Operating System Version 5.5

Particle Size (phi) Results Summary

Textural Size Classes

Gravel= 32.53% Sand= 67.47% Silt= 0.00% Clay= 0.00%

Gravel bearing detrital sediment

Sandy Gravel

Moment Method Parameters

Mean= -0.73 Sorting= 1.36 Skewness= -1.23 Kurtosis= 4.96

Graphical Method Parameters (Folk & Ward, 1957)

Mean= -0.58 Sorting= 1.35 Skewness= -0.23 Kurtosis= 1.68

Median= -0.56 C= -4.50 D35= -0.93 D65= -0.18

Textural Description

Poorly sorted, Coarse skewed, Very leptokurtic

Data Summary

Size (phi)	Size (mm)	Cumulative Weight (g)	Interval Frequency (%)	Cumulative Frequency (%)
-4.50	2.26e+1	53.89	5.92	5.92
-4.25	1.90e+1	53.89	0.00	5.92
-4.00	1.60e+1	53.89	0.00	5.92
-3.75	1.35e+1	53.89	0.00	5.92
-3.50	1.13e+1	63.94	1.10	7.02
-3.25	9.51e+0	66.47	0.28	7.30
-3.00	8.00e+0	67.87	0.15	7.45
-2.75	6.73e+0	70.87	0.33	7.78
-2.50	5.66e+0	73.42	0.28	8.06
-2.25	4.76e+0	83.42	1.10	9.16
-2.00	4.00e+0	96.19	1.40	10.56
-1.75	3.36e+0	121.70	2.80	13.36
-1.50	2.83e+0	165.91	4.85	18.21
-1.25	2.38e+0	223.94	6.37	24.58
-1.00	2.00e+0	296.28	7.94	32.53
-0.75	1.68e+0	374.24	8.56	41.08
-0.50	1.41e+0	481.30	11.75	52.84
-0.25	1.19e+0	567.26	9.44	62.27
0.00	1.00e+0	653.37	9.45	71.73
0.25	8.41e-1	722.26	7.56	79.29
0.50	7.07e-1	780.21	6.36	85.65
0.75	5.95e-1	829.40	5.40	91.05
1.00	5.00e-1	865.28	3.94	94.99
1.25	4.20e-1	881.31	1.76	96.75
1.50	3.54e-1	896.62	1.68	98.43
1.75	2.97e-1	902.85	0.68	99.12
2.00	2.50e-1	905.54	0.30	99.41
2.25	2.10e-1	910.90	0.59	100.00

Total Weight = 910.90 g

Particle Size Analysis
sediment collected from north side of ridge 4

Sample Identification: TS/87/09

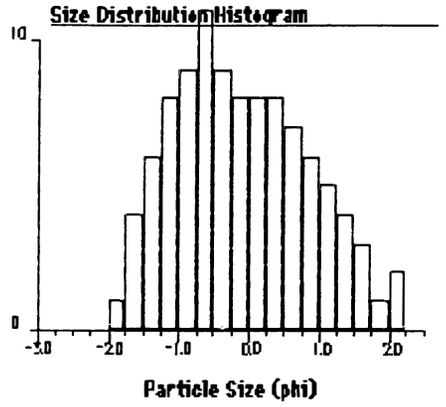

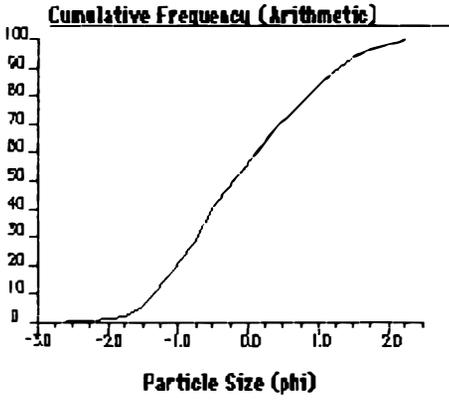

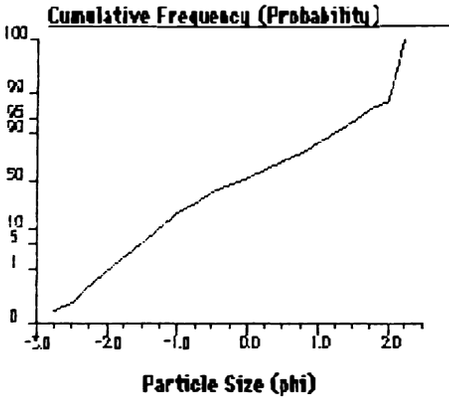

University of Waikato
Rapid Sediment Analyser
Operating System Version 5.5

Particle Size (phi) Results Summary

Textural Size Classes

Gravel= 20.15% Sand= 79.85% Silt= 0.00% Clay= 0.00%

Gravel bearing detrital sediment

Gravelly Sand

Moment Method Parameters

Mean= -0.11 Sorting= 0.98 Skewness= 0.17 Kurtosis= 2.40

Graphical Method Parameters (Folk & Ward, 1957)

Mean= -0.12 Sorting= 1.00 Skewness= 0.11 Kurtosis= 0.86

Median= -0.19 C= -2.01 D35= -0.60 D65= 0.29

Textural Description

Poorly sorted, Fine skewed, Platykurtic

Data Summary

Size (phi)	Size (mm)	Cumulative Weight (g)	Interval Frequency (%)	Cumulative Frequency (%)
-2.75	6.73e+0	1.31	0.27	0.27
-2.50	5.66e+0	1.92	0.13	0.40
-2.25	4.76e+0	2.98	0.22	0.62
-2.00	4.00e+0	4.85	0.39	1.01
-1.75	3.36e+0	11.56	1.40	2.41
-1.50	2.83e+0	28.97	3.63	6.04
-1.25	2.38e+0	58.84	6.23	12.27
-1.00	2.00e+0	96.68	7.89	20.15
-0.75	1.68e+0	137.87	8.59	28.74
-0.50	1.41e+0	188.90	10.64	39.38
-0.25	1.19e+0	230.85	8.74	48.12
0.00	1.00e+0	268.85	7.92	56.04
0.25	8.41e-1	306.53	7.85	63.90
0.50	7.07e-1	342.61	7.52	71.42
0.75	5.95e-1	375.56	6.87	78.29
1.00	5.00e-1	406.74	6.50	84.79
1.25	4.20e-1	432.47	5.36	90.15
1.50	3.54e-1	451.84	4.04	94.19
1.75	2.97e-1	466.15	2.98	97.17
2.00	2.50e-1	471.95	1.21	98.38
2.25	2.10e-1	479.72	1.62	100.00

Total Weight = 479.72 g

Particle Size Analysis
sediment collected from station 6

Sample Identification: TS/87/10

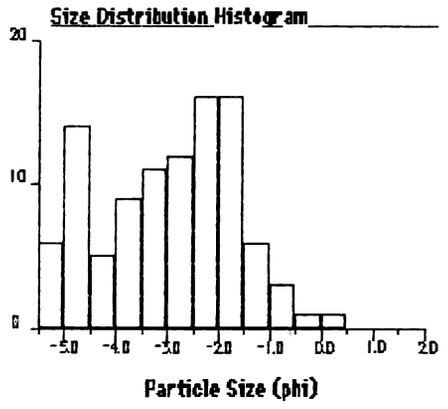

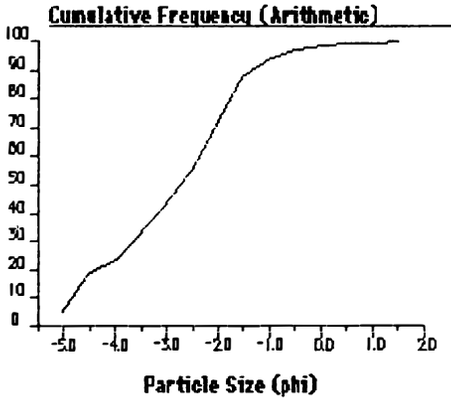

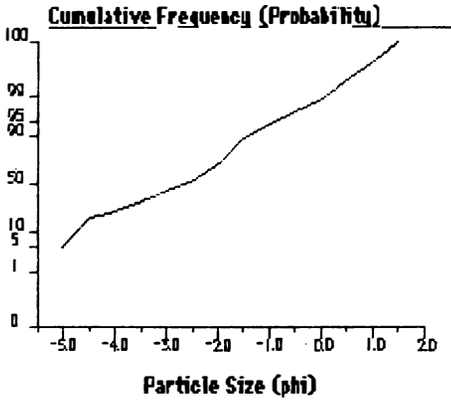

Particle Size (phi) Results Summary

Textural Size Classes

Gravel= 94.19% Sand= 5.81% Silt= 0.00% Clay= 0.00%

Gravel bearing detrital sediment

Gravel

Moment Method Parameters

Mean= -2.90 Sorting= 1.34 Skewness= -0.01 Kurtosis= 2.42

Graphical Method Parameters (Folk & Ward, 1957)

Mean= -2.99 Sorting= 1.37 Skewness= -0.18 Kurtosis= 0.84

Median= -2.73 C= -5.00 D35= -3.40 D65= -2.21

Textural Description

Poorly sorted, Coarse skewed, Platykurtic

Data Summary

Size (phi)	Size (mm)	Cumulative Weight (g)	Interval Frequency (%)	Cumulative Frequency (%)
-5.00	3.20e+1	46.67	5.59	5.59
-4.50	2.26e+1	160.41	13.61	19.20
-4.00	1.60e+1	198.21	4.52	23.72
-3.50	1.13e+1	274.85	9.17	32.90
-3.00	8.00e+0	363.61	10.62	43.52
-2.50	5.66e+0	465.10	12.15	55.67
-2.00	4.00e+0	600.56	16.21	71.88
-1.50	2.83e+0	734.83	16.07	87.95
-1.00	2.00e+0	786.97	6.24	94.19
-0.50	1.41e+0	812.55	3.06	97.25
0.00	1.00e+0	824.48	1.43	98.68
0.50	7.07e-1	830.38	0.71	99.39
1.00	5.00e-1	832.73	0.28	99.67
1.50	3.54e-1	835.51	0.33	100.00

Total Weight = 835.51 g

University of Waikato
Rapid Sediment Analyser
Operating System Version 5.5

Particle Size Analysis
sediment collected from north side of ridge 3

Sample Identification: TS/87/11

Size Distribution Histogram

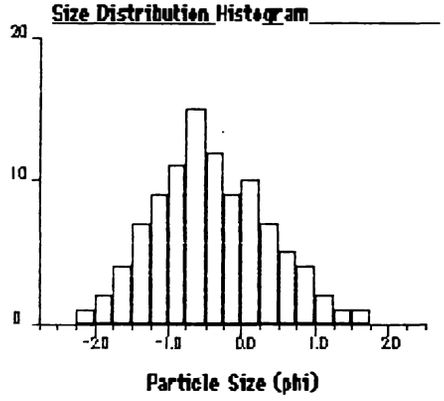

Cumulative Frequency (Arithmetic)

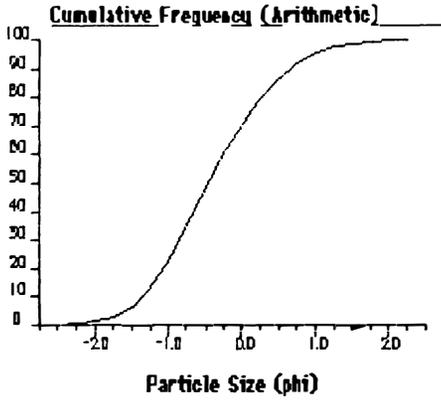

Cumulative Frequency (Probability)

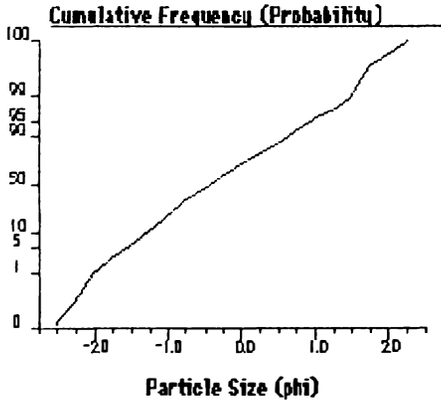

Particle Size (phi) Results Summary

Textural Size Classes

Gravel= 22.52% Sand= 77.48% Silt= 0.00% Clay= 0.00%

Gravel bearing detrital sediment

Gravelly Sand

Moment Method Parameters

Mean= -0.40 Sorting= 0.78 Skewness= 0.25 Kurtosis= 2.91

Graphical Method Parameters (Folk & Ward, 1957)

Mean= -0.41 Sorting= 0.78 Skewness= 0.11 Kurtosis= 0.97

Median= -0.47 C= -2.10 D35= -0.73 D65= -0.12

Textural Description

Moderately sorted, Fine skewed, Mesokurtic

Data Summary

Size (phi)	Size (mm)	Cumulative Weight (g)	Interval Frequency (%)	Cumulative Frequency (%)
-2.50	5.66e+0	0.55	0.13	0.13
-2.25	4.76e+0	2.01	0.35	0.48
-2.00	4.00e+0	5.63	0.86	1.34
-1.75	3.36e+0	12.80	1.71	3.05
-1.50	2.83e+0	27.76	3.56	6.61
-1.25	2.38e+0	55.21	6.53	13.14
-1.00	2.00e+0	94.63	9.38	22.52
-0.75	1.68e+0	142.95	11.50	34.02
-0.50	1.41e+0	204.10	14.55	48.57
-0.25	1.19e+0	253.46	11.75	60.31
0.00	1.00e+0	292.83	9.37	69.68
0.25	8.41e-1	333.28	9.63	79.31
0.50	7.07e-1	364.08	7.33	86.64
0.75	5.95e-1	385.62	5.13	91.76
1.00	5.00e-1	403.12	4.16	95.93
1.25	4.20e-1	410.19	1.68	97.61
1.50	3.54e-1	415.74	1.32	98.93
1.75	2.97e-1	418.48	0.65	99.58
2.00	2.50e-1	419.23	0.18	99.76
2.25	2.10e-1	420.23	0.24	100.00

Total Weight = 420.23 g

University of Waikato
Rapid Sediment Analyser
Operating System Version 5.5

Particle Size Analysis

sediment collected from south side of ridge 2

Sample Identification: TS/87/12

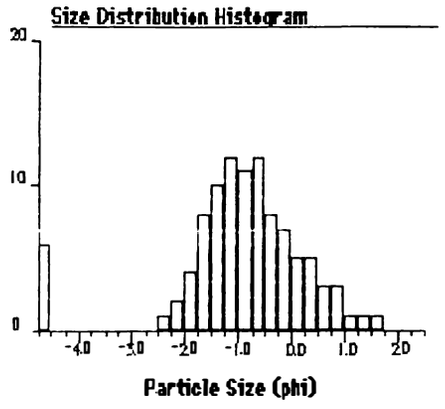

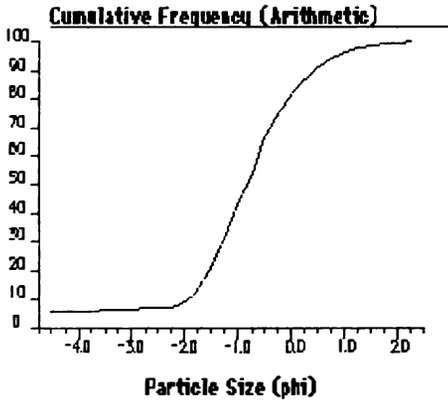

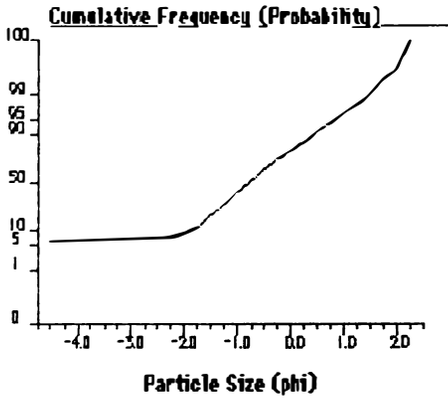

University of Waikato
Rapid Sediment Analyser
Operating System Version 5.5

Particle Size (phi) Results Summary

Textural Size Classes

Gravel= 42.12% Sand= 57.88% Silt= 0.00% Clay= 0.00%

Gravel bearing detrital sediment

Sandy Gravel

Moment Method Parameters

Mean= -0.92 Sorting= 1.26 Skewness= -1.18 Kurtosis= 5.45

Graphical Method Parameters (Folk & Ward, 1957)

Mean= -0.78 Sorting= 1.26 Skewness= -0.15 Kurtosis= 1.87

Median= -0.83 C= -4.50 D35= -1.15 D65= -0.51

Textural Description

Poorly sorted, Coarse skewed, Very leptokurtic

Data Summary

Size (phi)	Size (mm)	Cumulative Weight (g)	Interval Frequency (%)	Cumulative Frequency (%)
-4.50	2.26e+1	34.98	6.12	6.12
-4.25	1.90e+1	34.98	0.00	6.12
-4.00	1.60e+1	34.98	0.00	6.12
-3.75	1.35e+1	34.98	0.00	6.12
-3.50	1.13e+1	37.46	0.43	6.56
-3.25	9.51e+0	37.46	0.00	6.56
-3.00	8.00e+0	37.46	0.00	6.56
-2.75	6.73e+0	38.93	0.26	6.81
-2.50	5.66e+0	41.06	0.37	7.19
-2.25	4.76e+0	44.27	0.56	7.75
-2.00	4.00e+0	53.70	1.65	9.40
-1.75	3.36e+0	74.37	3.62	13.02
-1.50	2.83e+0	117.24	7.50	20.52
-1.25	2.38e+0	174.40	10.00	30.52
-1.00	2.00e+0	240.70	11.60	42.12
-0.75	1.68e+0	305.56	11.35	53.48
-0.50	1.41e+0	375.49	12.24	65.71
-0.25	1.19e+0	423.45	8.39	74.11
0.00	1.00e+0	461.78	6.71	80.82
0.25	8.41e-1	493.01	5.47	86.28
0.50	7.07e-1	519.77	4.68	90.96
0.75	5.95e-1	537.08	3.03	93.99
1.00	5.00e-1	551.50	2.52	96.52
1.25	4.20e-1	559.13	1.34	97.85
1.50	3.54e-1	564.50	0.94	98.79
1.75	2.97e-1	567.76	0.57	99.36
2.00	2.50e-1	568.77	0.18	99.54
2.25	2.10e-1	571.40	0.46	100.00

Total Weight = 571.40 g

Particle Size Analysis
sediment collected from south side of ridge 3

Sample Identification: TS/87/13

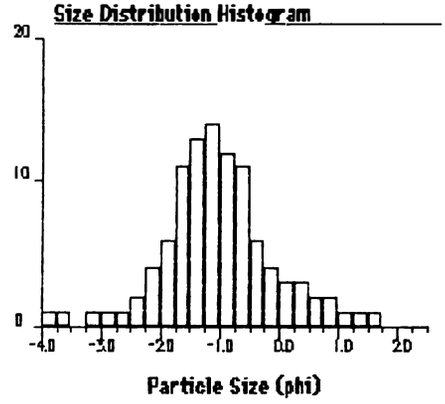

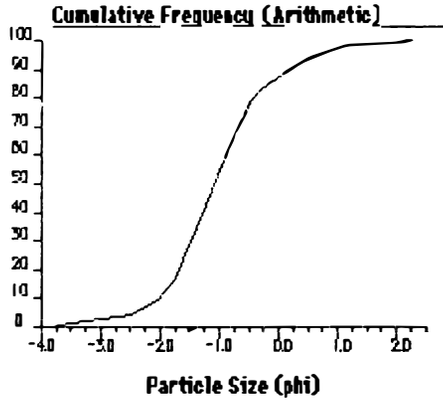

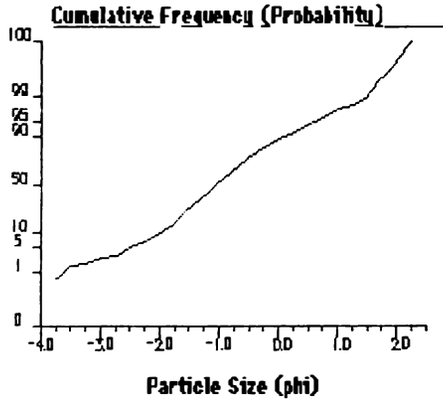

Particle Size (phi) Results Summary

Textural Size Classes

Gravel= 54.61% Sand= 45.39% Silt= 0.00% Clay= 0.00%

Gravel bearing detrital sediment

Sandy Gravel

Moment Method Parameters

Mean= -1.03 Sorting= 0.94 Skewness= 0.13 Kurtosis= 4.28

Graphical Method Parameters (Folk & Ward, 1957)

Mean= -1.03 Sorting= 0.86 Skewness= 0.10 Kurtosis= 1.28

Median= -1.08 C= -3.69 D35= -1.36 D65= -0.79

Textural Description

Moderately sorted, Near symmetrical, Leptokurtic

Data Summary

Size (phi)	Size (mm)	Cumulative Weight (g)	Interval Frequency (%)	Cumulative Frequency (%)
-3.75	1.35e+1	4.57	0.80	0.80
-3.50	1.13e+1	9.70	0.90	1.70
-3.25	9.51e+0	12.20	0.44	2.14
-3.00	8.00e+0	15.68	0.61	2.74
-2.75	6.73e+0	19.94	0.75	3.49
-2.50	5.66e+0	27.86	1.39	4.88
-2.25	4.76e+0	39.41	2.02	6.90
-2.00	4.00e+0	61.07	3.79	10.69
-1.75	3.36e+0	96.22	6.15	16.84
-1.50	2.83e+0	156.55	10.56	27.40
-1.25	2.38e+0	231.48	13.11	40.51
-1.00	2.00e+0	312.04	14.10	54.61
-0.75	1.68e+0	382.06	12.25	66.86
-0.50	1.41e+0	442.76	10.62	77.49
-0.25	1.19e+0	477.89	6.15	83.63
0.00	1.00e+0	501.81	4.19	87.82
0.25	8.41e-1	521.79	3.50	91.32
0.50	7.07e-1	537.00	2.66	93.98
0.75	5.95e-1	547.37	1.81	95.79
1.00	5.00e-1	556.42	1.58	97.38
1.25	4.20e-1	560.98	0.80	98.18
1.50	3.54e-1	565.06	0.71	98.89
1.75	2.97e-1	568.00	0.51	99.40
2.00	2.50e-1	569.26	0.22	99.63
2.25	2.10e-1	571.40	0.37	100.00

Total Weight = 571.40 g

University of Waikato
Rapid Sediment Analyser
Operating System Version 5.5

Particle Size Analysis

sediment collected from north side of ridge 1

Sample Identification: TS/87/14

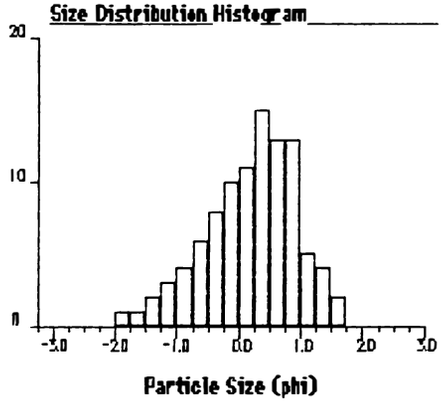

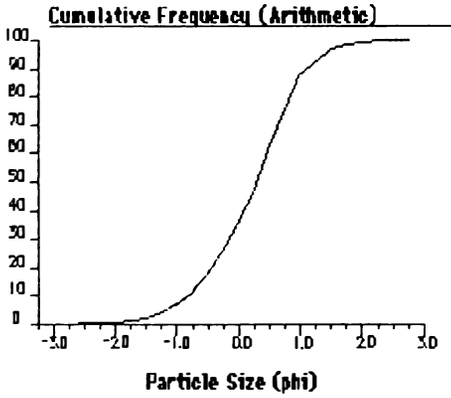

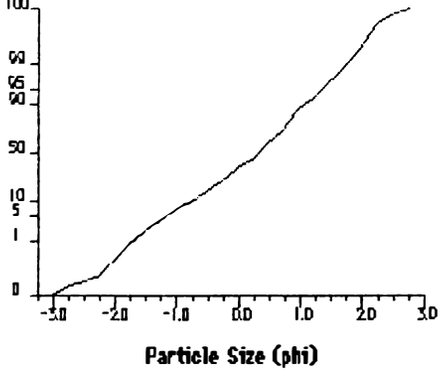

University of Waikato
Rapid Sediment Analyser
Operating System Version 5.5

Particle Size (phi) Results Summary

Textural Size Classes

Gravel= 7.54% Sand= 92.46% Silt= 0.00% Clay= 0.00%

Gravel bearing detrital sediment

Slightly Gravelly Sand

Moment Method Parameters

Mean= 0.20 Sorting= 0.78 Skewness= -0.49 Kurtosis= 3.55

Graphical Method Parameters (Folk & Ward, 1957)

Mean= 0.21 Sorting= 0.77 Skewness= -0.17 Kurtosis= 1.01

Median= 0.30 C= -1.84 D35= -0.02 D65= 0.55

Textural Description

Moderately sorted, Coarse skewed, Mesokurtic

Data Summary

Size (phi)	Size (mm)	Cumulative Weight (g)	Interval Frequency (%)	Cumulative Frequency (%)
-3.00	8.00e+0	0.45	0.09	0.09
-2.75	6.73e+0	1.06	0.12	0.21
-2.50	5.66e+0	1.52	0.09	0.30
-2.25	4.76e+0	2.03	0.10	0.40
-2.00	4.00e+0	3.30	0.25	0.66
-1.75	3.36e+0	6.10	0.56	1.21
-1.50	2.83e+0	12.68	1.31	2.52
-1.25	2.38e+0	22.65	1.98	4.50
-1.00	2.00e+0	38.01	3.05	7.54
-0.75	1.68e+0	59.46	4.26	11.80
-0.50	1.41e+0	92.00	6.46	18.26
-0.25	1.19e+0	132.54	8.05	26.31
0.00	1.00e+0	180.60	9.54	35.85
0.25	8.41e-1	236.53	11.10	46.95
0.50	7.07e-1	313.71	15.32	62.27
0.75	5.95e-1	376.71	12.51	74.78
1.00	5.00e-1	443.63	13.28	88.06
1.25	4.20e-1	467.91	4.82	92.88
1.50	3.54e-1	489.55	4.30	97.18
1.75	2.97e-1	498.39	1.75	98.93
2.00	2.50e-1	500.58	0.43	99.36
2.25	2.10e-1	502.48	0.38	99.74
2.50	1.77e-1	503.13	0.13	99.87
2.75	1.49e-1	503.78	0.13	100.00

Total Weight = 503.78 g

Particle Size Analysis
sediment collected from south side of ridge 4

Sample Identification: TS/87/15

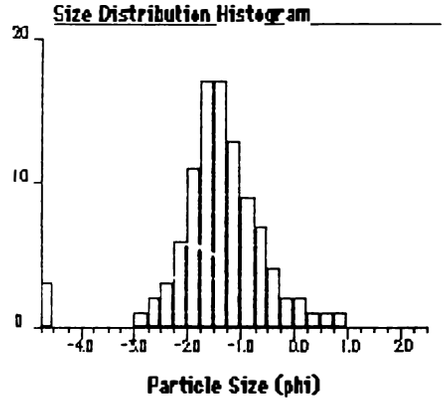

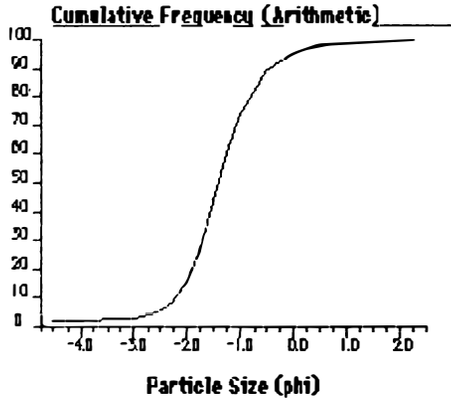

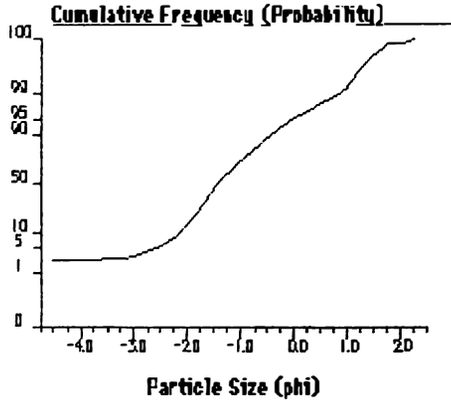

University of Waikato
Rapid Sediment Analyser
Operating System Version 5.5

Particle Size (phi) Results Summary

Textural Size Classes

Gravel= 73.46% Sand= 26.54% Silt= 0.00% Clay= 0.00%

Gravel bearing detrital sediment

Sandy Gravel

Moment Method Parameters

Mean= -1.40 Sorting= 0.88 Skewness= -0.71 Kurtosis= 6.89

Graphical Method Parameters (Folk & Ward, 1957)

Mean= -1.36 Sorting= 0.72 Skewness= 0.07 Kurtosis= 1.31

Median= -1.40 C= -4.50 D35= -1.62 D65= -1.16

Textural Description

Moderately sorted, Near symmetrical, Leptokurtic

Data Summary

Size (phi)	Size (mm)	Cumulative Weight (g)	Interval Frequency (%)	Cumulative Frequency (%)
-4.50	2.26e+1	15.50	2.61	2.61
-4.25	1.90e+1	15.50	0.00	2.61
-4.00	1.60e+1	15.50	0.00	2.61
-3.75	1.35e+1	15.50	0.00	2.61
-3.50	1.13e+1	16.92	0.24	2.85
-3.25	9.51e+0	16.92	0.00	2.85
-3.00	8.00e+0	18.99	0.35	3.19
-2.75	6.73e+0	26.65	1.29	4.48
-2.50	5.66e+0	35.61	1.51	5.99
-2.25	4.76e+0	52.22	2.79	8.79
-2.00	4.00e+0	89.91	6.34	15.13
-1.75	3.36e+0	156.69	11.23	26.36
-1.50	2.83e+0	258.50	17.13	43.49
-1.25	2.38e+0	357.28	16.62	60.11
-1.00	2.00e+0	436.68	13.36	73.46
-0.75	1.68e+0	490.47	9.05	82.51
-0.50	1.41e+0	530.15	6.68	89.19
-0.25	1.19e+0	552.05	3.68	92.87
0.00	1.00e+0	566.91	2.50	95.37
0.25	8.41e-1	576.51	1.62	96.99
0.50	7.07e-1	582.76	1.05	98.04
0.75	5.95e-1	586.52	0.63	98.67
1.00	5.00e-1	589.64	0.52	99.20
1.25	4.20e-1	591.39	0.29	99.49
1.50	3.54e-1	592.62	0.21	99.70
1.75	2.97e-1	593.50	0.15	99.85
2.00	2.50e-1	593.72	0.04	99.88
2.25	2.10e-1	594.42	0.12	100.00

Total Weight = 594.42 g

Particle Size Analysis
sediment collected from station 4

Sample Identification: TS/87/51

Size Distribution Histogram

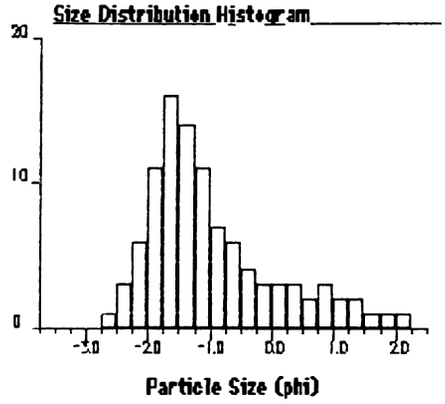

Cumulative Frequency (Arithmetic)

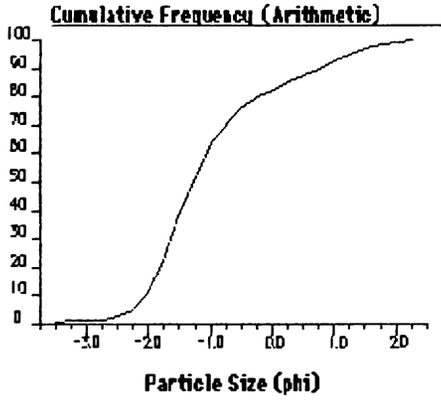

Cumulative Frequency (Probability)

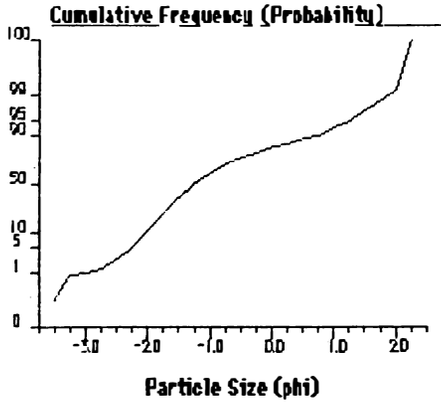

University of Waikato
Rapid Sediment Analyser
Operating System Version 5.5

Particle Size (phi) Results Summary

Textural Size Classes

Gravel= 62.68% Sand= 37.32% Silt= 0.00% Clay= 0.00%

Gravel bearing detrital sediment

Sandy Gravel

Moment Method Parameters

Mean= -1.00 Sorting= 1.07 Skewness= 0.88 Kurtosis= 3.49

Graphical Method Parameters (Folk & Ward, 1957)

Mean= -1.01 Sorting= 1.05 Skewness= 0.42 Kurtosis= 1.27

Median= -1.28 C= -3.17 D35= -1.54 D65= -0.92

Textural Description

Poorly sorted, Strongly fine skewed, Leptokurtic

Data Summary

Size (phi)	Size (mm)	Cumulative Weight (g)	Interval Frequency (%)	Cumulative Frequency (%)
-3.50	1.13e+1	2.47	0.46	0.46
-3.25	9.51e+0	5.14	0.50	0.96
-3.00	8.00e+0	5.81	0.13	1.09
-2.75	6.73e+0	7.84	0.38	1.47
-2.50	5.66e+0	15.31	1.40	2.86
-2.25	4.76e+0	28.86	2.53	5.39
-2.00	4.00e+0	60.13	5.84	11.24
-1.75	3.36e+0	117.13	10.65	21.89
-1.50	2.83e+0	202.07	15.88	37.77
-1.25	2.38e+0	275.56	13.74	51.50
-1.00	2.00e+0	335.37	11.18	62.68
-0.75	1.68e+0	375.32	7.47	70.15
-0.50	1.41e+0	407.89	6.09	76.24
-0.25	1.19e+0	427.11	3.59	79.83
0.00	1.00e+0	441.69	2.73	82.56
0.25	8.41e-1	455.07	2.50	85.06
0.50	7.07e-1	469.05	2.61	87.67
0.75	5.95e-1	481.54	2.33	90.00
1.00	5.00e-1	497.56	2.99	93.00
1.25	4.20e-1	507.01	1.77	94.76
1.50	3.54e-1	519.58	2.35	97.11
1.75	2.97e-1	527.53	1.49	98.60
2.00	2.50e-1	530.78	0.61	99.21
2.25	2.10e-1	535.02	0.79	100.00

Total Weight = 535.02 g

Particle Size Analysis

Sediment analysis of core from station #1

Sample Identification: CORE #1

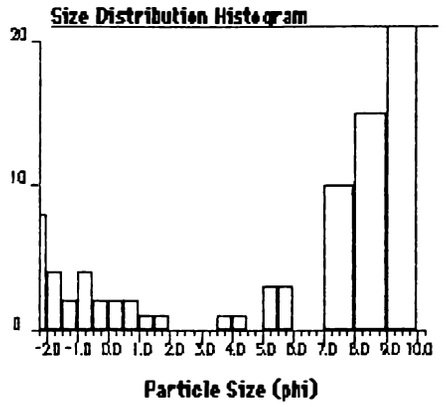

Particle Size (phi) Results Summary

Textural Size Classes

Gravel= 14.55% Sand= 12.48% Silt= 16.40% Clay= 56.57%

Gravel bearing detrital sediment

Slightly Gravelly Mud

Moment Method Parameters

Mean= 4.09 Sorting= 4.15 Skewness= 0.14 Kurtosis= 1.58

Graphical Method Parameters (Folk & Ward, 1957)

Median= 8.44 C= -2.00 D35= 7.17 D65= 9.33

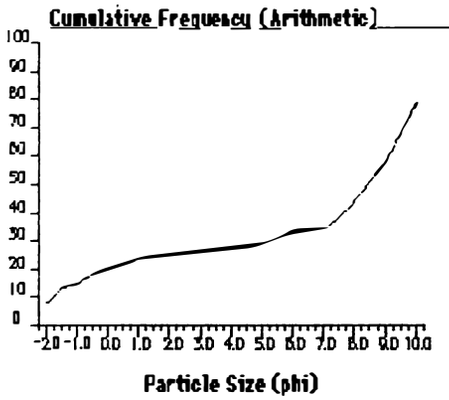

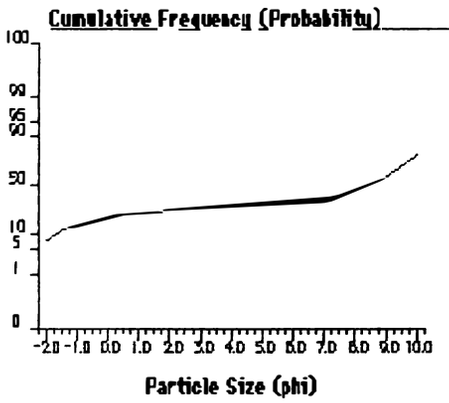

Data Summary

Size (phi)	Size (mm)	Cumulative Weight (g)	Interval Frequency (%)	Cumulative Frequency (%)
-2.00	4.00e+0	8.29	8.29	8.29
-1.50	2.83e+0	12.69	4.40	12.69
-1.00	2.00e+0	14.55	1.86	14.55
-0.50	1.41e+0	18.24	3.69	18.24
0.00	1.00e+0	20.28	2.04	20.28
0.50	7.07e-1	21.78	1.50	21.78
1.00	5.00e-1	23.61	1.83	23.61
1.50	3.54e-1	24.59	0.98	24.59
2.00	2.50e-1	25.33	0.74	25.33
2.50	1.77e-1	25.79	0.46	25.79
3.00	1.25e-1	26.21	0.42	26.21
3.50	8.84e-2	26.42	0.21	26.42
4.00	6.25e-2	27.03	0.61	27.03
4.50	4.42e-2	27.61	0.58	27.61
5.00	3.12e-2	27.61	0.00	27.61
5.50	2.21e-2	30.78	3.17	30.78
6.00	1.56e-2	33.32	2.54	33.32
7.00	7.81e-3	33.32	0.00	33.32
8.00	3.91e-3	43.43	10.11	43.43
9.00	1.95e-3	58.23	14.80	58.23
10.00	9.77e-4	78.80	20.57	78.80

Total Weight = 100.00 g

University of Waikato

Rapid Sediment Analyser

Operating System Version 5.5

Particle Size Analysis

Sediment analysis of core from station #2

Sample Identification: CORE #2

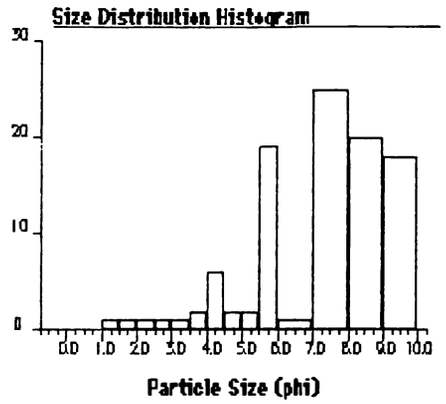

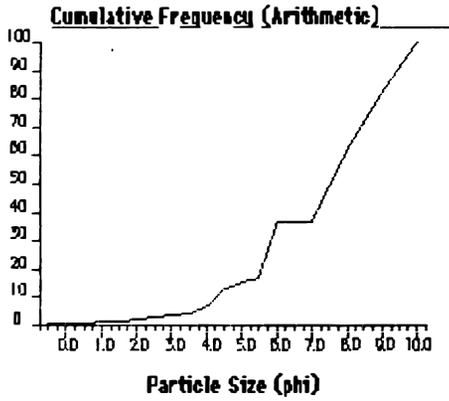

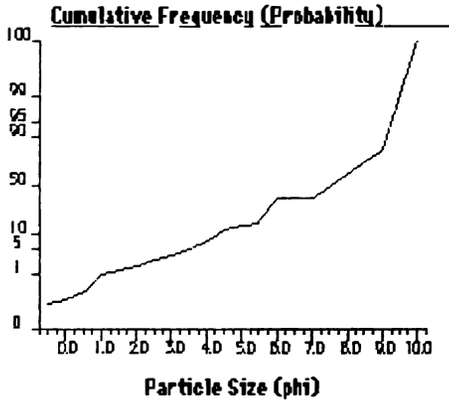

University of Waikato
Rapid Sediment Analyser
Operating System Version 5.5

Particle Size (phi) Results Summary

Textural Size Classes

Gravel= 0.00% Sand= 7.42% Silt= 54.66% Clay= 37.92%

Gravel free detrital sediment

Silt

Moment Method Parameters

Mean= 7.06 Sorting= 2.02 Skewness= -0.90 Kurtosis= 3.64

Graphical Method Parameters (Folk & Ward, 1957)

Mean= 7.28 Sorting= 1.90 Skewness= -0.23 Kurtosis= 0.87

Median= 7.51 C= 1.00 D35= 5.96 D65= 8.14

Textural Description

Poorly sorted, Coarse skewed, Platykurtic

Data Summary

Size (phi)	Size (mm)	Cumulative Weight (g)	Interval Frequency (%)	Cumulative Frequency (%)
-0.50	1.41e+0	0.32	0.43	0.43
0.00	1.00e+0	0.38	0.08	0.52
0.50	7.07e-1	0.48	0.14	0.65
1.00	5.00e-1	0.74	0.35	1.00
1.50	3.54e-1	1.11	0.50	1.50
2.00	2.50e-1	1.58	0.64	2.14
2.50	1.77e-1	2.06	0.65	2.79
3.00	1.25e-1	2.77	0.96	3.76
3.50	8.84e-2	3.63	1.17	4.92
4.00	6.25e-2	5.47	2.49	7.42
4.50	4.42e-2	9.69	5.72	13.14
5.00	3.12e-2	11.10	1.91	15.05
5.50	2.21e-2	12.51	1.91	16.96
6.00	1.56e-2	26.86	19.45	36.42
7.00	7.81e-3	27.54	0.92	37.34
8.00	3.91e-3	45.79	24.74	62.08
9.00	1.95e-3	60.82	20.38	82.46
10.00	9.77e-4	73.76	17.54	100.00

Total Weight = 73.76 g

Particle Size Analysis

Sediment analysis of core from station #3

Sample Identification: core #3

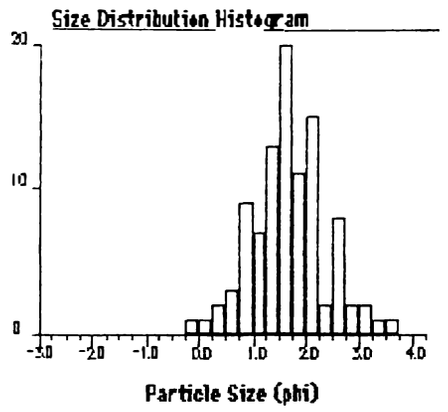

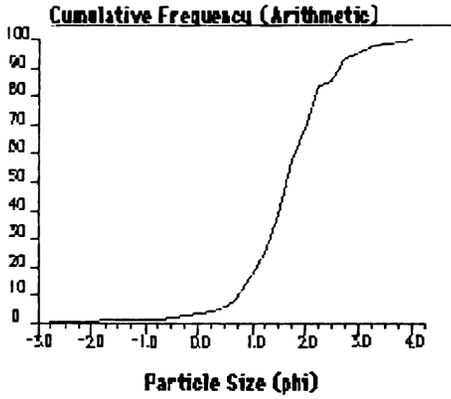

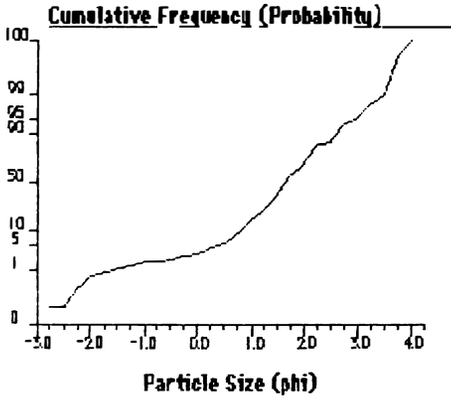

University of Waikato
Rapid Sediment Analyser
Operating System Version 5.5

Particle Size (phi) Results Summary

Textural Size Classes

Gravel= 1.76% Sand= 98.24% Silt= 0.00% Clay= 0.00%

Gravel bearing detrital sediment

Slightly Gravelly Sand

Moment Method Parameters

Mean= 1.63 Sorting= 0.87 Skewness= -1.18 Kurtosis= 7.70

Graphical Method Parameters (Folk & Ward, 1957)

Mean= 1.64 Sorting= 0.74 Skewness= -0.01 Kurtosis= 1.23

Median= 1.65 C= -1.70 D35= 1.44 D65= 1.92

Textural Description

Moderately sorted, Near symmetrical, Leptokurtic

Data Summary

Size (phi)	Size (mm)	Cumulative Weight (g)	Interval Frequency (%)	Cumulative Frequency (%)
-2.75	6.73e+0	0.59	0.32	0.32
-2.50	5.66e+0	0.59	0.00	0.32
-2.25	4.76e+0	1.18	0.32	0.63
-2.00	4.00e+0	1.47	0.16	0.79
-1.75	3.36e+0	1.74	0.15	0.94
-1.50	2.83e+0	2.35	0.33	1.26
-1.25	2.38e+0	2.75	0.22	1.48
-1.00	2.00e+0	3.28	0.28	1.76
-0.75	1.68e+0	3.63	0.19	1.95
-0.50	1.41e+0	4.34	0.38	2.33
-0.25	1.19e+0	4.95	0.33	2.66
0.00	1.00e+0	6.43	0.80	3.46
0.25	8.41e-1	8.07	0.88	4.34
0.50	7.07e-1	11.34	1.76	6.10
0.75	5.95e-1	17.42	3.27	9.37
1.00	5.00e-1	33.28	8.53	17.89
1.25	4.20e-1	46.34	7.02	24.92
1.50	3.54e-1	71.36	13.45	38.37
1.75	2.97e-1	107.68	19.53	57.90
2.00	2.50e-1	127.32	10.56	68.46
2.25	2.10e-1	154.92	14.84	83.29
2.50	1.77e-1	158.65	2.01	85.30
2.75	1.49e-1	173.61	8.04	93.34
3.00	1.25e-1	177.93	2.32	95.67
3.25	1.05e-1	182.00	2.19	97.85
3.50	8.84e-2	183.89	1.02	98.87
3.75	7.43e-2	185.40	0.81	99.68
4.00	6.25e-2	185.99	0.32	100.00

Total Weight = 185.99 g

Particle Size Analysis

Sediment analysis of core from station #4

Sample Identification: CORE #4

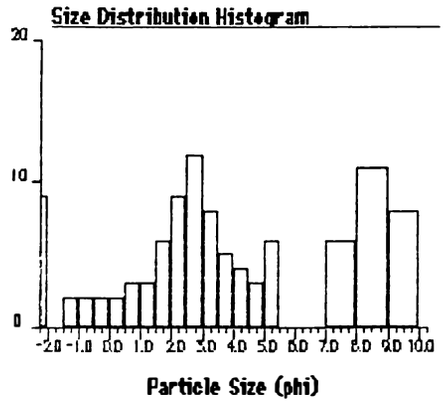

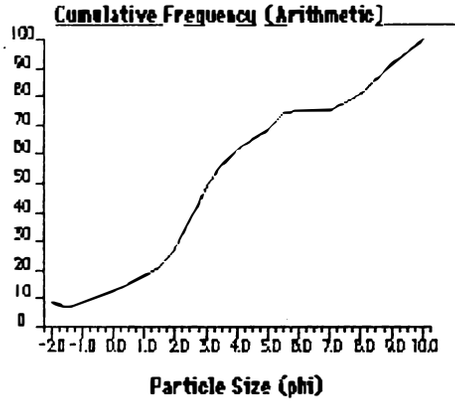

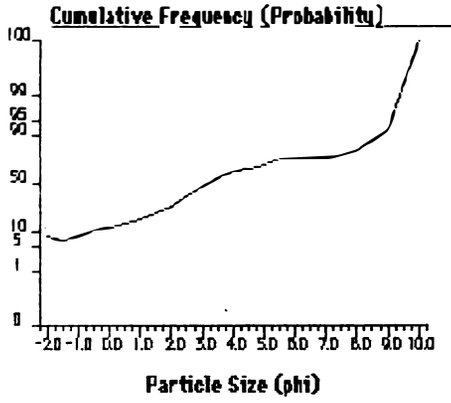

Particle Size (phi) Results Summary

Textural Size Classes

Gravel= 8.82% Sand= 53.01% Silt= 19.02% Clay= 19.15%

Gravel bearing detrital sediment

Slightly Gravelly Muddy Sand

Moment Method Parameters

Mean= 3.77 Sorting= 3.36 Skewness= 0.17 Kurtosis= 2.20

Graphical Method Parameters (Folk & Ward, 1957)

Mean= 4.00 Sorting= 3.64 Skewness= 0.23 Kurtosis= 0.89

Median= 3.10 C= -2.00 D35= 2.43 D65= 4.43

Textural Description

Very poorly sorted, Fine skewed, Platykurtic

Data Summary

Size (phi)	Size (mm)	Cumulative Weight (g)	Interval Frequency (%)	Cumulative Frequency (%)
-2.00	4.00e+0	7.92	8.82	8.82
-1.50	2.83e+0	6.10	-2.03	6.80
-1.00	2.00e+0	7.92	2.03	8.82
-0.50	1.41e+0	9.96	2.27	11.10
0.00	1.00e+0	11.93	2.19	13.29
0.50	7.07e-1	13.73	2.01	15.30
1.00	5.00e-1	16.62	3.22	18.52
1.50	3.54e-1	18.97	2.62	21.13
2.00	2.50e-1	24.27	5.90	27.04
2.50	1.77e-1	32.65	9.34	36.37
3.00	1.25e-1	43.43	12.01	48.38
3.50	8.84e-2	50.76	8.17	56.55
4.00	6.25e-2	55.50	5.28	61.83
4.50	4.42e-2	58.83	3.71	65.54
5.00	3.12e-2	61.29	2.74	68.28
5.50	2.21e-2	66.69	6.02	74.30
6.00	1.56e-2	66.87	0.20	74.50
7.00	7.81e-3	67.05	0.20	74.70
8.00	3.91e-3	72.57	6.15	80.85
9.00	1.95e-3	82.48	11.04	91.89
10.00	9.77e-4	89.76	8.11	100.00

Total Weight = 89.76 g

University of Waikato

Rapid Sediment Analyser

Operating System Version 5.5

Particle Size Analysis

Sediment analysis of core from station #12

Sample Identification: CORE #12

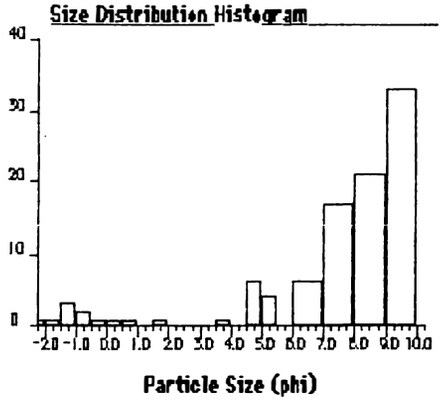

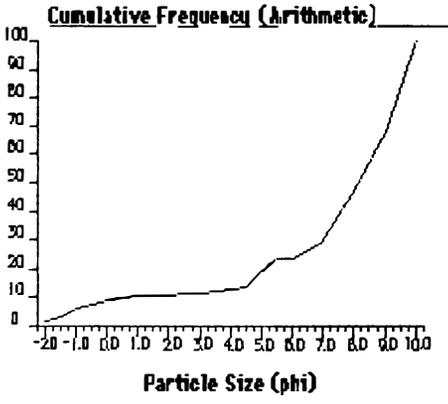

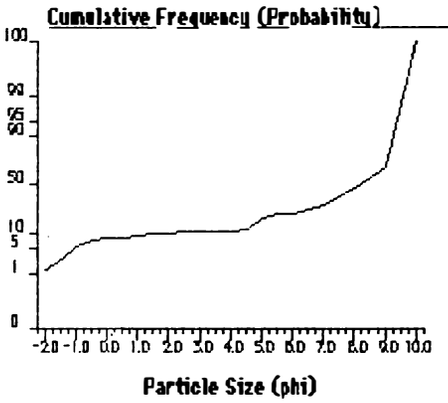

Particle Size (phi) Results Summary

Textural Size Classes

Gravel= 5.87% Sand= 6.53% Silt= 34.22% Clay= 53.38%

Gravel bearing detrital sediment

Slightly Gravelly Mud

Moment Method Parameters

Mean= 7.05 Sorting= 3.16 Skewness= -1.64 Kurtosis= 4.76

Graphical Method Parameters (Folk & Ward, 1957)

Mean= 7.48 Sorting= 2.85 Skewness= -0.56 Kurtosis= 1.52

Median= 8.16 C= -2.00 D35= 7.31 D65= 8.88

Textural Description

Very poorly sorted, Strongly Coarse skewed, Very leptokurtic

Data Summary

Size (phi)	Size (mm)	Cumulative Weight (g)	Interval Frequency (%)	Cumulative Frequency (%)
-2.00	4.00e+0	1.06	1.48	1.48
-1.50	2.83e+0	1.35	1.24	2.71
-1.00	2.00e+0	4.22	3.16	5.87
-0.50	1.41e+0	5.47	1.74	7.62
0.00	1.00e+0	6.13	0.92	8.53
0.50	7.07e-1	6.59	0.64	9.17
1.00	5.00e-1	7.04	0.63	9.80
1.50	3.54e-1	7.32	0.39	10.19
2.00	2.50e-1	7.70	0.53	10.72
2.50	1.77e-1	7.98	0.39	11.11
3.00	1.25e-1	8.21	0.32	11.43
3.50	8.84e-2	8.40	0.26	11.69
4.00	6.25e-2	8.91	0.71	12.40
4.50	4.42e-2	9.14	0.32	12.72
5.00	3.12e-2	13.59	6.20	18.92
5.50	2.21e-2	16.73	4.37	23.29
6.00	1.56e-2	16.73	0.00	23.29
7.00	7.81e-3	21.32	6.39	29.68
8.00	3.91e-3	33.49	16.94	46.62
9.00	1.95e-3	48.47	20.85	67.48
10.00	9.77e-4	71.83	32.52	100.00

Total Weight = 71.83 g

University of Waikato

Rapid Sediment Analyser

Operating System Version 5.5

APPENDIX THREE

G. LYONS SKETCH MAP OF TROUGH LAKE 1970.

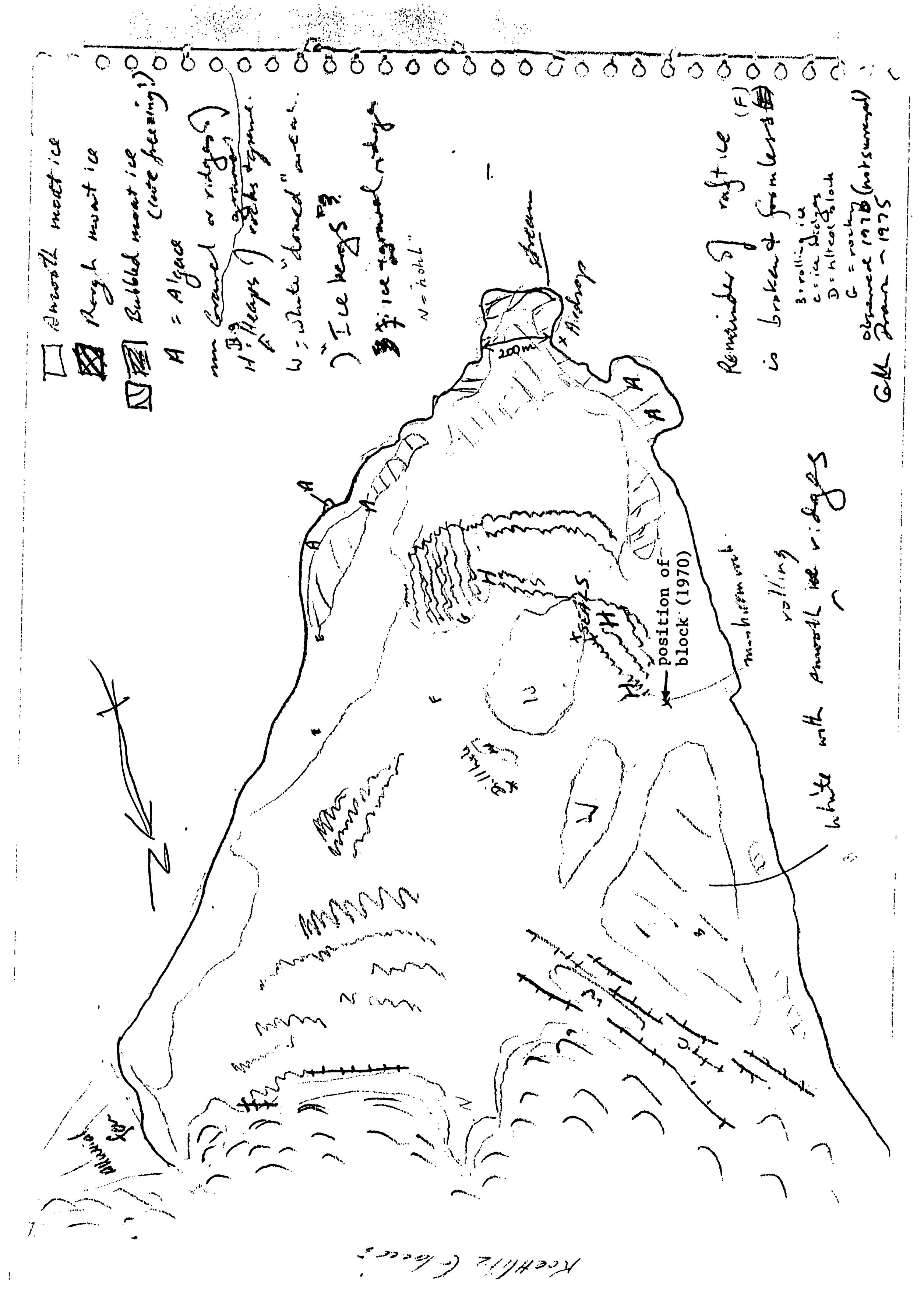
Smooth moat ice
Rough moat ice
Bubbled moat ice
A = Algae
W = white "domed" areas
Ice bergs?
Stream
Airdrop
200 m
SEALS
position of block (1970)
rolling
white with smooth ice ridges
N